

Electronic Thesis and Dissertation Repository

9-21-2016 12:00 AM

Molecular Characterization of the Potyviral First Protein (P1 Protein)

Qiuyue Pan, *The University of Western Ontario*

Supervisor: Aiming Wang, *The University of Western Ontario*

Joint Supervisor: Mark Bernards, *The University of Western Ontario*

A thesis submitted in partial fulfillment of the requirements for the Doctor of Philosophy degree in Biology

© Qiuyue Pan 2016

Follow this and additional works at: <https://ir.lib.uwo.ca/etd>

Recommended Citation

Pan, Qiuyue, "Molecular Characterization of the Potyviral First Protein (P1 Protein)" (2016). *Electronic Thesis and Dissertation Repository*. 4115.

<https://ir.lib.uwo.ca/etd/4115>

This Dissertation/Thesis is brought to you for free and open access by Scholarship@Western. It has been accepted for inclusion in Electronic Thesis and Dissertation Repository by an authorized administrator of Scholarship@Western. For more information, please contact wlsadmin@uwo.ca.

Abstract

The *Potyvirus* genus is the largest group of plant viruses and includes many agriculturally important viruses. The potyviral genome is a single-stranded, positive RNA molecule that contains one long open reading frame (ORF) and another relatively short ORF resulting from transcriptional slippage. The resulting two polyproteins are ultimately processed into 11 mature proteins by three viral protease domains. Of these 11 viral proteins, P1, the very first of the viral polyproteins, is one of the least studied. My research was directed to investigate the functional role(s) of P1 during viral infection. In this study, the localization of P1 within plant cells was investigated and three nuclear localization signals (NLSs) were identified. No interaction was identified between P1 and itself or any of the other 10 viral proteins using yeast two hybrid (Y2H) and bimolecular fluorescence complementation (BiFC) assays. An *Arabidopsis* cDNA library was used for a Y2H screen with *Turnip mosaic virus* (TuMV) P1 as bait. Results from this screen yielded 25 putative P1-interacting host factors. Three candidates, *AtNDL2*, *AtTPR* and *AtUCP3*, were chosen for further functional characterization. Homozygous *Arabidopsis* T-DNA insertion lines for these host factors were obtained and used for TuMV infection assays. *AtNDL2*, *AtTPR* and *AtUCP3* knockout/knockdown plants demonstrated reduced susceptibility to TuMV infection, which suggests that those proteins have critical functions in the potyviral infection cycle. These three plant proteins were also recruited into TuMV 6K2 vesicles in virus-infected cells. Besides, the infection ability of *Tobacco etch virus* (TEV) mutations indicated that P1 may be involved in other non-proteolytic functions such as viral amplification or cell-to-cell transportation. The findings generated in this study may contribute to the development of novel genetic resistance against potyviruses and related plant viruses.

Keywords: potyvirus, plant viruses, P1 protein, *Tobacco etch virus* (TEV), *Turnip mosaic virus* (TuMV), nuclear localization, yeast two hybrid (Y2H), viral replication, viral replication complex (VRC), host factor(s), recessive resistance.

Acknowledgments

Firstly, my earnest thanks go out to my supervisor and mentor, Dr. Aiming Wang, for his continuous patience, guidance and encouragement which have supported me throughout my journey of obtaining a Ph.D. degree. I really appreciate that he gave me the opportunity to join his wonderful team and to work on this fantastic project. His confidence, diligence, generosity and intelligence have inspired and helped me so much during my personal growth.

I am sincerely grateful to my co-supervisor, Dr. Mark Bernards, for his assistance and support during my graduate studies at Western. Many thanks for all the stimulating discussions and valuable and constructive suggestions on my project. I wish to thank my advisory committee, Dr. Jim Karagiannis, Dr. Susanne Kohalmi and Dr. Rima Menassa, for their helpful feedback and critical advice. I couldn't have made it this far without all of their help.

I would like to express my heartfelt thanks to Jamie McNeil for technical support and also to Jamie and Dr. Cinta Hernández Sebastià for editing this thesis. Their time and assistance are genuinely appreciated. I wish to extend my warmest appreciation to the current and former members of the Wang lab. They have made my time in the lab pleasant and I am grateful for their companionship and discussions. I would also like to thank members of Agriculture and Agri-Food Canada (AAFC) for their generous assistance.

My deepest gratitude goes to my parents and my brother. Their ever-lasting understanding, love and sacrifices have supported me throughout my most stressful and frustrating times of doing research and writing this thesis.

Lastly, I wish to thank the China Scholarship Council for providing me a four-year scholarship and Western University for providing me the financial assistance to pursue my academic aspirations. The financial support from Dr. Wang throughout my studies is also gratefully acknowledged.

Table of Contents

| | |
|---|------|
| Abstract | i |
| Acknowledgments..... | ii |
| Table of Contents | iii |
| List of Tables | vii |
| List of Figures | viii |
| List of Abbreviations | x |
| Chapter 1 Introduction | 1 |
| 1.1 Overview of plant viruses | 1 |
| 1.2 <i>Potyvirus</i> , the largest plant virus group | 3 |
| 1.2.1 Genomic organization of potyviruses | 4 |
| 1.2.2 Functions of potyviral proteins | 5 |
| 1.3 The first potyviral protein, P1 | 7 |
| 1.3.1 P1 as a serine proteinase | 8 |
| 1.3.2 P1's potential function in virus amplification..... | 8 |
| 1.3.3 P1's involvement in suppression of RNA silencing..... | 9 |
| 1.3.4 P1's other functions | 10 |
| 1.4 Plant defence mechanisms against viruses and required host factors for viral infection | 10 |
| 1.4.1 Dominant resistance..... | 12 |
| 1.4.2 Recessive resistance..... | 15 |
| 1.4.3 Gene silencing and its suppression | 17 |
| 1.5 Research objectives and goals | 20 |
| Chapter 2 Materials and Methods..... | 22 |
| 2.1 Plant materials..... | 22 |

| | | |
|-----------|---|----|
| 2.2 | Virus materials | 22 |
| 2.3 | Growth conditions of bacterial and yeast strains | 27 |
| 2.4 | Gateway-based plasmid construction | 27 |
| 2.5 | <i>Agrobacterium</i> -mediated transient expression | 34 |
| 2.6 | Confocal microscopy | 34 |
| 2.7 | Y2H cDNA library construction and screen | 34 |
| 2.8 | Plant genomic DNA isolation | 35 |
| 2.9 | Plant RNA extraction | 36 |
| 2.10 | PCR | 36 |
| 2.10.1 | Reverse transcription polymerase chain reaction (RT-PCR) | 36 |
| 2.10.2 | Quantitative real-time polymerase chain reaction (qRT-PCR) | 37 |
| 2.11 | Protein extraction and Western blot | 39 |
| 2.12 | Functional analysis of <i>Arabidopsis</i> T-DNA insertion lines | 39 |
| 2.12.1 | Selection of T-DNA insertion lines | 39 |
| 2.12.2 | Screening for homozygous <i>Arabidopsis</i> T-DNA insertion lines | 39 |
| 2.12.3 | Gene expression analysis of <i>Arabidopsis</i> T-DNA insertion lines | 46 |
| 2.13 | Mechanical inoculation | 46 |
| 2.14 | Biolistic bombardment | 47 |
| Chapter 3 | Results | 48 |
| 3.1 | Subcellular localization of P1 in plant cells | 48 |
| 3.1.1 | Nuclear localization of P1 protein | 48 |
| 3.1.2 | Determination of TEV nuclear localization signals (NLSs) | 51 |
| 3.2 | Interactions between P1 and viral proteins | 56 |
| 3.3 | Y2H screen of P1 interacting host proteins | 56 |
| 3.4 | Screening of homozygous <i>Arabidopsis</i> T-DNA knockout/knockdown lines | 59 |
| 3.5 | Characterization of the <i>Arabidopsis</i> gene, <i>AtNDL2</i> | 65 |

| | | |
|----------------------------|--|-----|
| 3.5.1 | Interactions between AtNDL2 and 11 potyviral proteins | 65 |
| 3.5.2 | Verification of <i>Arabidopsis AtNDL2</i> T-DNA insertion lines | 69 |
| 3.5.3 | TuMV infection is partially inhibited in the <i>Arabidopsis AtNDL2</i> T-DNA knockout line..... | 72 |
| 3.5.4 | Co-localization of AtNDL2 with VRC | 75 |
| 3.6 | Characterization of the <i>Arabidopsis</i> gene, <i>AtTPR</i> | 76 |
| 3.6.1 | Interactions between AtTPR and 11 potyviral proteins | 76 |
| 3.6.2 | Verification of <i>Arabidopsis AtTPR</i> T-DNA insertion lines | 79 |
| 3.6.3 | TuMV infection is partially inhibited in <i>Arabidopsis AtTPR</i> T-DNA knockout lines | 82 |
| 3.6.4 | Co-localization of AtTRP with VRC | 85 |
| 3.7 | Characterization of the <i>Arabidopsis</i> gene, <i>AtUCP3</i> | 86 |
| 3.7.1 | Interactions between AtUCP3 and 11 potyviral proteins | 86 |
| 3.7.2 | Verification of <i>Arabidopsis AtUCP3</i> T-DNA insertion lines | 89 |
| 3.7.3 | Partial resistance of the <i>Arabidopsis AtUCP3</i> T-DNA knockout line to TuMV | 93 |
| 3.7.4 | Co-localization of AtUCP3 with VRC | 96 |
| 3.8 | P1 functions other than being a protease | 97 |
| Chapter 4 Discussion | | 101 |
| 4.1 | Subcellular localization of the P1 protein | 101 |
| 4.2 | Protein-protein interaction | 104 |
| 4.2.1 | P1's potyviral interaction partners | 105 |
| 4.2.2 | P1's host interaction partners..... | 106 |
| 4.3 | Host proteins identified to be involved in potyviral infection | 107 |
| 4.4 | P1 functions | 109 |
| 4.5 | Major findings and future directions..... | 109 |
| References..... | | 111 |

Curriculum Vitae 132

List of Tables

| | |
|---|-----|
| Table 1 Primers used for engineering cDNAs of TuMV infectious clone | 24 |
| Table 2 Primers used for engineering cDNAs of TEV infectious clone..... | 25 |
| Table 3 Primers for plasmid construction of TEV proteins | 29 |
| Table 4 Primers for plasmid construction of TuMV proteins..... | 30 |
| Table 5 Primers for confirmation of TEV P1 NLSs | 31 |
| Table 6 Primers for plasmid construction to express <i>Arabidopsis</i> proteins..... | 32 |
| Table 7 Other primers used for this study..... | 33 |
| Table 8 Primers for RT-PCR. | 38 |
| Table 9 Primers used for screening of <i>Arabidopsis</i> homozygous insertion lines..... | 41 |
| Table 10 Primers used for detecting gene expression of <i>Arabidopsis</i> homozygous insertion lines..... | 44 |
| Table 11 TuMV P1 interacting host candidates resulting from Y2H screen..... | 58 |
| Table 12 List of <i>Arabidopsis</i> candidate genes and corresponding T-DNA insertion lines. .. | 61 |
| Table 13 List of homozygous <i>Arabidopsis</i> T-DNA insertion lines. | 62 |
| Table 14 List of homozygous <i>Arabidopsis</i> T-DNA knockout/knockdown lines for TuMV infection assay..... | 63 |
| Table 15 List of predicted NLSs of potyviral P1s using ELM | 103 |

List of Figures

| | | |
|-----------|--|----|
| Figure 1 | Genomic organization of the genus <i>Potyvirus</i> | 5 |
| Figure 2 | Subcellular localization of P1 protein in <i>N. benthamiana</i> leaf cells | 50 |
| Figure 3 | The determination of TEV P1 NLSs | 55 |
| Figure 4 | Gene expression analysis of homozygous <i>Arabidopsis</i> T-DNA insertion mutants | 64 |
| Figure 5 | TuMV infection assay on <i>Arabidopsis</i> mutant and wild type plants..... | 65 |
| Figure 6 | Protein-protein interactions between full-length <i>Arabidopsis</i> AtNDL2 and potyviral proteins..... | 68 |
| Figure 7 | Subcellular localization of AtNDL2 in <i>N. benthamiana</i> | 68 |
| Figure 8 | Genotyping and RT-PCR analysis of <i>Arabidopsis</i> AtNDL2 T-DNA insertion lines | 71 |
| Figure 9 | TuMV infection assay on <i>Arabidopsis atndl2</i> mutant and wild type plants | 74 |
| Figure 10 | Co-localization of AtNDL2 with VRC in TuMV-infected <i>N. benthamiana</i> epidermal cells | 75 |
| Figure 11 | Protein-protein interactions between <i>Arabidopsis</i> AtTRP and TuMV proteins.... | 77 |
| Figure 12 | Subcellular localization of AtTRP in <i>N. benthamiana</i> | 78 |
| Figure 13 | Genotyping and RT-PCR analysis of <i>Arabidopsis</i> AtTPR T-DNA insertion lines | 81 |
| Figure 14 | TuMV infection assay on <i>Arabidopsis attrp</i> mutant and wild type plants..... | 84 |
| Figure 15 | Co-localization of AtTRP with VRC in TuMV-infected <i>N. benthamiana</i> leaves. | 85 |
| Figure 16 | Interactions between full-length <i>Arabidopsis</i> AtUCP3 and potyviral proteins..... | 87 |
| Figure 17 | Subcellular localization of AtUCP3 in <i>N. benthamiana</i> at 48 hpi | 88 |

| | |
|--|-----|
| Figure 18 Genotyping and RT-PCR analysis of <i>Arabidopsis AtUCP3</i> T-DNA insertion lines | 92 |
| Figure 19 TuMV infection assay on <i>Arabidopsis atucp3-1</i> and wild type plants | 95 |
| Figure 20 Co-localization of AtUCP3 with VRC in TuMV-infected <i>N. benthamiana</i> leaf tissues | 96 |
| Figure 21 Diagrammatic representation of relevant portions of the p35TEV and p35TuMV plasmids | 98 |
| Figure 22 TEV infection assay on <i>N. benthamiana</i> plants | 100 |

List of Abbreviations

| | |
|---------------|---|
| +ss | Positive-sense single-stranded |
| 6K1 | The first 6-kDa peptide |
| 6K2 | The second 6-kDa peptide |
| AAFC | Agriculture and Agri-Food Canada |
| ABA | Abscisic acid |
| ABRC | <i>Arabidopsis</i> Biological Resource Center |
| Ade | Adenine |
| ADF3 | Actin depolymerizing factor 3 |
| AGO | Argonaute |
| <i>Apaf-1</i> | Apoptotic protease activating factor-1 |
| <i>AtAct2</i> | <i>Arabidopsis Actin2</i> |
| <i>Avr</i> | Avirulence |
| BaMMV | <i>Barley mild mosaic virus</i> |
| BaYMV | <i>Barley yellow mosaic virus</i> |
| BD | Binding domain |
| BIFC | Bimolecular fluorescence complementation |
| bp | Base pair |
| cDNA | Complementary DNA |
| CED-4 | <i>Caenorhabditis elegans</i> death-4 |
| CFP | Cyan fluorescent proteins |
| CI | Cylindrical inclusion protein |
| CIYVV | <i>Clover yellow vein virus</i> |
| CMV | <i>Cucumber mosaic virus</i> |
| CP | Coat protein |
| CTAB | Cetyltrimethyl-ammonium bromide |
| CYVV | <i>Clover yellow vein virus</i> |
| DCL | Dicer-like endoribonuclease |
| DDO | Double dropout medium: SD/–Leu/–Trp |
| DIC | Differential interference contrast |
| DO | Drop out |
| dpi | Days post infiltration/inoculation |
| dsRNA | Double-stranded RNA |
| EDTA | Ethylenediaminetetraacetic acid |
| <i>eIF</i> | Eukaryotic translation initiation factor |
| endo-siRNA | Endogenous siRNA |
| ER | Endoplasmic reticulum |
| GFP | Green fluorescent protein |
| GUS | Beta-glucuronidase reporter gene |
| HC-Pro | The helper component-protease |
| His | Histidine |
| hpi | Hours post infiltration/inoculation |

| | |
|----------------|---|
| HR | Hypersensitive response |
| <i>HRT</i> | HR to TCV infection |
| HSP70 | Heat shock protein 70 |
| HSP90 | Heat shock protein 90 |
| I-2 | Resistance to <i>Fusarium oxysporum</i> |
| INA | Invasive nucleic acid |
| IPME | Plant invertase/pectin methylesterase inhibitor domain-containing protein |
| IR | Induced resistance |
| Iso | Isoform |
| ISR | Induced systemic resistance |
| JA | Jasmonic acid |
| kb | Kilobase |
| kDa | Kilodalton |
| LAR | Localised acquired resistance |
| LB | Luria-Bertani |
| Leu | Leucine |
| LKR1 | Lysine ketoglutarate reductase trans-splicing related 1 |
| LMV | <i>Lettuce mosaic virus</i> |
| LRR | Leucine-rich repeat |
| Mi-1 | Resistance to root-knot nematodes and potato aphids |
| min | Minute |
| miRNA | MicroRNA |
| MNSV | <i>Melon necrotic spot virus</i> |
| MP | Movement protein |
| mRFP | Monomeric red fluorescent proteins |
| NB | Nucleotide-binding |
| <i>NbActin</i> | <i>Nicotiana benthamiana</i> actin |
| NDL2 | Protein N-MYC downregulated-like 2 |
| NES | Nuclear export signal |
| Nla | Nuclear inclusion "a" protein |
| Nlb | Nuclear inclusion "b" protein |
| NLS | Nuclear localization signal |
| NoLS | Nucleolar localization signal |
| nt | Nucleotide |
| ORF | Open reading frame |
| P1 | The first protein |
| P1a | The first copy of P1 |
| P1b | The second copy of P1 |
| P3 | The third protein |
| P3N-PIPO | PIPO as a translational fusion with the N-terminal of P3 |
| p50 | 50-kDa helicase/replicase fragment |
| PABP | Poly(A) binding proteins |
| PAGE | Polyacrylamide gel electrophoresis |
| PAMP/MAMP | Pathogen/microbe-associated molecular pattern |
| PCD | Programmed cell death |
| PCR | Polymerase chain reaction |

| | |
|-------------|---|
| PD | Plasmodesmata |
| PFK4 | 6-phosphofructokinase 4 |
| PIPO | Pretty Interesting Potyvirus ORF |
| PISPO | Pretty Interesting Sweet potato Potyviral ORF |
| PPV | <i>Plum pox virus</i> |
| pri-miRNA | Primary-miRNA |
| PRR | Pathogen/pattern-recognition receptor |
| PRSV-P | <i>Papaya ringspot virus</i> type P |
| PSbMV | <i>Pea seed-borne mosaic virus</i> |
| PTGS | Post-transcriptionally gene silencing |
| PTI | PAMP-induced immunity |
| <i>Pto</i> | Resistance to <i>Pseudomonas syringae</i> |
| PVA | <i>Potato virus A</i> |
| PVMV | <i>Pepper veinal mottle virus</i> |
| PVX | <i>Potato virus X</i> |
| PVY | <i>Potato virus Y</i> |
| QDO | Quadruple dropout medium: SD/–Ade/–His/–Leu/–Trp |
| QDO/X/A | SD/–Ade/–His/–Leu/–Trp supplemented with X-a-Gal and Aureobasidin A |
| qRT-PCR | Quantitative real-time polymerase chain reaction |
| <i>R</i> | Resistance |
| <i>RCY1</i> | Resistance to CMV infection |
| RdRp | RNA-dependent RNA polymerase |
| RISC | RNA-induced silencing complex |
| RNA | Ribonucleic acid |
| RNAi | RNA interference |
| ROI | Oxygen intermediates |
| <i>RPM1</i> | Resistance to <i>P. syringae</i> expressing AvrRPM1 |
| <i>PPP8</i> | Resistance to <i>Hyaloperonospora arabidopsidis</i> , isolate Emco5 |
| <i>RPS2</i> | Resistance to <i>P.syringae</i> expressing AvrRPT2 |
| RSS | RNA silencing suppression |
| RT-PCR | Reverse transcription polymerase chain reaction |
| <i>Rx</i> | Resistance to PVX infection |
| RYMV | <i>Rice yellow mottle virus</i> |
| <i>s</i> | Second |
| SA | Salicylic acid |
| SAR | Systemic acquired resistance |
| SD | Synthetic defined |
| SDS | Sodium dodecyl sulfate |
| SEL | Size exclusion limit |
| siRNA | Small/short interfering RNA |
| SMV | <i>Soybean mosaic virus</i> |
| SPFMV | <i>Sweet potato feathery mottle virus</i> |
| ssRNA | Single-stranded RNA |
| SYSV | <i>Shallot yellow stripe virus</i> |
| TCV | <i>Turnip crinkle virus</i> |
| TDO | Triple dropout medium: SD/–His/–Leu/–Trp |

| | |
|------|---|
| TEV | <i>Tobacco etch virus</i> |
| TGS | Transcriptional gene silencing |
| TIR | <i>Drosophila Toll</i> and mammalian interleukin-1 receptor |
| TMV | <i>Tobacco mosaic virus</i> |
| TPR | Tetratricopeptide repeat |
| Trp | Tryptophan |
| TRSV | <i>Tobacco ringspot virus</i> |
| TuMV | <i>Turnip mosaic virus</i> |
| UCP | Uncharacterized protein |
| UTR | Untranslated region |
| VIGS | Virus-induced gene silencing |
| VPg | Viral genome-linked protein |
| VRC | Viral replication complex |
| VSR | Viral suppressor of RNA silencing |
| WSMV | <i>Wheat streak mosaic virus</i> |
| WT | Wild type |
| WYMV | <i>Wheat yellow mosaic virus</i> |
| Y2H | Yeast two hybrid |
| YFP | Yellow fluorescent protein |
| YPDA | YPD medium supplemented with adenine hemisulfate |

Chapter 1 Introduction

1.1 Overview of plant viruses

Viruses were not distinguished as an individual pathogen group until the late nineteenth century (Beijerinck, 1898, as cited in Hull, 2013), despite numerous historic records and paintings. The birth of virology is generally believed to be the discovery of Beijerinck, describing the infectious agent extracted from tobacco (*Tobacco mosaic virus*, TMV) as "*contagium vivum fluidum*" (Latin for contagious living fluid). Judging from the name, viruses are microscopic particles smaller than bacteria yet, interestingly, the largest identified virus, named mimivirus, possesses a genome even larger than that of some bacteria and can even be infected by another virus (La Scola et al., 2003; La Scola et al., 2008; Pearson, 2008). This fact makes viruses more alive than ever and causes great excitement in virology.

Nevertheless, in general, viruses are still defined as obligate, miniscule and acellular parasites, that exclusively live and multiply in living host cells. One of the common characteristics shared by most, if not all viruses, is their relatively small genome (usually 3~15 kb), which typically encodes a very limited number of essential proteins. Due to their simple structural and physicochemical properties, viruses must hijack cellular pathways and manipulate necessary components at every stage of their infection cycle (Nelson and Citovsky, 2005; Thresh, 2006; Roossinck, 2010; Wang, 2015). Thus, intimate interactions between viral genomes/genome-encoded products and host factors are required for a successful infection (Verma et al., 2014). Few viruses can stay viable for long outside of living tissues and their survival mainly depends on the continuous availability of host supplies. Viral infection is a very complicated process. For example, in the case of positive-sense single-stranded (+ss) RNA viruses, which make up the great majority of known viruses, the viral life cycle can be divided into several major steps, including viral particle disassembly, viral genome translation, viral replication

complex (VRC) formation, virion assembly, cell-to-cell movement, and long-distance transport (Thivierge et al., 2005; Pallas and García, 2011; Verma et al., 2014).

Viruses are known to have the ability to infect a wide range of organisms, such as plants, animals, fungi, algae, bacteria, and even other viruses. Plant viruses usually establish systemic infections in their hosts and persist throughout the life of the infected plants (Faoro and Gozzo, 2015). Viral transmission is largely reliant on insect, mite, fungi or nematode vectors. Among them, aphids are the most common group of plant virus vectors. The acquisition phase is in which an aphid feeds on a virus-infected plant and acquires sufficient viral particles to transmit the virus. It lasts seconds to days depending on the virus type. When the aphid migrates to another healthy host to feed, the retention (transmission) period begins. Viruses are classified as non-persistent and persistent according to the length of transmission time. Most known aphidborne viruses are non-persistent. Non-persistent viruses can infect a healthy plant immediately but the retention time is only a few minutes (Ng and Perry, 2004; Hull, 2013). Additionally, viruses can also be spread through mechanical inoculation using virus-containing sap isolated from contagious materials, as well as through pollen and seeds from infected plants (Hull, 2009; Hull, 2013).

Most agricultural crops are under the threat of various virus diseases, and plant viruses are one of the most important plant pathogens. Infected plants may display a variety of symptoms ranging from mild to catastrophic, such as yellowing, stunting, leaf curling, wilting, mosaic, ringspot, necrosis, and developmental abnormalities of the flower or fruit, resulting in either significant global damage or severe local losses (Thresh, 2006; Hull, 2013; Verma et al., 2014; Yadav and Khurana, 2015). Ironically, viral infections in some plants are not regarded negatively. For instance, tulip petals with striped patterns caused by viruses were prized as special varieties and priced at a premium (Hull, 2013). However, at least one-tenth of worldwide food production is lost to plant diseases, and the total cost of global crop damages is estimated as \$60 billion annually

(Strange and Scott, 2005; Thresh, 2006; Hull, 2013). Viruses are considered the second most notorious contributor to these losses after fungi. More than 700 known plant viruses can cause dreadful diseases and often have a wide spectrum of hosts (Strange and Scott, 2005).

Once systemic infection is established, plant viruses are rarely eliminated naturally from their hosts and there are limited recovery phenomena equivalent to that of the immunological response of animals (Thresh, 2006; Ziebell, 2016). It is hard to counteract viral pathogens after infection starts and there have been no efficient therapeutic approaches available to fight plant virus diseases in the field. Thus, preventative measures have become the most economical and effective strategy to control viral diseases. Recently, one of the most desired qualities in current crop selection is resistance to damage by pests or parasites, specifically viral pathogens (Thompson and Tepfer, 2010; Wang, 2013; Rosa and Falk, 2014). Modern breeding programs, which use advanced molecular biology techniques and biotechnology methods to improve crops with desirable traits, are playing decisive roles in the success of today's agriculture (Ma et al., 2015).

1.2 *Potyvirus*, the largest plant virus group

The *Potyvirus* genus belongs to the family *Potyviridae*. Potyviruses, which account for approximately 30% of known plant viruses, constitute the largest group of plant viruses including many agriculturally important viruses, e.g., *Turnip mosaic virus* (TuMV), *Tobacco etch virus* (TEV), *Soybean mosaic virus* (SMV), *Potato virus Y* (PVY) and *Plum pox virus* (PPV) (Atreya, 1992; Riechmann et al., 1992; Rajamäki et al., 2009; Verma et al., 2014; Rybicki, 2015). Many potyviruses can be efficiently transmitted by aphids in a non-persistent manner and have a worldwide distribution, making them difficult to control (Rybicki, 2015). Notably, potyviruses are considered one of the most important viral groups affecting vegetables worldwide, specifically necrotic PVY isolates, which are still potentially responsible for extraordinary economic losses in

various vegetable crops such as potato, tobacco, tomato and pepper (Scholthof et al., 2011; Rybicki, 2015). PPV, which causes sharka, is the most devastating viral disease of stone fruit crops, specifically in Europe (Clemente-Moreno et al., 2015). TuMV is another widespread and economically important potyvirus. TuMV was ranked amongst the five most devastating virus infecting field-grown vegetables worldwide (Tomlinson, 1987; Sanchez et al., 2003). In addition to its wide range of crops and other plants which have been found naturally, TuMV is able to infect model plants, *A. thaliana* and *N. benthamiana*, which makes TuMV an ideal model to research host-potyvirus interactions from both host and virus perspectives (Walsh and Jenner, 2002). TEV, which can infect *N. benthamiana*, has also been traditionally used as one of the model viruses to study potyvirus molecular biology and plant-virus interactions (Bedoya and Daròs, 2010). Unlike some other potyviruses, like some cultivars of PPV, which are seed-borne, neither TuMV nor TEV is known to be transmitted by seeds (Sanchez et al., 2003; Bedoya and Daròs, 2010; Clemente-Moreno et al., 2015).

1.2.1 Genomic organization of potyviruses

Potviruses produce flexuous, non-enveloped, rod-shaped particles 680~900 nm long and 11~15 nm wide. They are composed of a +ss RNA, about 10 kb long, surrounded by approximately 2000 copies of coat protein (CP) units. The RNA genome carries a viral genome-linked protein (VPg) covalently bound to its 5' end, and a poly(A) tail at its 3' end (Figure 1, Yambao et al., 2003). The potyviral genome contains a long open reading frame (ORF) that translates into a long polyprotein of about 350 kDa in mass. This protein is ultimately processed by three different virus-encoded proteases into 10 mature proteins: the first protein (P1), the helper component-protease (HC-Pro), the third protein (P3), the first 6-kDa peptide (6K1), the cylindrical inclusion protein (CI), the second 6-kDa peptide (6K2 or 6K), the nuclear inclusion "a" protein (NIa), which is further cleaved into the VPg protein (NIa-VPg or VPg) and the protease (NIa-Pro or NIa), the nuclear inclusion "b" protein (NIb) and CP (Adams et al., 2005a). In 2008, a novel ~25 kDa viral protein termed P3N-PIPO (Pretty Interesting Potyvirus ORF),

resulting from a +2 frameshift in the P3 coding sequence, was reported (Chung et al., 2008). This short ORF is well-conserved among all members of the *Potyviridae* family. More recently, a third truncated ORF called PISPO (Pretty Interesting Sweet potato Potyviral ORF) was predicted by bioinformatics analysis within the P1 cistron of four potyviruses infecting sweet potato, all within the monophyletic group of *Sweet potato feathery mottle virus* (SPFMV) (Clark et al., 2012; Olsper et al., 2015; Mingot et al., 2016; Untiveros et al., 2016), which suggests PISPO is not conserved amongst potyviruses.

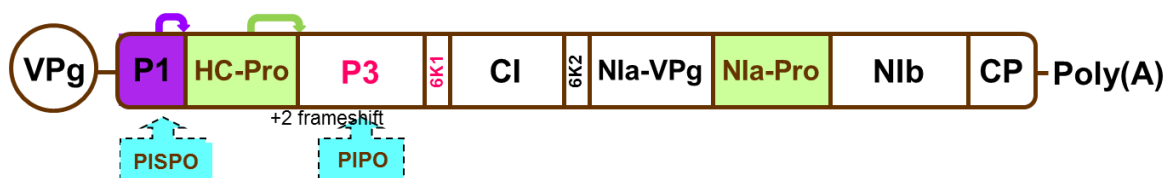


Figure 1 Genomic organization of the genus *Potyvirus*. The potyviral genomic RNA carries a VPg covalently bound to its 5' end, and a poly(A) tail at its 3' end. It encodes ten mature proteins produced by proteolytic cleavage (arrow heads) of the polyprotein translated from a long open reading frame (ORF). A short peptide named PIPO results from a +2 frameshift in the P3 cistron. A third truncated protein named PISPO results from P1 cistron in four sweet potato-infected potyviruses. HC-Pro is self-cleaved at its C-termini.

1.2.2 Functions of potyviral proteins

Most, if not all, potyviral proteins are believed to be multifunctional and their roles in the infection cycle have been revealed in extensive studies on various potyviruses. Usually, the functionality of a protein from one potyvirus has been shown to be

conserved within other potyvirus members due to the high genomic similarity within the genus (Urcuqui-Inchima et al., 2001).

Potyviral genome amplification requires two fundamental processes, viral RNA translation for the synthesis of virus-encoded proteins, and RNA replication. Viral replication is associated with plant membrane systems, such as the endoplasmic reticulum (ER), which are involved the formation of VRC containing viral RNA, virus-encoded replication related proteins and host factors (Cotton et al., 2009; Verchot, 2014; Heinlein, 2015). So far, HC-Pro, P3, CI, 6K2, VPg and NIb have been shown to participate in viral genome replication (Riechmann et al., 1992; Fernández et al., 1997; Kasschau et al., 1997; Kasschau and Carrington, 1998; Puustinen and Mäkinen, 2004; Cui et al., 2010), while some other viral proteins have been suggested to be part of VRC, like P1 (Merits et al., 1999). 6K2 plays a crucial role in virus replication through the anchoring of VRCs to the ER (Schaad et al., 1997) and induction of the unfolded protein responses (Zhang et al., 2015b). Due to the lack of a 5'-cap structure in potyvirus RNA, VPg has been suggested to serve this primary function by binding the 5'-termini of potyviral RNA to host translation factors, i.e., eIF4E and eIF(iso)4E (Léonard et al., 2004). The 6K2-VPg-NIa-Pro complex is found within vesicular compartments (the site of potyviral replication) derived from the ER (Jiang and Laliberté, 2011). NIb, as the RNA-dependent RNA polymerase (RdRp), is the core peptide that catalyzes the synthesis of potyviral RNA (Buck, 1996). Each of the vesicles initiates from a single genome, thus showing that the existence of all viral proteins within the vesicles are generated through translation within the vesicular compartments (Cotton et al., 2009).

Another essential process of the virus life cycle is viral particle movement, which can be divided into short- and long-distance. Potyviruses move intercellularly by modifying the size exclusion limit (SEL) of plasmodesmata (PD) and infect systemically through phloem by interacting with host proteins and several chaperones. Usually, viral

movement is directed by the movement protein (MP), but in the case of potyviruses, there can be several movement-related proteins, rather than a specific one. HC-Pro, P3N-PIPO, CI, VPg and CP have all been shown to be involved with viral movement (Kasschau et al., 1997; Carrington et al., 1998; Wei et al., 2010; Heinlein, 2015). These MPs serve many biological functions: binding the viral RNA, directing the viral genome to PD, gating PD, transport through PD, and trafficking through phloem (Urcuqui-Inchima et al., 2001; Cotton et al., 2009; Solovyev and Savenkov, 2014; Heinlein, 2015). TuMV P3N-PIPO is a PD-located protein and facilitates virus movement by targeting CI to PD (Wei et al., 2010; Wei et al., 2013). CI can direct the viral transport complex to PD through intracellular translocation (Carrington et al., 1998). Subsequently, CP and HC-Pro have the ability to increase the SEL of PD (Rojas et al., 1997).

In addition, HC-Pro is also crucial for long-distance movement by suppressing posttranscriptional gene silencing mechanisms in host plant (Maia et al., 1996; Kasschau et al., 2003; Roth et al., 2004) and aphid-transmission (Blanc et al., 1997; Blanc et al., 1998). 6K2 is also involved in viral long-distance movement and symptom induction (Spetz and Valkonen, 2004). CP plays an important functional role in aphid-transmission (Blanc et al., 1997). 6K1 and P3 have been shown to be pathogenicity determinants and part of VRCs (Urcuqui-Inchima et al., 2001; Cui and Wang, 2016).

1.3 The first potyviral protein, P1

Interestingly, P1, the first viral protein that is translated, is one of the least studied potyviral proteins. P1 protein was the last identified peptidase after HC-Pro and NIa (Verchot et al., 1991). In the last 25 years, although massive amounts of information on P1 have been accumulated and assimilated, P1 remains largely mysterious. The molecular mechanisms underlying P1-associated biological phenomena are still elusive, and the exact role of P1 in the potyvirus life cycle has yet to be determined.

1.3.1 P1 as a serine proteinase

P1 is a serine-type proteinase that catalyzes auto-proteolytic cleavage at a Tyr-Ser dipeptide site between itself and HC-Pro (Verchot et al., 1991). This cleavage is required for viral infectivity (Verchot and Carrington, 1995b; Verchot and Carrington, 1995a). Serine, aspartic and cysteine proteinases are not unusual and have been discovered in both prokaryotic and eukaryotic organisms (Rawlings and Barrett, 1993; Barrett, 1994). All virus-encoded proteinases are endopeptidases and play significant roles during viral infection cycles because of their ability to process viral polypeptides and involvement in a wide range of biological reactions (Barrett, 1994; Rohožková and Navrátil, 2011). As a group, serine peptidases are characterized by the presence of an active site domain that contains a Ser in addition to two other amino acid residues, Asp and His (Adams et al., 2005b; Valli et al., 2007). The catalytic triad in P1, which is located at the C-terminal region, is conserved among all potyviral P1s, but P1 protein is still the most divergent in potyviruses with regard to both length and amino acid sequence (Valli et al., 2007). The conserved His and Asp residues are present upstream of the reactive Ser. The substitution of His or Ser residues abolishes the proteolytic activity of P1 (Verchot et al., 1991; Verchot and Carrington, 1995b). It has been suggested that the non-conservative N-terminal region of the TEV P1 is dispensable for its known biological functions, such as protease activity and viral amplification and movement (Verchot et al., 1992; Verchot and Carrington, 1995a; Verchot and Carrington, 1995b; Moreno et al., 1998; Moreno et al., 1999; Rajamäki et al., 2005).

1.3.2 P1's potential function in virus amplification

Verchot and Carrington (1995b) suggested that the TEV P1 protein operated *in trans* as an accessory, or regulatory factor, to enhance viral genome amplification. However, it is not clear whether P1 functions directly through interaction with VRC components or the viral genome, or indirectly by stimulating viral RNA translation during the RNA replication process. The RNA binding ability of P1 (Brantley and Hunt, 1993;

Soumounou and Laliberté, 1994) may play a critical role in this proposed accessory function. Arbatova et al. (1998) revealed the association between P1 and cytoplasmic inclusion bodies, supporting P1's possible participation in virus replication. The interactions of P1 with other viral proteins, such as CI, were identified *in vitro*, further suggesting that P1 might be recruited to become a component of the VRC through interactions with other viral replicase proteins (Merits et al., 1999). Consistently, Martínez and Daròs (2014) found that P1 binds the host 60S ribosomal subunits in the TEV-infected cells and likely stimulates translation of viral proteins during the early stages of potyviral infection.

1.3.3 P1's involvement in suppression of RNA silencing

Accumulated evidence suggests that viruses from different genera of the *Potyviridae* family may have evolved independently to establish different viral proteins with RNA silencing suppression (RSS) capacity. It is recognized that most members from the *Potyvirus* and *Rymovirus* genera encode HC-Pro to suppress RNA silencing (Anandalakshmi et al., 1998; Llave, 2010). For these viruses, although P1 itself is not a viral suppressor of RNA silencing (VSR), it acts in conjunction with and enhances the RSS function of HC-Pro (Kasschau et al., 2003). Such an effect on RSS may be related to its accessory function of stimulating viral multiplication. In order to understand the mechanism(s) behind P1's function in overcoming host defences, the involvement of P1 in the interaction between potyvirus and its host was investigated using several potyviruses (Anandalakshmi et al., 1998; Tavert-Roudet et al., 1998; Mäki-Valkama et al., 2000b; Mäki-Valkama et al., 2000a). The RSS activity of P1/HC-Pro seems to act at the post-transcriptional level (Pruss et al., 1997; Kasschau and Carrington, 1998). Recently, Pasin et al. (2014) provided evidence that the hypervariable region of P1 that precedes the protease domain negatively regulates P1 proteolytic activity *in vitro* and removal of the P1 protease antagonistic regulator accelerates early replication and enhances symptom severity in PPV-infected leaves. Thus, P1 may regulate viral infection by fine modulation of the viral protease activity to keep viral amplification

below host detrimental levels, and to maintain higher long-term replicative capacity (Pasin et al., 2014).

Some SPFMV-related potyviruses were predicted to encode a novel frame-shift protein, P1N-PISPO, and this protein has proven to be a potent player in RSS (Clark et al., 2012; Mingot et al., 2016). In the case of some viruses in the *Potyviridae* family that do not encode HC-Pro (e.g., species in the genera *Tritimovirus* and *Poacevirus*), P1 plays the RSS function (Tatineni et al., 2012; Young et al., 2012). Interestingly, ipomoviruses suppress host gene silencing using either P1 or the second copy of P1, a tritimo-like P1b (Valli et al., 2006; Mbanzibwa et al., 2009; Giner et al., 2010; Carbonell et al., 2012).

1.3.4 P1's other functions

In addition to functions discussed above, P1 is thought to make great contributions to the successful adaptation of the potyviruses to a wide range of host species, thanks to its high variability (Brigneti et al., 1998; Salvador et al., 2008). It has been shown that point mutations in P1 of *Clover yellow vein virus* (CYVV) confer CYVV the ability to break eIF4E-mediated recessive resistance (Nakahara et al., 2010). It is also reported that some regions of P1 can tolerate short or even long insertions without interfering with virus infection (Kekarainen et al., 2002; Rajamäki et al., 2005).

Notwithstanding progress from these studies, the exact role of P1 in the potyviral life cycle remains to be determined and the molecular mechanisms underlying the above-described P1-associated biological phenomena are still relatively vague.

1.4 Plant defence mechanisms against viruses and required host factors for viral infection

Unlike animals, plants are sessile and cannot flee from intruders. Thus, they have developed various countermeasure mechanisms to ward off pathogen attackers, such as viruses (Palukaitis, 2011; Srivastava and Prasad, 2014; Sanfaçon, 2015). Passive protection through waxy cuticular “skin” layers and anti-microbial compounds normally

protects plants against most pathogens that are not specialized to attack a specific host (Dangl and Jones, 2001). Some plants, in which a virus cannot replicate, either in protoplasts or in plant cells, are considered to be immune or non-host. In hosts or infectible plants, viruses are able to infect and multiply in protoplasts. Cases in which plants can prevent either viral replication, or spread to neighboring cells, are called extreme resistance. These resistant plants restrict viral infection into a small area, and necrosis patterns may develop. Susceptible plants allow viral replication as well as systemic movement (Hull, 2013). Plant resistance can be divided into two main groups, genetic resistance and induced resistance (IR). The first category is pre-existent in the plant and can limit viral ability of replication and/or transmission in the host. The second resistance type is not active in non-attacked plants and is only induced by pathogen attack, stresses or chemicals. Nevertheless, the difference between these two types of resistance is not completely clear (Palukaitis et al., 2008; Ziebell, 2016).

Innate immunity in plants relies on specialized immune receptors by which plants can detect and defend themselves against broad classes of microbes (Zipfel, 2008). One group of receptors is formed by the transmembrane pathogen/pattern-recognition receptors (PRRs), which detect pathogen/microbe-associated molecular patterns (PAMPs/MAMPs) (Pålsson-McDermott and O'Neill, 2007). PRRs are often highly conserved in both structure and function, while PAMPs are also very conservative and correlate with a wide range of pathogens (Nicaise et al., 2009; de Ronde et al., 2014). PAMP-triggered immunity (PTI), a plant's first active response to pathogens, is generally "low-impact" and effective in fighting against most pathogens (Chisholm et al., 2006). The other group, containing the polymorphic disease resistance (R) proteins, is relatively "high impact" (Jones, 2006; Nicaise et al., 2009). Amongst *R* genes, dominant genes typically trigger active defence via the initiation of extreme resistance or hypersensitive response (HR), which is a type of programmed cell death (PCD) occurring around the infection site, whereas recessive genes are usually associated with the loss or mutation of host factors required for parasitic infection cycle (Zaitlin and

Palukaitis, 2000; Robaglia and Caranta, 2006). In the last few decades, enormous progress in isolating host factors required for successful infection by pathogens has been achieved at an unexpected scale and extent (Bruening, 2006; Palukaitis and MacFarlane, 2006; Wang, 2015). Significant value can be added through the use of identified *R* genes in traditional breeding or genetic engineering (Gottula and Fuchs, 2009; Reddy et al., 2009; Thompson and Tepfer, 2010; Galvez et al., 2014), since plant genetic resistance against viruses is regarded as the most effective and common way to control virus replication, spread and symptom induction (Kang et al., 2005a).

Overall, understanding the mechanisms underlying plant viral defence, as well as identification of host factors, will provide the foundation for selection of new sources of natural resistance and the design of engineered resistance (Kang et al., 2005a; Maule et al., 2007; Carr et al., 2010).

1.4.1 Dominant resistance

About half of the *R* genes identified so far are dominant and monogenic. Dominant *R* proteins are highly variable and traditionally believed to confer resistance through a race-specific or gene-for-gene method of targeting the corresponding dominant avirulence (*Avr*) effector proteins encoded by pathogens, including viruses (Maule et al., 2002; Moffett, 2009). Thus, the consequence of an attempted infection is mainly determined by the genotypes of both the parasite and the host (Kopp et al., 2015). The *R/Avr* interaction usually activates HR at the pathogen's infection site. This is referred to as local acquired resistance (LAR), and is followed by systemic acquired resistance (SAR), which is no longer restricted to the inoculation site but also spreads into non-inoculated plant tissue and is effective against a broad range of pathogens (Durrant and Dong, 2004; Caplan and Dinesh-Kumar, 2006). Salicylic acid (SA) appears to be involved in the HR and may play a functional role in localizing the virus (Hammerschmidt, 2009).

To date, the majority of known dominant *R* genes belong to one of the largest and most variable gene families, the NB-LRR family, so named because members of this family possess a C-terminal transmembrane and extracellular leucine-rich repeat (LRR), a central conserved nucleotide-binding (NB) region and, usually, a variable N-terminal domain (Ritzenthaler, 2005; Padmanabhan et al., 2009; Sacco and Moffett, 2009). Although a few have been indicated as serving in the downstream signaling pathways leading to HR-PCD, most NB-LRR proteins function as pathogen receptors and have demonstrated the ability to bind diverse cellular recognition co-factors/baits (Tameling and Joosten, 2007). The LRR domains of NB-LRRs are responsible for the mediation of *R/Avr* recognition specificity by co-opting with baits in many, or most, cases (Rafiqi et al., 2009). Since the LRR domains are flexible to tolerate duplications and deletions of entire repeats, they have the capacity to evolve new interaction specificities, which allow the activated resistance to respond to other types of pathogens (Collier and Moffett, 2009). In other words, NB-LRR proteins can induce reactions against completely different parasites once resistance has been initiated. For instance, *RPM1* (resistance to *Pseudomonas syringae* expressing AvrRPM1) product was reported to bind multiple pathogen ligands (Bisgrove et al., 1994), and some members of the *Arabidopsis RPP8/HRT* family, like *RPP8* (resistance to *Hyaloperonospora arabidopsidis*, isolate Emco5), *HRT* [HR to *Turnip crinkle virus* (TCV) infection] and *RCY1* [resistance to *Cucumber mosaic virus* (CMV) infection], have been shown to confer resistance to both oomycete and virus (McDowell et al., 1998; Cooley et al., 2000; Takahashi et al., 2002). However, the interaction between NB-LRR and bait proteins still requires specificity on certain levels, hence the gene transfer between different species may fail to work properly due to the incompatibilities of altered recognition models (Palukaitis and MacFarlane, 2006). On the other hand, the NB region found in plant NB-LRR proteins has been shown to be a molecular switch and regulator of R protein activity (Martin et al., 2003). The NB region is now separated into a core NB site combined with another two ARC domains, ARC1 and ARC2, which are so defined because of their similarities with human Apaf-1 (Apoptotic protease

activating factor-1) protein, plant R proteins and CED-4 (*Caenorhabditis elegans* death-4) (Van Der Biezen and Jones, 1998). The NB-ARC domain contains the P-loop which is specific for binding nucleotides (ATP/ADP) and hydrolysis. Several NB-LRR proteins have proven to have this ability, like I-2 (resistance to *Fusarium oxysporum*), Mi-1 (resistance to root-knot nematodes and potato aphids) and N (Tameling et al., 2002; Ueda et al., 2006). It is believed that the nucleotide is buried at the interface of the pocket formed by the three subdomains (Rafiqi et al., 2009). Many dominant *R* genes have been cloned and studied in detail. For instance, the first isolated antiviral *R* gene is the *N* gene from tobacco that mediates resistance to *Tobacco mosaic virus* (TMV) (Whitham et al., 1994; Les Erickson et al., 1999). Sequence analysis of the *N* gene revealed that it encodes a 131 kDa protein with a subclass NB-LRR domain which contains a *Drosophila Toll* and mammalian interleukin-1 receptor (TIR) region at the N-terminus (TIR-NB-LRR). The *N* protein has been clearly demonstrated to directly interact with a 50 kDa replicase fragment (p50) that contains the putative helicase domain required to initiate the HR at TMV infection (Padgett and Beachy, 1993; Ueda et al., 2006). And, a plausible but unproven model has been proposed to explain the TMV recognition mechanism in tobacco. Upon infection with TMV, the *N* protein is targeted and forms a complex with ATP, which enhances ATP hydrolysis. The ATP/*N* factor complex then changes its conformation, probably from an ATP-bound form to an ADP-bound form, thus facilitating further interaction with other factor(s) to activate the downstream signaling pathway (Ueda et al., 2006).

Although the precise mechanism behind the interactions of viral proteins and antiviral *R* gene-encoded proteins is not clear, various models have been postulated. For example, it has been suggested that the recognition is largely based on protein-protein interaction rather than the specific function of viral proteins. The most commonly identified counterpart of *R* proteins in viruses is the CP protein, which has been determined to interact with several antiviral *R* proteins, such as proteins encoded by *R* genes *Rx1*, *Rx2* [resistance to *Potato virus X* (PVX) infection], *N*, *HRT*, and *RCY1* (Saito et al., 1989;

Bendahmane et al., 1995; Zhao et al., 2000; Takahashi et al., 2001). Another noteworthy model involves R protein-signalling complexes. As most proteins cooperate in complexes, it is optimal for them to co-evolve in plant disease response (Dangl and Jones, 2001; Belkhadir et al., 2004). One of these R interaction partners has been identified as heat shock protein 90 (HSP90), which is a highly conserved eukaryotic ATP-dependent chaperone that mediates protein folding and activation (Picard, 2002; Liu et al., 2004). HSP90 has proven to be indispensable for resistance mediated by *R* genes, like *RPM1*, *RPS2* (resistance to *P. syringae* expressing AvrRPT2) and *Pto* (resistance to *P. syringae*) (Lu et al., 2003; Takahashi et al., 2003).

1.4.2 Recessive resistance

As RNA viruses, such as potyviruses, encode only a limited number of essential proteins (CPs, MPs, RdRps, etc.), they must rely on host proteins (also host factors) to establish infection (Wang, 2015). These “host factors” may have diversified during the course of evolution and in some cultivars or species the variants cannot be utilized by the viruses, leading to incompatibility for infection. This has been defined as passive/recessive resistance because no activity is required by the plant host (Fraser and Van Loon, 1986). Unlike dominant resistance targeting parasites in an active recognition manner, recessive resistance operates by a mechanism in which the lack of required host factors for the viral life cycle make replication impossible (Faoro and Gozzo, 2015). In general, dominant resistance is more easily broken by plant RNA viruses than by other types of plant parasites. And, therefore, recessive resistance is more common for plant viruses while dominant *R* genes contribute to the majority of plant resistance sources against fungi or bacteria (Diaz-Pendon et al., 2004; Ritzenthaler, 2005; Takács et al., 2014). So far, about half of the ~200 reported plant *R* genes against viruses are recessively inherited, which makes the use of such genes a novel source in breeding programs to control plant viral diseases (Kang et al., 2005a).

Moreover, recessive *R* factors are over-represented in the interaction between potyviruses and their plant hosts. More than 50% of the recessive *R* genes have been identified as mediating resistance against potyviruses, while other plant viruses interact with only one-fifth of recessive *R* genes (Wang and Krishnaswamy, 2012). Further analysis has indicated that most of the recessive resistance genes to potyviruses encode translation initiation factors of the *4E* (*eIF4E*) and *4G* (*eIF4G*) families. These include *pvr1/pvr2* against PVY (*Potyvirus*) in peppers (Ruffel et al., 2002; Kang et al., 2005b), *mo1* against *Lettuce mosaic virus* (LMV, *Potyvirus*) in lettuce (Nicaise et al., 2003), *sbm1* against *Pea seed-borne mosaic virus* (PSbMV, *Potyvirus*) in peas (Gao et al., 2004), *pot-1* against PVY and TEV (*Potyvirus*) in tomatoes (Ruffel et al., 2005), *rym4/5* against *Barley yellow mosaic* and *Barley mild mosaic virus* (BaYMV and BaMMV, *Potyvirus*) in barley (Stein et al., 2005), *rymv1* against *Rice yellow mottle virus* (RYMV, *Sobemovirus*) in rice, and *nsv* against *Melon necrotic spot virus* (MNSV, *Carmovirus*) in melons (Nieto et al., 2006). Even though most potyviruses seem to require one specific *eIF4E* isoform for replication in a specific host, others are able to utilize more than one of them. For instance, *Pepper veinlet mottle virus* (PVMV) can use both *eIF4E* and *eIF(iso)4E* to achieve pepper infection whereas PVY and TEV need one specific *eIF4E* isoform (Ruffel et al., 2006).

Extensive studies have indicated that virus infection is associated with the direct interaction between *eIF4E/eIF(iso)4E* and potyviral VPg, which appears to control both qualitative and quantitative aspects of viral multiplication (Moury et al., 2014). This physical interaction may have served as the selective force which led to the coevolution between these two proteins in the arms race between plants and potyviruses (Robaglia and Caranta, 2006). Most resistance-breaking potyvirus isolates have been characterized to compensate for the interruption in the VPg-*eIF4E/eIF(iso)4E* interaction, e.g. PVY (Moury et al., 2004), TuMV (Charron et al., 2008) and LMV (Abdul-Razzak et al., 2009). Although its exact function has not yet been elucidated, the VPg from all those isolates possesses one or more mutations in the middle region of the protein, which is

thought to be exposed on the surface, suggesting that this region is involved in the interaction with *eIF4E* isoforms (Roudet-Tavert et al., 2007). It has been proposed that the VPg-eIF4E/eIF(iso)4E complex may play a direct role in potyvirus RNA translation and replication (Thivierge et al., 2008; Jiang and Laliberté, 2011). Another plausible hypothesis is that the VPg-eIF4E/eIF(iso)4E complex may disrupt nuclear functions since it localizes in subnuclear structures during TuMV infection (Beauchemin et al., 2007). On the other hand, amino acid substitutions in two other potyviral proteins have been described to be associated with the breakdown of *eIF4E/eIF(iso)4E*-mediated resistances: CI against LMV in lettuce (Abdul-Razzak et al., 2009) and P1 against *Clover yellow vein virus* (CIYVV) in peas (Nakahara et al., 2010). It is striking to note that a single deletion of *eIF4E* isoforms has no detectable impact on plant growth, which indicates functional redundancy of *eIF4Es*. Nevertheless, this functional overlay does not expand to their role in virus replication (Robaglia and Caranta, 2006; Sorel et al., 2014).

1.4.3 Gene silencing and its suppression

Unlike mammals, plants lack interferon and antibody-based immune systems, so “recovery” after viral infection was originally thought to be impossible. However, a recovery phenomenon was first reported in the year of 1928 (Wingard, 1928). Wingard observed that only the initially infected leaves of tobacco plants showed symptoms after being attacked by *Tobacco ringspot virus* (TRSV) and that the newly emerged leaves somehow became immune to the virus and resistant to later infection. However, the recovery mystery was not solved until the discovery of gene silencing at the end of the last century (Covey, 1997), and the gene silencing mediated by viral RNA is called virus-induced gene silencing (VIGS) (Hannon, 2002; Palukaitis et al., 2013). Since strategies applied in gene silencing are also involved in the control of endogenous gene expression, the border between gene silencing and normal gene regulation is vague, which makes it difficult to clearly define gene silencing-based resistance (Pumplin and Voinnet, 2013). Nowadays, gene silencing, or more strictly RNA silencing (or RNA

interference, RNAi), has been found to fight against the injurious effects of invasive nucleic acid (INA) in a sequence-specific manner in the four Eukaryote kingdoms (protists, fungi, plants and animals), with the exception of yeasts (Palukaitis, 2011; Zvereva and Pooggin, 2012). Nonetheless, this phenomenon is believed to be more apparent and more important in plants than in other eukaryotes (Wassenegger, 2002b; Gilliland et al., 2006; Anurag, 2013).

Two key mechanisms of RNAi have evolved and are utilized: transcriptional gene silencing (TGS) to block RNA biosynthesis and post-transcriptional gene silencing (PTGS) to eliminate existing RNA (Wassenegger, 2002a; Vaucheret, 2006; Csorba et al., 2015). In particular, PTGS is a cytoplasmic mechanism working through miRNA and other RNAi-associated pathways by recognition of dsRNAs and targeting of sequence-related single-stranded RNAs (ssRNAs) (Baulcombe, 2004; Zvereva and Pooggin, 2012). Both TGS and PTGS are largely mediated by a variety of 20- to 27-nucleotide (nt) small non-coding RNAs which are generated from the cleavage of double-stranded RNAs (dsRNAs) and primary-microRNA (pri-miRNA) by a dsRNA-specific nuclease named Dicer (RNase III family) in animals or dicer-like endoribonucleases (DCLs) in plants (Waterhouse et al., 2001; Huang et al., 2012). Dicer/DCL facilitates the activation of a multiprotein complex, RNA-induced silencing complex (RISC), which can incorporate small RNAs as a template to recognize complementary messenger RNA (mRNA). Once located, the main catalytic element of RISC, called Argonaute (AGO), can catalyze the degradation of target mRNA (Pumplin and Voinnet, 2013; Sanfaçon, 2015; Wieczorek and Obrepalska-Stęplowska, 2015). Generally, the most crucial small RNAs are members of two classes: host endogenous miRNAs and small/short interfering RNAs (siRNAs) (Moissiard and Voinnet, 2004; Sharma et al., 2013; Tenoever, 2013). RNAi has been studied extensively and additionally revealed as a promising therapeutic strategy for degrading pathogenic gene expression (Voinnet, 2005; Sibley et al., 2010; Zhang et al., 2015).

Soon after the discovery that RNAi can act as an antiviral defence barrier in plants, it became clear that viruses, in turn, have developed various strategies to evade RNA silencing, such as the expression of VSRs (Alvarado and Scholthof, 2009; Kon and Ikegami, 2009). Several previously identified viral pathogenicity determinants have actually turned out to be involved in RSS activities (Ghoshal and Sanfaçon, 2015; Zhao et al., 2016). P1/HC-Pro from potyviruses is one of the first and best characterized VSRs (Anandalakshmi et al., 1998). Subsequently, numerous VSRs have been discovered in nearly all plant virus families (Roth et al., 2004). The great diversity in sequence and domain structure of VSRs suggests that they have evolved independently and work under different mechanisms (Siddiqui et al., 2008; Bivalkar-Mehla et al., 2011; Omarov and Scholthof, 2012).

Molecular analysis has demonstrated that VSRs may counteract plant antiviral defences by the binding/sequestration of small RNAs away from the RISC, destabilization/inactivation of host factors associated with RISC formation, or inhibition of Dicer/DCLs or its co-factor DRB4 (Burgyán, 2006; Omarov and Scholthof, 2012; Pumplin and Voinnet, 2013). The potyviral HC-Pro and the tombusviral p19 are archetypical examples of VSRs that sequester siRNAs, which are the most conserved RNAi components (Brigneti et al., 1998; Kasschau et al., 2003; Vargason et al., 2003; Bartels et al., 2016). The cucumoviral 2b and ipomoviral P1 inactivate and/or destabilize AGO proteins, thus preventing RISC assembly (Zhang et al., 2006; Giner et al., 2010). GW/WG motifs have been shown in several VSRs to be responsible for mimicking and possibly displacing plant interactors which interact with key AGO proteins (Giner et al., 2010; Jin and Zhu, 2010; Karran and Sanfaçon, 2014). In addition, jasmonic acid (JA)-signalling pathways have been postulated to be influenced by RNAi directly or indirectly through interaction with VSRs (Westwood et al., 2014).

1.5 Research objectives and goals

Upon entry into the plant cell, the first step in potyviral replication is translation of the viral genome. Since P1 is the first protein of the polyprotein, and its separation from HC-Pro is required for viral viability, P1 may play an important role in virus infection. This research was directed to investigate the functional role of P1 in the viral infection process. The long term goal was to develop novel strategies against plant potyviruses and related viruses. The specific objectives of this research were:

1. Subcellular localization of the P1 protein in plant cells. In general, proper targeting is required for a protein to exert its functional role in the cellular biological processes in which it is involved. Therefore, subcellular localization of P1 is essential to explore its molecular functions within virus-plant interactions as well as in the virus infection process.
2. Determination whether P1 interacts with itself and/or any of the other 10 viral proteins in yeast and plant cells. Numerous important viral activities, such as the construction of the VRC, disassembly and assembly of virions, and short- and long-distance virus movement, rely on various protein complexes formed through protein-protein interactions. Analysis of protein-protein interactions naturally becomes a popular approach to studying protein functions and understanding the molecular mechanisms underlying these biological processes.
3. Examination of P1's functions other than that of a protease. It is well recognized that P1 protein is one of the three peptidases which processes the potyviral polyprotein, but its other potential involvements during the virus infection cycle are largely unknown. Since most, if not all, potyviral proteins have proved to be multifunctional, it is reasonable to believe that P1 might perform other functions than protease in the viral infection process.

4. Screen for *Arabidopsis thaliana* proteins that interact with TuMV P1 using the yeast two hybrid (Y2H) system. Since the establishment of successful viral infection requires numerous protein-protein interactions with host proteins, the study of the intimate relationship between plant viruses and their hosts will be vital to understand biological functions and the development of viral disease processes. The list of host factors identified from this screen can help to gain insights into the interactions between TuMV and its host.

5. Investigation of the roles that important host proteins play during virus infection. Functional characterization of host proteins during infection will elucidate precious knowledge on viral pathogenicity and the defined host proteins may serve as potential targets for the development of novel antiviral strategies.

Chapter 2 Materials and Methods

2.1 Plant materials

Arabidopsis thaliana ecotype Columbia (Col-0) and *Nicotiana benthamiana* were used in this research. *A. thaliana* and wild type *N. benthamiana* plants were grown in a growth chamber maintained under constant conditions of 60% relative humidity with a day/night photoperiod of 16h light at 22°C followed by 8h dark at 18°C. All *Arabidopsis* T-DNA insertion lines were purchased from the *Arabidopsis* Biological Resource Center (ABRC). T-DNA insertion mutant information was obtained from the Salk Institute Genomic Analysis Laboratory website (<http://signal.salk.edu/>).

2.2 Virus materials

The pCambiaTunos/GFP plasmid, which contains the full-length genome of TuMV and a free green fluorescent protein (GFP) between P1 and HC-Pro, and pCambiaTunos/6KGFP plasmid, with a GFP tagged at the C-terminal of an additional 6K2 protein at the junction of P1 and HC-Pro in the TuMV full-length genome plasmid were obtained from Dr. Jean-Francois Laliberte at the National Institute of Scientific Research (Quebec, Canada) (Cotton et al., 2009).

Since the full TuMV infectious plasmid was too large for functional cloning, a truncated fragment, TuMV-11740~3528, was amplified from pCambiaTunos/GFP using the forward primer 5'- CTCCTCTTAGAATTCCTCCGGGAC -3' and reverse primer 5'- CCGTGACCCATTTGGTACCG -3'. The GFP between P1/HC-Pro was deleted on the fragment by overlapping polymerase chain reaction (PCR) using the primer set listed (Table 1). The mutated PCR product and pCambiaTunos/GFP were both digested with *Xma*I and *Kpn*I, and then ligated using T4 DNA ligase (Invitrogen) to generate the plasmid p35TuMV.

Another truncated sequence, TuMV-9786~11116, was amplified from pCambiaTunos/GFP using the forward primer 5'- AGATACGCAAGTTCTACGCG -3' and reverse primer 5'- ATGTTACTAGATCGTCGACTC -3'. A free GFP was inserted between NIB/CP in TuMV-9786~11116 by overlapping PCR, using the primer pair described in Table 1. The mutated PCR fragment was digested with *MluI* and *SalI* and ligated into p35TuMV, which was also digested with the same enzymes, to create the infectious clone p35TuMV/GFP.

In this study, all mutagenesis of P1/HC-Pro was carried out on the TuMV-11740~3528 fragment using the overlapping primer pairs listed (Table 1). The mutated PCR products were digested and ligated into p35TuMV/GFP as described previously. The proper insertion sequences and direction were confirmed using DNA sequencing.

The p35TEV plasmid containing TEV full-length genome was provided by Dr. José-Antonio Daròs from the Polytechnic University of Valencia (Valencia, Spain) (Bedoya and Daròs, 2010). A truncated fragment, TEV-7453~9373, was amplified from p35TEV using the forward primer 5'- GAGCATATAAGCCAAGTCGAC -3' and reverse primer 5'- CTCTGTAGACCATACCTAGG -3'. A GFP was inserted between NIB/CP on this fragment by overlapping PCR using primer pair described in Table 2. The mutated PCR product was digested with *SalI* and *AvrII* and ligated into p35TEV, which was also digested with the same enzymes, to generate the infectious clone p35TEV/GFP. Another fragment, TEV-11740~3510, was amplified using primer pair, 5'- GCATTTATCAGGGTTATTGTCTC -3' and 5'- GGACACTCGAGACTGTGAT -3' and used for mutagenesis of P1/HC-Pro using the overlapping primer sets listed (Table 2). The mutated PCR products and p35TEV/GFP were ligated after digestion with *NotI* and *AatII*.

Table 1 Primers used for engineering cDNAs of TuMV infectious clone. Mutated nucleotides are underlined.

| Primer Name | Primer Sequence (5'-3') | Plasmid created |
|--------------------|--|--|
| TuMV-P1GFP-F | CAAGATTGTGCACTTTGCTGCCGCGGGAATGAGTAAAGG | p35TuMV-P1GFP, P1/HC-Pro cleavage site 363 S mutated to A |
| TuMV-P1GFP-R | CTCATTCCCCGCGGCAGCAAAGTGCACAATCTTGTGACTC | |
| TuMV-GFP-del-R | GAAGTTGGCTCCCGCGGCACTAAAGTGCACAATCTTGTGACTC | p35TuMV, GFP deleted from pCambiaTunos/GFP |
| TuMV-GFP-del-F | CAAGATTGTGCACTTTAGTGCCGCGGGAGCCAACCTTCTG | |
| TuMV-NIb-GFP-R | <u>CTCATTCCCCGCGGCTGCCTGGTGATAAACACAAGCCTC</u> | p35TuMV/GFP, free mGFP5 flanked by NIb/CP cleavage site ENLYFQ/S, which is cut by NIa, inserted between NIb/CP |
| TuMV-NIb-GFP-F | <u>CTGAGGCTTGTGTTTATCACCAGGCAGCCGCGGGAATGAGTAAAGG</u> | |
| TuMV-GFP-CP-R | <u>CAAGCGTTTCACCTGCCTGGTGATAGACACAAGCTTTG</u> | |
| TuMV-GFP-CP-F | <u>CAAAGCTTGTGTCTATCACCAGGCAGGTGAAACGCTTGATGC</u> | |
| TuMV-P1S313A-R | CCAACGACTATGCC <u>AGCC</u> CAACCTGCGCAA ACT ACTC | p35TuMV/GFP-P1S, P1 protease active site 313 S mutated to A |
| TuMV-P1S313A-F | GTTTGCGCAGGTTGG <u>GCT</u> GGCATAGTCGTTGGAAATGG | |
| TuMV-P1(null)/HC-R | GAAGTTGGCTCCCGCGGCTGCAAAGTGCACAATCTTGTGACTC | p35TuMV/GFP-P1(null)/HC, P1/HC-Pro cleavage site 305 S mutated to A |
| TuMV-P1(null)/HC-F | CAAGATTGTGCACTTTG <u>CAG</u> CCGCGGGAGCCAACCTTCTG | |
| TuMV-P1(nia)/HC-R | <u>CGCGGCTGCCTGATGATAGACACAAGCAAAGTGCACAATCTTGTGACTC</u> | p35TuMV/GFP-P1(nia)/HC, NIb/CP cleavage site ACVYHQ/A cut by NIa inserted between P1/HC-Pro |
| TuMV-P1(nia)/HC-F | <u>GTGCACTTTGCTTGTGTCTATCATCAGGCAGCCGCGGGAGCCAACCTTCTG</u> | |
| TuMV-P1-del-R | <u>GTTGGCTCCCGCGGCACTT</u> GTA ACT GCTGCCATTTGGTTTG | p35TuMV/GFP-ΔP1, whole P1 deleted after the fifth amino acid |
| TuMV-P1-del-F | <u>CCAAATGGCAGCAGTTACAAGT</u> GCCGCGGGAGCCAACCTC | |

Table 2 Primers used for engineering cDNAs of TEV infectious clone. Mutated nucleotides are underlined.

| Primer Name | Primer Sequence (5'-3') | Plasmid created |
|--------------------|---|--|
| TEV-NIb(nia)/GFP-R | <u>CAGATCTACCATACTCTGAAAATAAAGATTCTCAGTCG</u> | p35TEV/GFP, free mGFP5 flanked by NIb/CP cleavage site ENLYFQ/S cut by NIa inserted between NIb/CP |
| TEV-NIb(nia)/GFP-F | <u>GAATCTTTATTTTCAGAGTATGGTAGATCTGACTAGTAAAG</u> | |
| TEV-GFP-(nia)-R | <u>ACTCTGAAAATAAAGATTCTCCACGTGGTGGTGGTGGTG</u> | |
| TEV-(nia)-CP-F | <u>CACGTGGAGAATCTTTATTTTCAGAGTGGCACTGTGGGTGCTG</u> | |
| TEV-P1S256A-F | CGAAGCTCACTTTTGGTTCAG <u>CTGGCCTAGTTTTGAGGCAAGGC</u> | p35TEV/GFP-P1S, P1 protease active site 256 S mutated to A |
| TEV-P1S256A-R | GCCTTGCCTCAAACTAGGCC <u>AGCTGAACCAAAAGTGAGCTTCG</u> | |
| TEV-P1(null)/HC-F | TTGTCACTCAATGACACATTATT <u>GCCGACAAATCAATCTCTGAGGC</u> | p35TEV/GFP-P1(null)/HC, P1/HC-Pro cleavage site 305 S mutated to A |
| TEV-P1(null)/HC-R | GCCTCAGAGATTGATTTGT <u>CGGCATAATGTGTCATTGAGTGACAA</u> | |
| TEV-P1(nia)/HC-F | <u>GAGAATCTTTATTTTCAGAGTAGCGACAAATCAATCTCTGAGG</u> | p35TEV/GFP-P1(nia)/HC, NIb/CP cleavage site ENLYFQ/S cut by NIa inserted between P1/HC-Pro |
| TEV-P1(nia)/HC-R | <u>ACTCTGAAAATAAAGATTCTCATAATGTGTCATTGAGTGACAAAC</u> | |
| TEV-P1-del-F | <u>AGCTCGTATGAGCGACAAATCAATCTCTGAGGC</u> | p35TEV/GFP-ΔP1, whole P1 deleted after the 22nd amino acid |
| TEV-P1-del-R | <u>ATTTGTCGCTCATAACGAGCTCCACCGAACACTTCC</u> | |
| TEV-VNN-R | GGTGAATGGCAATCAATAG <u>GTTGTTAACATTGACGTAATACACAATCTC</u> | p35TEV/GFP-VNN, NIb 347~349 GDD mutated to VNN |
| TEV-VNN-F | GAGATTGTGTATTACGTCAAT <u>GTTAACAACCTATTGATTGCCATTCACC</u> | |
| TEV-HisP1-R | <u>GTATGATGGTGATGGTGATGGCCAAAGATGAGTGCCATGG</u> | p35TEV/GFP-6HisP1, 6× His fused at N-terminal of P1 |
| TEV-HisP1-F | <u>GCCATCACCATCACCATCATAACGCTAACATCCTG</u> | |
| TEV-StrepP1-R | <u>GTCTTTTCAAATTGAGGATGAGACCAGCCAAAGATGAGTGCCATGG</u> | p35TEV/GFP-StrepIIP1, StrepII (TGGTCTCATCCTCAATTTGAAAAG) fused at N-terminal of P1 |
| TEV-StrepP1-F | <u>GCTGGTCTCATCCTCAATTTGAAAAGACAGTCAACGCTAACATCCTG</u> | |
| TEV-P1Strep-R | <u>TGCTTTTCAAATTGAGGATGAGACCAACAACAGCGAACGTTACCT</u> | p35TEV/GFP-P1StrepII, StrepII fused at C-terminal of P1 |
| TEV-P1Strep-F | <u>GTTGGTCTCATCCTCAATTTGAAAAGCACTCAATGACACATTATAGC</u> | |

Table 2 (continued)

| | | |
|---------------|------------------------------------|---|
| TEV-P1N34A-R | CAAAATGCTTCC <u>AGCC</u> GCTCCAGCC | p35TEV/GFP-P1S256A, P1 34 N mutated to A |
| TEV-P1N34A-F | GGCTGGAGCGGCTGGAAGCATTTTG | |
| TEV-P1K40A-R | GTCTCTTCTG <u>CCGC</u> CTTCAAAATGC | p35TEV/GFP-P1S256A, P1 40 K mutated to A |
| TEV-P1K40A-F | GCATTTTGAAGGCGGCAGAAGAGAC | |
| TEV-P1K242A-R | CTCTCTCATT <u>CGC</u> AAATCTTTTAGC | p35TEV/GFP-P1S256A, P1 242 K mutated to A |
| TEV-P1K242A-F | GCTAAAAGATTTGCGAATGAGAGAG | |

2.3 Growth conditions of bacterial and yeast strains

The *Escherichia coli* strains DH10 β , DH5 α and DB3.1 were grown at 37°C in Luria-Bertani (LB) liquid medium (1% tryptone, 1% NaCl, 0.5% yeast extract) or on LB solid medium supplemented with 1.5% w/v agar. Selection for plasmids was maintained by the addition of ampicillin (100 μ g/mL), kanamycin (50 μ g/mL) or spectinomycin (20 μ g/mL). *Agrobacterium tumefaciens* strain GV3101 was cultured at 28°C in LB medium supplemented with 25 μ g/mL gentamicin, 10 μ g /mL of rifamycin and 50 μ g /mL of kanamycin.

The yeast (*Saccharomyces cerevisiae*) strain (Y2HGold) was grown at 28°C in rich YPD medium supplemented with adenine hemisulfate (YPDA) or minimal synthetic defined (SD) base liquid medium (0.17% yeast nitrogen base without amino acids, 2% glucose) combined with the appropriate drop out (DO) supplement powder. SD was supplemented with 1.5% w/v agar for solid medium. Selective medium for plasmids was maintained by supplementing the minimal SD base combined with -Ade (adenine) /-His (histidine) /-Leu (leucine)/-Trp (tryptophan) DO powder.

2.4 Gateway-based plasmid construction

Plasmid constructs were generated using the Gateway[®] Technology (Invitrogen, Burlington, Ontario, Canada) unless stated otherwise. DNA sequences were obtained by PCR amplification using Phusion[®] High-Fidelity DNA Polymerase (New England Biolabs, Pickering, Ontario, Canada) for cloning purposes or GoTaq[®] Flexi DNA Polymerase (Promega, Madison, WI, USA) for other analysis. Gene sequences were confirmed by Sanger DNA sequencing when needed.

The coding regions of P1, HC-Pro, P3, 6K1, CI, 6K2, VPg, NIa, NIb and CP of TuMV (GenBank accession no. NC002509) and TEV (GenBank accession no. NC001555) were amplified by PCR from vectors pCambiaTunos/GFP and p35TEV, respectively, with relevant primers (Table 3 and Table 4). In addition, P3N-PIPO was obtained by overlapping PCR using the primer sets indicated (Table 3 and Table 4). Partial fragments of TEV P1, P1-1~318 (N-terminal part, N), P1-319~486 (Middle part, M), P1-486~912

(C-terminal part, C), P1-1~486 (NM part, NM) and P1-319~912 (MC part, MC) were amplified using forward primers, TeP1-GW319-F and TeP1-GW487-F, and reverse primers, TeP1-GW318-R and TeP1-GW486-R (Table 5). Overlapping PCR primers used to delete predicted nuclear localization signals (NLSs) from partial fragments of TEV P1 are shown in Table 4. Predicted P1 NLSs were amplified and fused with a Beta-glucuronidase reporter gene (GUS) (Table 5). The full length of *Arabidopsis* genes *NDL2* (AT5G11790), *TPR* (AT1G78915) and *UCP3* (AT1G26650) were retrieved from Col-0 complementary DNA (cDNA, primers shown in Table 6). All of the resulting DNA fragments were purified and transferred into the entry vector pDONR221 using BP clonase II (Invitrogen) and then verified by DNA sequencing.

Gateway compatible vectors pGWB454 and 554 were used to express monomeric red fluorescent proteins (mRFP) (Nakagawa et al., 2007) and pEarlyGate101, 102 and 103 were used to express yellow (YFP), cyan (CFP) and green fluorescent proteins (GFP) respectively (Earley et al., 2006). The GUS coding region was amplified from plasmid pENTR-GUS (Invitrogen) using the primer pair listed in Table 6. In order to construct a new gateway destination vector pPanGate-GUS-YFP, the PCR product was digested with *Xba*I and *Pac*I and ligated into pEarlyGate101 (Earley et al., 2006), which was also digested with the same enzymes. pPanGate-2YFP was obtained by digestion of pEarly101 with *Avr*II and insertion of another YFP fragment digested with the same enzyme. The proper insertion sequences and direction were confirmed using DNA sequencing.

Protein expressing vectors for bimolecular fluorescence complementation (BiFC) assays were created based on pEarlyGate vectors 201 and 202, renamed pEarlyGate201-YN and pEarlyGate201-YC, respectively (Lu et al., 2010). To construct vectors used in Y2H assays, the afore-mentioned entry clone pDONR221 constructs were ligated with modified Gateway compatible vectors pGBKT7-DEST (bait) and pGADT7-DEST (prey) generated from pGKBT7 and pGADT7-Rec vectors (Lu et al., 2010) using LR recombination reactions (Invitrogen).

Table 3 Primers for plasmid construction of TEV proteins. The *attB* recognition site is underlined.

| Primer Name | Primer Sequence (5'-3') |
|----------------|--|
| TeP1-GW-F | GGGGACAAGTTTGTACAAAAAAGCAGGCTTCATGGCACTCATCTTTGGCACA |
| TeP1-GW-R | GGGGACCACTTTGTACAAGAAAGCTGGGTCATAATGTGTTCATTGAGTGACAAAC |
| TeHC-GW-F | GGGGACAAGTTTGTACAAAAAAGCAGGCTTCATGAGCGACAAATCAATCTCTGAG |
| TeHC-GW-R | GGGGACCACTTTGTACAAGAAAGCTGGGTCCTCAACATTGTAAGTTTTCATTC |
| TeCI-GW-F | GGGGACAAGTTTGTACAAAAAAGCAGGCTTCATGAGTTTGGATGATTACGTTACA AC |
| TeCI-GW-R | GGGGACCACTTTGTACAAGAAAGCTGGGTCCTGGAGATAGATAGTTTCCAGG |
| TeVPg-GW-F | GGGGACAAGTTTGTACAAAAAAGCAGGCTTCATGGGGAAGAAGAATCAGAAG CAC |
| TeVPg-GW-R | GGGGACCACTTTGTACAAGAAAGCTGGGTCCTCAAACGTCAAGTCCTCACT |
| TeP3-GW-F | GGGGACAAGTTTGTACAAAAAAGCAGGCTTCATGGGGATGAACCGAGATATGGT |
| TeP3-GW-R | GGGGACCACTTTGTACAAGAAAGCTGGGTCCTGTTCAACGAGGTCTTCCT |
| Te6K1-GW-F | GGGGACAAGTTTGTACAAAAAAGCAGGCTTCATGGCAAACAACCGGAGATAGC |
| Te6K1-GW-R | GGGGACCACTTTGTACAAGAAAGCTGGGTCCTGCGTGTAGATGATCTCCC |
| Te6K2-GW-F | GGGGACAAGTTTGTACAAAAAAGCAGGCTTCATGTCAGATAGCGAAGTGGCTAAG |
| Te6K2-GW-R | GGGGACCACTTTGTACAAGAAAGCTGGGTCCTGGAAATAGACTGGTTCATTG |
| TePro-GW-F | GGGGACAAGTTTGTACAAAAAAGCAGGCTTCATGGGAGAAAGCTTGTTTAAGGGA |
| TePro-GW-R | GGGGACCACTTTGTACAAGAAAGCTGGGTCCTGCGAGTACACCAATTCCT |
| TeNIb-GW-F | GGGGACAAGTTTGTACAAAAAAGCAGGCTTCATGGGGGAGAAGAGGAAATGGG |
| TeNIb-GW-R | GGGGACCACTTTGTACAAGAAAGCTGGGTCCTGAAAATAAAGATTCTCAGTCG |
| TeCP-GW-F | GGGGACAAGTTTGTACAAAAAAGCAGGCTTCATGAGTGGCACTGTGGGTGCTG |
| TeCP-GW-R | GGGGACCACTTTGTACAAGAAAGCTGGGTCCTGGCGGACCCCTAATAGT |
| TePIPO-GW-R | GGGGACCACTTTGTACAAGAAAGCTGGGTCGGAAGCATGCTGTAGATTTTG |
| TePIPO-F1 | GCATGAAATGTTGGGAAAAAACTATG |
| TeP3N-R1 | GTTTTTTTCCCAACATTTTCATGCACC |
| TeP1-6His-GW-R | GGGGACCACTTTGTACAAGAAAGCTGGGTCATGATGGTGTGGTGTGATAATG TGTCATTGAGTGACAAAC |
| 6His-TeP1-GW-F | GGGGACAAGTTTGTACAAAAAAGCAGGCTTCATGCATCACCATCACCATCATGC ACTCATCTTTGGCACAGT |

Table 4 Primers for plasmid construction of TuMV proteins.The *attB* recognition site is underlined.

| Primer Name | Primer Sequence (5'-3') |
|---------------|---|
| TuMVP1-GW-F | <u>GGGGACAAGTTTGTACAAAAAAGCAGGCTTC</u> CATGGCAGCAGTTACATTTCGC |
| TuMVP1-GW-R | GGGGACCACTTTGTACAAGAAAGCTGGGTCAAAGTGCACAATCTTGTGACTC |
| TuMVHC-GW-F | <u>GGGGACAAGTTTGTACAAAAAAGCAGGCTTC</u> CATGAGTGCAGCAGGAGCCAAC |
| TuMVHC-GW-R | GGGGACCACTTTGTACAAGAAAGCTGGGTCTCCAACGCGGTAGTGTTC |
| TuMVP3-GW-F | <u>GGGGACAAGTTTGTACAAAAAAGCAGGCTTC</u> CATGGGAACAGAATGGGAGGACAC |
| TuMVP3-GW-R | GGGGACCACTTTGTACAAGAAAGCTGGGTCTTGATGAACCACCGCCTTTTC |
| TuMV6K1-GW-F | <u>GGGGACAAGTTTGTACAAAAAAGCAGGCTTC</u> CATGGCGAAGAGACAATCCGAGC |
| TuMV6K1-GW-R | GGGGACCACTTTGTACAAGAAAGCTGGGTCTGATGGTAGACTGTAGGTTTC |
| TuMVCI-GW-F | <u>GGGGACAAGTTTGTACAAAAAAGCAGGCTTC</u> CATGACTCTCAATGATATAGAGGATG |
| TuMVCI-GW-R | GGGGACCACTTTGTACAAGAAAGCTGGGTCTTGATGGTGAAGTGCCTCAAG |
| TuMV6K2-GW-F | <u>GGGGACAAGTTTGTACAAAAAAGCAGGCTTC</u> CATGAACACCAGCGACATGAGCAA |
| TuMV6K2-GW-R | GGGGACCACTTTGTACAAGAAAGCTGGGTCTTCATGGGTACGGGTTCCG |
| TuMVVPg-GW-F | <u>GGGGACAAGTTTGTACAAAAAAGCAGGCTTC</u> CATGGCGAAAGGTAAGAGGCAAAG |
| TuMVVPg-GW-R | GGGGACCACTTTGTACAAGAAAGCTGGGTCTCGTGGTCCACTGGGAC |
| TuMVNIa-GW-F | <u>GGGGACAAGTTTGTACAAAAAAGCAGGCTTC</u> CATGAGTAACTCCATGTTTCAGAGGG |
| TuMVNIa-GW-R | GGGGACCACTTTGTACAAGAAAGCTGGGTCTTGTCGTAGACTGCCGTG |
| TuMVNIb-GW-F | <u>GGGGACAAGTTTGTACAAAAAAGCAGGCTTC</u> CATGACCCAGCAGAATCGGTGGA |
| TuMVNIb-GW-R | GGGGACCACTTTGTACAAGAAAGCTGGGTCTCGGTGATAAACACAAGCCTC |
| TuMVCP-GW-F | <u>GGGGACAAGTTTGTACAAAAAAGCAGGCTTC</u> CATGGCAGGTGAAACGCTTGATGC |
| TuMVCP-GW-R | GGGGACCACTTTGTACAAGAAAGCTGGGTCCAACCCCTGAACGCCAG |
| TuMVPIPO-GW-R | <u>GGGGACCACTTTGTACAAGAAAGCTGGGTCT</u> CCGTTGTAAGATGACATG |
| TuMVP3N-R1 | GATAACTTTTTTCCCAAAATGGAGATGC |
| TuMVPIPO-F1 | TCTCCATTTTGGGAAAAAAGTTATCTAC |

Table 5 Primers for confirmation of TEV P1 NLSs. The *attB* recognition site or mutated nucleotides are underlined.

| Primer Name | Primer Sequence (5'-3') |
|--------------------|---|
| TeP1-GW318-R | <u>GGGGACCACTTTGTACAAGAAAGCTGGGTCTCTCCTGTTCCCTCTTGTTATTC</u> |
| TeP1-GW319-F | <u>GGGGACAAGTTTGTACAAAAAAGCAGGCTTCATGAGGAAAGTGGCCAAAA</u> CGTAC |
| TeP1-GW486-R | <u>GGGGACCACTTTGTACAAGAAAGCTGGGTCTCTCCTGTTCCCTCTTGTTATTC</u> |
| TeP1-GW487-F | <u>GGGGACAAGTTTGTACAAAAAAGCAGGCTTCATGTTCTTGCCCCGCACTTCAC</u> |
| TeP1-NLS1-GUS-GW-F | <u>GGGGACAAGTTTGTACAAAAAAGCAGGCTTCATGGGCAAGAGACGCAAAG</u> TTATGGTCCGTCCTGTAGAAACCC |
| TeP1-NLS2-GUS-GW-F | <u>GGGGACAAGTTTGTACAAAAAAGCAGGCTTCATGAAGCGTAAGAAGCAGA</u> AAAACATGGTCCGTCCTGTAGAAACCC |
| TeP1-NLS3-GUS-GW-F | <u>GGGGACAAGTTTGTACAAAAAAGCAGGCTTCATGGCTAAAAGATTTAAGA</u> ATGAGAGAATGGTCCGTCCTGTAGAAACCC |
| GUS-GW-R | <u>GGGGACCACTTTGTACAAGAAAGCTGGGTCTTGTGTTGCCTCCCTGCTGCGG</u> |
| TeP1-ΔNLS1-F | CATGGCGCGGCAGCCGAGTTTCTGTGAATAACAAGAGG |
| TeP1-ΔNLS1-R | AGAAACTGCGGCTGCCGCGCCATGGGTGAGCGCGCG |
| TeP1-ΔNLS2-F | ATGCCAGCGGCTGCGGCGCAGAAAACTTCTTGCCCG |
| TeP1-ΔNLS2-R | TTTCTGCGCCGAGCCGCTGGCATACTATTATGCACAAGT |
| TeP1-ΔNLS3-F | CTTGCTGCAGCAGCTGCGAATGAGAGAGTGGATCAATC |
| TeP1-ΔNLS3-R | CTCATTCGCAGCTGCTGCAGCAAGGTCTAGAAGTGTCTC |

Table 6 Primers for plasmid construction to express *Arabidopsis* proteins. The *attB* recognition site is underlined.

| Primer Name | Primer Sequence (5'-3') |
|-------------|--|
| NDL2-GW-F | <u>GGGGACAAGTTTGTACAAAAAAGCAGGCTTC</u> ATGGCGGATTCAAGCGATTC |
| NDL2-GW-R | GGGGACCACTTTGTACAAGAAAGCTGGGTCTAGAGCGAGTCGTGTCTTTATC |
| TPR-GW-F | <u>GGGGACAAGTTTGTACAAAAAAGCAGGCTTC</u> ATGTTGATGACACTAGCGGGC |
| TPR-GW-R | GGGGACCACTTTGTACAAGAAAGCTGGGTCTAGTTTGGAGTATCTATCCACAAG |
| UCP3-GW-F | <u>GGGGACAAGTTTGTACAAAAAAGCAGGCTTC</u> ATGGAGACGGAAACGAATCAG |
| UCP3-GW-R | GGGGACCACTTTGTACAAGAAAGCTGGGTCCTCAGCATCCACAACCGTAAC |
| IPME-GW-F | <u>GGGGACAAGTTTGTACAAAAAAGCAGGCTTC</u> ATGGCTCCTACACAAAATCTC |
| IPME-GW-R | GGGGACCACTTTGTACAAGAAAGCTGGGTCAAGATGTACGTCGTGGGGTTTG |
| DDP-GW-F | <u>GGGGACAAGTTTGTACAAAAAAGCAGGCTTC</u> ATGGATATTAGCCGGCGTGA |
| DDP-GW-R | GGGGACCACTTTGTACAAGAAAGCTGGGTCACTTCGTCGCTATCGTTCCC |
| ADF3-GW-F | <u>GGGGACAAGTTTGTACAAAAAAGCAGGCTTC</u> ATGGCTAATGCAGCATCAGG |
| ADF3-GW-R | GGGGACCACTTTGTACAAGAAAGCTGGGTCATTGGCTCGGCTTTTGAAAAC |
| UCH3-GW-F | <u>GGGGACAAGTTTGTACAAAAAAGCAGGCTTC</u> ATGGCGACCGCAAGCGAGAG |
| UCH3-GW-R | GGGGACCACTTTGTACAAGAAAGCTGGGTCGGTTCTCTTAGAGATGGCTATC |
| SNT7-GW-F | <u>GGGGACAAGTTTGTACAAAAAAGCAGGCTTC</u> ATGGCTACAATATCTCCGGG |
| SNT7-GW-R | GGGGACCACTTTGTACAAGAAAGCTGGGTCCTCTCTCTGGGGATCCATC |
| UCP1-GW-F | <u>GGGGACAAGTTTGTACAAAAAAGCAGGCTTC</u> ATGGAAACAATAGCAGTTCAAATG |
| UCP1-GW-R | GGGGACCACTTTGTACAAGAAAGCTGGGTCCCGGAGCTGTAAACTCGCC |
| UCP2-GW-F | <u>GGGGACAAGTTTGTACAAAAAAGCAGGCTTC</u> ATGGATTTGTATGGAATGAGAGTTG |
| UCP2-GW-R | GGGGACCACTTTGTACAAGAAAGCTGGGTCGGTGTCATCAGTAACATCCTTAC |
| PKP-GW-F | <u>GGGGACAAGTTTGTACAAAAAAGCAGGCTTC</u> ATGGGATGTTTCGGACGCAC |
| PKP-GW-R | GGGGACCACTTTGTACAAGAAAGCTGGGTCAGTTGCTTGATCTGAGCATATC |
| ELS1-GW-F | <u>GGGGACAAGTTTGTACAAAAAAGCAGGCTTC</u> ATGACGATGTCGGAGAACTC |
| ELS1-GW-R | GGGGACCACTTTGTACAAGAAAGCTGGGTCTTGTAGAAAATCTGTAAGAGAAGC |
| ABCG25-GW-F | <u>GGGGACAAGTTTGTACAAAAAAGCAGGCTTC</u> ATGTCAGCTTTTGACGGCGTTG |
| ABCG25-GW-R | GGGGACCACTTTGTACAAGAAAGCTGGGTCATGTTTGATACGTCTCAAAGCTAG |

Table 6 (continued)

| | |
|-----------------|--|
| PFK4-GW-F | <u>GGGGACAAGTTTGTACAAAAAAGCAGGCTTCATGGAAGCTTCGATTTTCGTTTC</u> |
| PFK4-GW-R | <u>GGGGACCACTTTGTACAAGAAAGCTGGGTTCGATAGAAGAGATCTTCATGTTATC</u> |
| CtaG/Cox11-GW-F | <u>GGGGACAAGTTTGTACAAAAAAGCAGGCTTCATGTCGTGGTCGAAAGCTTG</u> |
| CtaG/Cox11-GW-R | <u>GGGGACCACTTTGTACAAGAAAGCTGGGTTCATTGGTTTCTTGAAGTGGAAACAG</u> |
| AGTP-GW-F | <u>GGGGACAAGTTTGTACAAAAAAGCAGGCTTCATGTCCGATGGTTATCGTAG</u> |
| AGTP-GW-R | <u>GGGGACCACTTTGTACAAGAAAGCTGGGTTCGCCAGATTCTCGTTTGCAG</u> |
| RP1-GW-F | <u>GGGGACAAGTTTGTACAAAAAAGCAGGCTTCATGTCTCACAGGAAGTTTGAG</u> |
| RP1-GW-R | <u>GGGGACCACTTTGTACAAGAAAGCTGGGTTCCTTCGTGACACGGTTGAAAAC</u> |
| UCP4-GW-F | <u>GGGGACAAGTTTGTACAAAAAAGCAGGCTTCATGGAATCGCTAACATCTATTTTC</u> |
| UCP4-GW-R | <u>GGGGACCACTTTGTACAAGAAAGCTGGGTCTTTATTATCCCTCAAGTCCTC</u> |
| RD2-GW-F | <u>GGGGACAAGTTTGTACAAAAAAGCAGGCTTCATGGAGGCTTTGCCGGAGG</u> |
| RD2-GW-R | <u>GGGGACCACTTTGTACAAGAAAGCTGGGTTCGGGTTTAGGATCTTCTGAG</u> |
| HHP2-GW-F | <u>GGGGACAAGTTTGTACAAAAAAGCAGGCTTCATGCAGAAACGGAGAACGG</u> |
| HHP2-GW-R | <u>GGGGACCACTTTGTACAAGAAAGCTGGGTCAAAGGCACAAGAAGGAGAAG</u> |
| LKP1-GW-F | <u>GGGGACAAGTTTGTACAAAAAAGCAGGCTTCATGGAACATGGTTTACCGTC</u> |
| LKP1-GW-R | <u>GGGGACCACTTTGTACAAGAAAGCTGGGTCTGTTGTAGTCTCTTCAGCTTTC</u> |
| NST-GW-F | <u>GGGGACAAGTTTGTACAAAAAAGCAGGCTTCATGGAGTGGCCATGGTCGG</u> |
| NST-GW-R | <u>GGGGACCACTTTGTACAAGAAAGCTGGGTTCGTCGTTGCCTTCGGGAAAG</u> |

Table 7 Other primers used for this study. The *attB* recognition site and the restriction sites are underlined.

| Primer Name | Primer Sequence (5'-3') |
|-------------|---|
| YFP-AvrII-F | AAGTGGTGCCTAGGGTGAGC |
| YFP-AvrII-R | TCTGTGCCTAGGCTTGTACAGCTCGTCCATGC |
| GUS-XbaI-F | TGTGTGTCTAGAAATGGTCCGTCCTGTAGAAAC |
| GUS-PacI-R | TGTGTGTTAATTAATTATTGTTTGCCTCCCTGCTG |
| mGFP5-GW-F | <u>GGGGACAAGTTTGTACAAAAAAGCAGGCTTCATGGTAGATCTGACTAGTAAAGG</u> |
| mGFP5-GW-R | <u>GGGGACCACTTTGTACAAGAAAGCTGGGTCCACGTGGTGGTGGTGGTGG</u> |

2.5 *Agrobacterium*-mediated transient expression

For transient expression in *N. benthamiana*, the relevant Gateway destination clones, as described previously, were transformed into *A. tumefaciens* strain GV3101 using electroporation. Agrobacterial cultures were grown overnight in LB medium containing the appropriate selective antibiotics. Agrobacteria were harvested by centrifugation, and then resuspended in infiltration buffer (10 mM MgCl₂, 10mM MES and 100 μM acetosyringone). After a minimum of 2 h incubation at room temperature, the cultures were diluted to an optical density of 0.1~1.0 (at OD 600 nm) and infiltrated into four-week-old *N. benthamiana* lower leaf epidermal cells using a 1 mL syringe without needle, by applying gentle pressure (Wei et al., 2010).

2.6 Confocal microscopy

For BiFC assays, reconstitution of YFP fragments was determined by *Agrobacterium*-mediated transient co-expression of the selected protein pairs in *N. benthamiana*. Plants were kept for protein expression under appropriate growing conditions. The infiltrated leaf tissues were collected and observed using a Leica TCS SP2 inverted confocal microscope with a 60× water immersion objective, at room temperature. CFP was excited at 458 nm and the emitted light was captured at 440 to 470 nm; GFP was excited at 488 nm and the emitted light was captured at 505 to 555 nm; YFP was excited at 514 nm, and the emitted light was captured at 525 to 650 nm; mRFP was excited at 543 nm and the emitted light was captured at 590~630 nm; chlorophyll autofluorescence was emitted at 630~680 nm. Captured images were recorded digitally and handled using the Leica LCS software (Cui et al., 2010).

2.7 Y2H cDNA library construction and screen

The yeast two-hybrid screen was conducted using Mate & Plate™ Library - Universal *Arabidopsis* (Normalized) and Screening Kits (Clontech, <http://www.clontech.com/>) following the supplier's instruction manual. The TuMV P1 coding sequence was amplified and cloned into the bait vector pGBKT7-DEST to generate the plasmid pGBKT7-TuP1. The resulting plasmid was confirmed by DNA sequencing, and then transformed into the yeast strain Y2HGold using the LiAc transformation method. Tests

of pGBKT7-TuP1 were performed and demonstrated no toxicity or autoactivation. The *Arabidopsis* Mate & Plate™ library was transformed into the yeast strain Y187. The yeast mating method was performed according to the manufacturer's protocol (Clontech) and the mated culture was spread on selective agar plates SD/-Ade/-His/-Leu/-Trp supplemented with X-a-Gal and Aureobasidin A (QDO/X/A), and incubated at 28°C for 7 days. Blue colonies, which were considered as positive clones, were extracted and transformed into the *E. coli* DH5α strain for plasmid preparation and DNA sequencing. The resulting sequence of the rescued cDNA clones were BLAST searched against the National Center for Biotechnology Information (NCBI) database.

To confirm interactions between TuMV P1 and candidate genes from the screen, the full lengths of candidate genes were amplified from *Arabidopsis* leaf tissue cDNA and recombined into plasmid pGBKT7 and pGADT7. Paired bait and prey plasmids were co-transformed into yeast strain Y2HGold and spread on selective plates (SD/-His/-Leu/-Trp) and grown for 4 days at 28°C. Then BiFC method was used to validate the protein interactions.

2.8 Plant genomic DNA isolation

Arabidopsis leaves were collected, frozen in liquid nitrogen, and stored at -80°C until use. Leaf tissue (200 mg) was ground in the presence of liquid nitrogen, transferred into a 1.5 mL polypropylene centrifuge tube with 500 μL CTAB extraction buffer [10 mM Tris-HCl, 1.4 M NaCl, 20 mM ethylenediaminetetraacetic acid (EDTA), 2% cetyltrimethylammonium bromide (w/v) (CTAB)] (Porebski et al., 1997), vigorously mixed well and incubated at 65°C for 15 minutes (min). Five hundred microliter of chloroform:isoamyl alcohol (24:1) was added and mixed by inversion to form an emulsion, followed by centrifugation at 10,000 g for 5 min at room temperature. The upper aqueous solution was transferred to a new 1.5 mL centrifuge tube. DNA was precipitated by adding 0.7 volumes of isopropanol and mixed by inversion (if required, the solution may be left at -20°C for an extended period, or even overnight precipitation). DNA pellets were collected by centrifugation at 10,000 g for 20 min, and then washed with 500 μL 75%

ethanol, air-dried for 10~20 min at room temperature and finally resuspended in 50 μ L of milli-Q water.

2.9 Plant RNA extraction

Plant tissue samples were harvested, frozen in liquid nitrogen, and stored at -80°C until use. Tissue sample (100 mg) was homogenized in the presence of liquid nitrogen, transferred into 1.5 mL centrifuge tubes with 1 mL of TRIZOL[®] Reagent (Invitrogen) and incubated for 5 min at room temperature to permit the complete dissociation of nucleoprotein complexes. Two hundred microliter of chloroform was added, shaken vigorously by hand for 15 seconds (s) and incubated at room temperature for 2 to 3 min. The mixture was separated into a lower, red phenol-chloroform phase, an interphase, and a colorless upper aqueous phase after centrifugation at 12,000 g for 15 minutes at 4°C . The top aqueous solution, about 60% of the volume of TRIZOL[®] Reagent used for homogenization, was transferred into a fresh 1.5 mL centrifuge tube. RNA was precipitated by adding 0.5 mL of isopropyl alcohol and incubated at room temperature for 10 min (if required, the solution may be left at -20°C for an extended period or even overnight precipitation). After centrifugation at 12,000 g for 10 minutes at 4°C , the RNA pellets were washed with 1 mL 75% ethanol, air-dried for 5~10 min at room temperature and finally resuspended in 30 μ L of milli-Q water.

2.10 PCR

2.10.1 Reverse transcription polymerase chain reaction (RT-PCR)

The RNA materials for TuMV and TEV infection assays were extracted from newly emerged leaf tissues. The total RNA (1 μ g) was treated with DNase I and synthesized into cDNA using the Superscript III First-Strand Synthesis System for RT-PCR kit (Invitrogen) following the manufacturer's instructions. The PCR reaction was performed to analyze both the internal standard and target genes using the specific gene primers listed (Table 8). The RT-PCR viral target genes were CP of TuMV or TEV, and P1 for detection of potyviruses. The *A. thaliana* or *N. benthamiana* actin gene was used as the internal control independently.

2.10.2 Quantitative real-time polymerase chain reaction (qRT-PCR)

Quantitative real-time PCR reactions were carried out using the CFX96 Real-Time PCR Detection System (Bio-Rad) following the manufacturer's instructions. For each pair of primers, gel electrophoresis and melting curve analysis were conducted to ensure that only one single PCR product of the expected length and melting temperature was generated. The expression of CP fragment of TuMV or TEV was detected to determine the potyviral accumulation level using primer pairs listed (Table 8). In the meantime, *A. thaliana Actin2* (*AtActin2*) or *N. benthamiana Actin* (*NbActin*) were used as the endogenous reference gene using the primer sets described (Table 8). All amplicons of the internal references or target genes were designed to be 100~150 bp. Three technical repeats were carried out for each biological replicates and three biological replicates were performed for each sample analysis. All results were shown as means of three biological replicates with corresponding standard errors.

Table 8 Primers for RT-PCR.

| Primer Name | Primer Sequence (5'-3') |
|--------------------|--------------------------------|
| AtActin2-qrt-F | AGTTGTAAGAGATAAACCCGCC |
| AtActin2-qrt-R | CCGGAGATTCAAAACGGCTG |
| NbActin-qrt-F | CGAGCGGGAAATTGTTAGGG |
| NbActin-qrt-R | GCTCGTAGCTCTTCTCCACG |
| TuMV-CP-qrt-F | GACAGACGAGCAAAAGCAGG |
| TuMV-CP-qrt-R | CTTGTGCAACATCCTTGCC |
| TuMV-P1-qrt-F | GGCTAGTTTGAAGAGAAGCTC |
| TuMV-P1-qrt-R | GCGCTTTAGCTTCATTGCCC |
| TuMV-HC-qrt-F | CGCATACCGTAGTGACAATC |
| TuMV-HC-qrt-R | GTTATCTTTCCGCATGGGAAC |
| TEV-CP-qrt-F | GCTGCAGTACGAAACAGTGG |
| TEV-CP-qrt-R | GCATGTTACGGTTCACATCG |
| TEV-P1-qrt-F | GAGGCAAGGCTCGTACGG |
| TEV-P1-qrt-R | CAGCGAACGTTACCTTCGC |
| TEV-HC-qrt-F | CCGAGAACTACTCACAAGG |
| TEV-HC-qrt-R | GTGAATGGAGCTTGTTTGCG |

2.11 Protein extraction and Western blot

Plant tissues were collected in liquid nitrogen and stored at -80°C until use. Samples were ground to a fine powder under liquid nitrogen and thawed in the protein extraction buffer [50 mM Tris-HCl, pH 7.5, 50 mM DTT, 10% (v/v) Glycerol, 150 mM NaCl, 0.1% Triton X100, 1 pill of protease inhibitor cocktail (Roche) to 50 mL extraction buffer right before use]. Protein extracts were mixed vigorously and incubated for 20 min at room temperature or overnight under -20°C . The cell debris was removed by centrifugation at 20,000 g at 4°C for 20 min. Supernatants were boiled with the 6 \times SDS loading buffer [1.2 g sodium dodecyl sulfate (SDS), 6 mL glycerol, 0.006 g bromophenol blue, 0.462 g DTT to 10 mL, 3.75 mL 1M Tris, pH 6.8] at 99°C for 10 min and chilled on ice for 5 min. After centrifugation at 20,000 g at 4°C for 10 min, the total protein extract was resolved on sodium dodecyl sulfate polyacrylamide gel electrophoresis (SDS-PAGE), electro-transferred to a nitrocellulose membrane, and subjected to Western blot analysis using the relevant primary and secondary antibody set following the manufacturer's instructions. The immuno-stained proteins were visualized by ECL Western Blotting Detection Reagents (Amersham) according to the protocols recommended by the supplier.

2.12 Functional analysis of *Arabidopsis* T-DNA insertion lines

2.12.1 Selection of T-DNA insertion lines

The corresponding T-DNA insertion lines of *Arabidopsis* were selected for each candidate gene based on their availability and genotype, with a preference for insertions in the exon or 5'-untranslated region (5'-UTR). Seed stocks of *Arabidopsis* T-DNA insertion mutants were purchased from ABRC. Information of mutant lines and insertions was obtained from the Salk Institute Genomic Analysis Laboratory website (<http://signal.salk.edu/>).

2.12.2 Screening for homozygous *Arabidopsis* T-DNA insertion lines

The genotyping of T-DNA line was confirmed by the PCR screen using the T-DNA left border specific primer, LBb1.3, and a gene specific primer set, LP and RP (Table 9),

following the protocols suggested by ABRC (<http://signal.salk.edu/tdnaprimers.2.html>). Primer sets of LP and RP were used to amplify the target alleles in order to identify the wild-type allele, while primers Lb1.3 and RP were used to detect the mutant allele. The heterozygous T-DNA insertion lines were grown and self-pollinated for their next generations. The descendant plants were genotyped again as described previously. All genotyping primers were designed using the T-DNA iSect tool (<http://signal.salk.edu/tdnaprimers.2.html>).

Table 9 Primers used for screening of *Arabidopsis* homozygous insertion lines.

| Primer Name | Primer Sequence (5'-3') | Gene Inserted |
|-----------------|---------------------------|---|
| LBb1.3 | ATTTTGCCGATTTCGGAAC | Of pBIN-pROK2 for SALK lines |
| SALK_059302C-LP | TATGGAGGCATTGTCTCTTGG | Protein N-MYC downregulated-like 2 (<i>NDL2</i>) |
| SALK_059302C-RP | ACCTCATGGCCAAGAGGAC | |
| SALK_074252C-LP | TGGGTATATCGACAACACAAGTC | |
| SALK_074252C-RP | TCACCAATCGGTCAAAAAGTC | |
| SALK_013645-LP | TCGATAACCCAATTCGTTTTG | |
| SALK_013645-RP | GTCATCAGCTGAGAGCAAAGG | |
| SALK_022668-LP | TGCCTCAGGTTGATATCGAAC | Tetratricopeptide repeat-containing protein (<i>TPR</i>) |
| SALK_022668-RP | TTTTACGTCCGAAGAAACCAG | |
| SALK_030248C-LP | GTCTTTTGTACGTCCCTCCTC | Uncharacterized protein 3 (<i>UCP3</i>) |
| SALK_030248C-RP | CTTCGAGGTTATGGGAAGGAC | |
| SALK_123978C-LP | TTGGAACGTAGACAAGATCCG | |
| SALK_123978C-RP | ATTACTCAGCATCCACAACCG | |
| SALK_080927C-LP | TTATTTAAACCATGCGAACCG | |
| SALK_080927C-RP | TTCTCCGGTACAATCTTGGTG | |
| SALK_026550-LP | ACTCATGGGCAGATACAGTGG | 6-phosphofruktokinase 4 (<i>PFK4</i>) |
| SALK_026550-RP | CAGTTGATGAATATCAACTGACCTG | |
| SALK_026549-RP | TTCACCAGTCAAGAAACTCGG | |
| SALK_012602C-LP | ACCACTGTATCTGCCCATGAG | |
| SALK_012602C-RP | AGGCGAACTTTTGTGAGTTCC | |
| SALK_066115C-LP | TGGGATGAAGATCTTGGAGTG | Lysine ketoglutarate reductase trans-splicing related 1 (<i>LKRI</i>) |
| SALK_066115C-RP | TGAATCAAAAAGTCGCAGAACC | |
| SALK_129295C-LP | CCATTGATCCATGTTTCCATC | |
| SALK_129295C-RP | TCTTGCATGTGCGTAGATCAG | |
| SALK_014631C-LP | TTCCATGACGATTTACCCTG | |
| SALK_014631C-RP | CACTTACCATCTGGGTTTTGC | |
| SALK_139265C-LP | TTTCAGCTTGCAGTCATCATG | Actin depolymerizing factor 3 (<i>ADF3</i>) |
| SALK_139265C-RP | TCAGAAGTTTGAAACAAACAGC | |
| SALK_065622C-LP | AAGGGAAGACGTGGATGACTC | |
| SALK_065622C-RP | TAGGTTGGCAACTTGGCATAG | |

Table 9 (continued)

| | | |
|-----------------|---------------------------|--|
| SALK_040467-LP | ACAGGCTTCGAATCTCCTCTC | Uncharacterized protein 4 (<i>UCP4</i>) |
| SALK_040467-RP | TTGTTAAATTTTGCCTCCACG | |
| SALK_130660C-LP | GAGATAGCTGCTGGGTCACAG | |
| SALK_130660C-RP | CTTGCCTTACAAACTCATCGG | |
| SALK_133531C-LP | GAGATAGCTGCTGGGTCACAG | |
| SALK_133531C-RP | CTTGCCTTACAAACTCATCGG | |
| CS843375-LP | GGGTGGATTAGGAAATGAAGC | Plant invertase/pectin methylesterase inhibitor domain-containing protein (<i>IPME</i>) |
| CS843375-RP | GCCATAAAAATCAGCCTCTCC | |
| CS436734-LP | TGGTTAATCAAATTTGCTGTTTGGT | IPME, vector pAC161 |
| CS436735-RP | TCTTCTTCCCACCGAGTCT | |
| SALK_018458C-LP | TTGTGGGTTGGCTCTGTAAAG | D111/G-patch domain- containing protein (<i>DDP</i>) |
| SALK_018458C-RP | GATCGAAGACTCGGTTTAGGG | |
| SALK_105440C-LP | CCACGACGACTTAGGAAACTG | |
| SALK_105440C-RP | GAACGTGAGCAGAAGATCCAG | |
| SALK_073254C-LP | GAGCTTGTGGGAATAGCTGTG | Serine/threonine-protein kinase (<i>SNT7</i>) |
| SALK_073254C-RP | TAGTTGAACATGCGTGAGTCG | |
| SALK_134469-LP | TCAACACTTGCTGGTTTGATG | |
| SALK_134469-RP | GAACCAAAGTAATCCAGGGC | |
| SALK_072531C-LP | GTTTTGGCCTTAAATGTTGGC | |
| SALK_072531C-RP | CTACTCCAGGAGCAGTGATCG | |
| SALK_025646C-LP | AGAACCAAAACGACATCAACG | Sugar transporter ERD6-like 3 (<i>ESL1</i>) |
| SALK_025646C-RP | TCCCCATTTTCCCTATACACC | |
| CS859783-LP | AGAACCAAAACGACATCAACG | |
| CS859783-RP | TCCCCATTTTCCCTATACACC | Dessication responsive protein (<i>RD2</i>) |
| SALK_104907C-LP | ACCAAGGATGGAGGTATCAGG | |
| SALK_104907C-RP | TCTGCAAGGAAGCAGAGAAAG | ABC transporter G family member 25 (<i>ABCG25</i>) |
| SALK_016500C-LP | ACATGAGACCACAAAGGATCG | |
| SALK_016500C-RP | AAAAAGCATAACCACGTGTTTAGG | |
| SALK_128873C-LP | TCGTGGAAACGTATTTTCATCC | |
| SALK_128873C-RP | AAGAACACGATTGGCTGATTC | |

Table 9 (continued)

| | | |
|-----------------|--------------------------|--|
| SALK_056437-LP | GGGAACATACGGTTACTGTGC | Protein kinase family protein (<i>PKP</i>) |
| SALK_056437-RP | AGATACCTGACACATGCTGCG | |
| SALK_019586-LP | ATCACGAGAACAACACTTCCATGG | Beta-1,4-N-acetylglucosaminyl-transferase family protein (<i>AGTP</i>) |
| SALK_019586-RP | TTGGGAGGAACAACACTGAACAAG | |
| SALK_019130C-LP | GCAATGGTACCACCATTGATC | 60S ribosomal protein L3-1 (<i>RPI</i>) |
| SALK_019130C-RP | CATCCCTTTCCTCTTCCTTTG | |
| SALK_045063C-LP | ATACGGTGGCAGCAGTAACAC | |
| SALK_045063C-RP | CGCCTTCACTGATAAACCAAC | |
| SALK_003794-LP | GCAATGGTACCACCATTGATC | |
| SALK_003794-RP | TCTTCCTTTGCGTGAATTCAC | |
| SALK_003445C-LP | CTCTACAAGCTTTCGACCACG | Cytochrome c oxidase assembly protein CtaG/Cox11 |
| SALK_003445C-RP | GGAGGGTGTACAAGAAGGAGG | |
| CS875926-LP | AAATTCGACTGAACGGATGTG | |
| CS875926-RP | TTTGCGTTGAACAGTACCTCC | |
| SALK_026233C-LP | TACGGTTCATTTCGATTTTTG | Heptahelical transmembrane protein2 (<i>HHP2</i>) |
| SALK_026233C-RP | TTCTCCGTTTCTGCATGATTC | |
| SALK_149660C-LP | ACAAATCCCCCAAAAAGATTG | |
| SALK_149660C-RP | ATGAATCAACCCTCCTTGAG | |
| SALK_048056-LP | TTAAACGTGACACACACTCGC | |
| SALK_048056-RP | CACTCAAAGAGCGAGAATTGC | |
| SALK_061798C-LP | GCTTATTCTGCTGCAATGTC | Selenoprotein, Rdx type (<i>Rdx</i>) |
| SALK_061798C-RP | CGCAGAAGGAAAGAACTCTTC | |
| SALK_038796C-LP | AGTGTGACTGGTGTTCATCCC | |
| SALK_038796C-RP | TCCAAAGGAGTTTGTGATGG | |
| SALK_140822-LP | CGAATCTGATTTTGTGATTCG | Ubiquitin C-terminal hydrolase 3 (<i>UCH3</i>) |
| SALK_140822-RP | GAATTTGGTAGGTGCATAGCG | |
| SALK_020444-LP | GATGTGAAACTACCCCTTCCC | Glycerol-3-phosphate dehydrogenase [NAD(+)] (<i>GPDHC1</i>) |
| SALK_020444-RP | CTGTGGAGCTGCTAAATGGAG | |
| CS412653-LP | TGGAAGAACGCATGATTCTGGA | Nucleotide/sugar transporter family protein (<i>NST</i>) , vector pAC161 |
| CS412653-RP | CCCAAAGCCTTTCTCAGGC | |
| pAC161LB-R | GACGTGAATGTAGACACGTC | LB primer for vector pAC161 |

Table 10 Primers used for detecting gene expression of *Arabidopsis* homozygous insertion lines.

| Primer Name | Primer Sequence (5'-3') |
|--------------------|--------------------------------|
| NDL2-NF | ATGGCGGATTCAAGCGATTC |
| NDL2-NR | CATGGCCAAGAGGACTGATG |
| NDL2-CF | CTAGACAGACGATACGGTGC |
| NDL2-CR | CTAGAGCGAGTCGTGTCTTTATC |
| TRP-NF | TATGAAGGCAGTATCGCTGC |
| TRP-NR | GTCTTCAGGATGAGCACTG |
| TRP-CF | AATGTTTCATCCAGGCGCGC |
| TRP-CR | AGATAACAGTTCCTGAACTTC |
| UCP3-NF | CTGCTTTGCTCTTACCAAAC |
| UCP3-NR | CAACTACTTCCCTCGAGTAAG |
| UCP3-CF | GGAGCATTGATGAGAGCTAG |
| UCP3-CR | CACTGCACTCATCATCGAATC |
| UCP4-NF | CCATAATTCTTCCTCCGGC |
| UCP4-NR | CCAAGTGAAGCGCCTTCTC |
| UCP4-CF | CGACATGCGTCGGAAACTTG |
| UCP4-CR | GTCTAGCCTGCTTTGTCTG |
| IPME-NF | ATGGCTCCTACACAAAATCTC |
| IPME-NR | CTGCACCATTATGACGACC |
| IPME-CF | TCACTATGCGTCCGTACTC |
| IPME-CR | GTAAAGCGCGTTGCTCGTAA |
| LKR1-NF | CAGCCTTGTATAGAAGTGG |
| LKR1-NR | GTACTGTACACATTAGCACC |
| LKR1-CF | CCTTTTGGTATCATGCAACC |
| LKR1-CR | GATCCCACCATTGATCCATG |
| PFK4-NF | ATGGAAGCTTCGATTTCGTTTC |
| PFK4-NR | CGTCTTCTAGGACAAACCC |
| PFK4-CF | CTGGGTAICTCAGGTTTCAC |
| PFK4-CR | GAGATCTTCATGTTATCGATC |
| DDP-NF | GGTCTTGAAAGCAAGAGC |

Table 10 (continued)

| | |
|-----------|------------------------|
| DDP-NR | GTTGTTTGCGAGCATCAGC |
| DDP-CF | GGCTAAGACCACGGTTGC |
| DDP-CR | CTTCGTCGCTATCGTTCCC |
| Rdx-NF | CTGCAGTCACCATGAAGAAG |
| Rdx-NR | GCCTGAGCTTTGAAGGTAAG |
| Rdx-CF | ATTGAAAGAAGGTAGATTCCC |
| Rdx-CR | TCAGTAGCTGCTGCCTGTG |
| UCH3-NF | CATCTAAGAGATGGCTTCCAC |
| UCH3-NR | CCTTGTCTTGCTCGATTCTC |
| UCH3-CF | GCTGGTGATACACCTGCTTC |
| UCH3-CR | CAGGTTCTCTTAGAGATGGC |
| SNT7-NF | CAGACTATCATGAGACAACTC |
| SNT7-NR | GCTCATGATGTATTGCTCAG |
| SNT7-CF | GTGGCAGATGAATTTGCCAG |
| SNT7-CR | CGATTCCACCGTCTAGATC |
| GPDHC1-NF | CTGCTCTTGAACCAGTTCC |
| GPDHC1-NR | CCTCCCATTACTTCATGTGTC |
| GPDHC1-CF | CAGGGTGTTTCTGCAGTGG |
| GPDHC1-CR | CTGACCAAGAAGGGAAGGC |
| PKP-NF | ATGGGATGTTTCGGACGC |
| PKP-NR | CTTCATCTTCAACATTAGTATC |
| PKP-CF | GTCTCGCTGATCATCCAAATC |
| PKP-CR | CGTGATATCCTTCATCGATC |
| ESL1-NF | CGAATGTCGTATCACTGCTG |
| ESL1-NR | GACCCATGAGATCTGCAAC |
| ESL1-CF | CTGAAGAAGCCAACACTATC |
| ESL1-CR | CATTGAGCCAATGCTGCTTG |
| ABCG25-NF | GGTTCAGACTCTTGCCGGG |
| ABCG25-NR | GTTACACCGTCAGTCTGAC |
| ABCG25-CF | GCAACATGGTTTAGCCAACTC |
| ABCG25-CR | GGACGCACGCTCTCTAGTG |

Table 10 (continued)

| | |
|---------|-----------------------|
| AGTP-NF | CTCTTCACTCTCCTGCCAC |
| AGTP-NR | GTTACTGAACAAGGCAGCATC |
| AGTP-CF | CACACATTCAGGGAGATTATC |
| AGTP-CR | CAGCCAGATTCTCGTTTGC |
| NST-NF | ATGGAGTGGCCATGGTCGG |
| NST-NR | GATTCTGTCTCCTCAGTGC |
| NST-CF | GGTGGATGCTTCTTGCAGC |
| NST-CR | CCGTAGCTAACTGCGCTGC |

2.12.3 Gene expression analysis of *Arabidopsis* T-DNA insertion lines

The gene expression was verified by RT-PCR with the gene specific primers (Table 10) to confirm T-DNA line as a true mutant. The total RNA used for cDNA synthesis was extracted from *Arabidopsis* leaf tissues. All positive T-DNA insertion lines were grown and self-pollinated for next generation and genotyped again by PCR for T-DNA insertion and RT-PCR for gene expression determination prior to the virus infection assay.

2.13 Mechanical inoculation

Approximately 1 g of fresh leaf tissues of TEV/TuMV infected *N. benthamiana* were used as the source of viral material. Plant tissues were ground using a mortar and pestle in 10 mL inoculation buffer, which was prepared by adding 1.0 g of polyvinylpyrrolidone-40 (Sigma) and 0.1 g of sodium diethyldithiocarbamate trihydrate (Sigma) into 1× PBS buffer [pH 7.4, 1.35 M sodium chloride, 27 mM potassium chloride, 43 mM sodium phosphate (dibasic, anhydrous), 14 mM potassium phosphate (monobasic, anhydrous)]. Two well-expanded young leaves of *N. benthamiana* (approximately 3~4 weeks old) and *A. thaliana* (approximately 4 weeks old) intended for inoculation were dusted with carborandum powder followed by gently rubbing to spread the inoculum over the leaf surface with gloved fingers to facilitate virus entry, while supporting leaves with

the other hand. The control plants were rubbed with inoculation buffer alone as mock inoculations.

2.14 Biolistic bombardment

N. benthamiana plants (approximately 3~4 weeks old) were biolistically inoculated using the Helios Gene Gun System (Bio-Rad, Hercules, CA, U.S.A.). Microcarrier cartridges were prepared with 1.0 μm gold particles coated with TEV infectious plasmids at a DNA loading ratio of 2 $\mu\text{g}/\text{mg}$ of gold and a microcarrier loading quantity of 0.5 mg/shooting, according to the manufacturer's instructions. A helium pressure of 100 psi was used. Two cartridges were shot onto different leaves of the same plant from the leaf adaxial side.

Chapter 3 Results

3.1 Subcellular localization of P1 in plant cells

3.1.1 Nuclear localization of P1 protein

As the size of P1-YFP or P1-CFP is about 62 kDa which is around the maximal size for protein diffusion through the nuclear pore, P1-coding regions of both TEV and TuMV were introduced into the expression vector pPanGate-GUS-YFP to explore the subcellular localization of P1 *in planta*. The plasmids were introduced into GV3101 and then infiltrated into *N. benthamiana* leaves for transient expression. The infiltrated leaves were sampled at 48 hours post infiltration (hpi) and observed using the Leica TCS SP2 inverted confocal microscopy. P1s of TEV and TuMV were both present in the cytoplasm and nucleus while as a control, GUS-YFP, was only observed in the cytoplasm (Figure 2A, B and D). The coding region of TEV VPg, a well-known nuclear localized protein, was inserted into the vector pEarlyGate102 and the resulting clone was used to express VPg as a nuclear marker (Sadowy et al., 2001).

To determine the P1 localization during viral infection, TEV P1 was cloned into the Gateway vector pGWB 454 and transiently expressed in TEV-GFP-infected *N. benthamiana*. The infectious clone p35TuMV-P1GFP was generated to express a GFP tagged at the C-terminal of P1. The localization of P1 was not altered in virus-infected plants; in other words, P1 still remained in the cytoplasm and nucleus (Figure 2C and E).

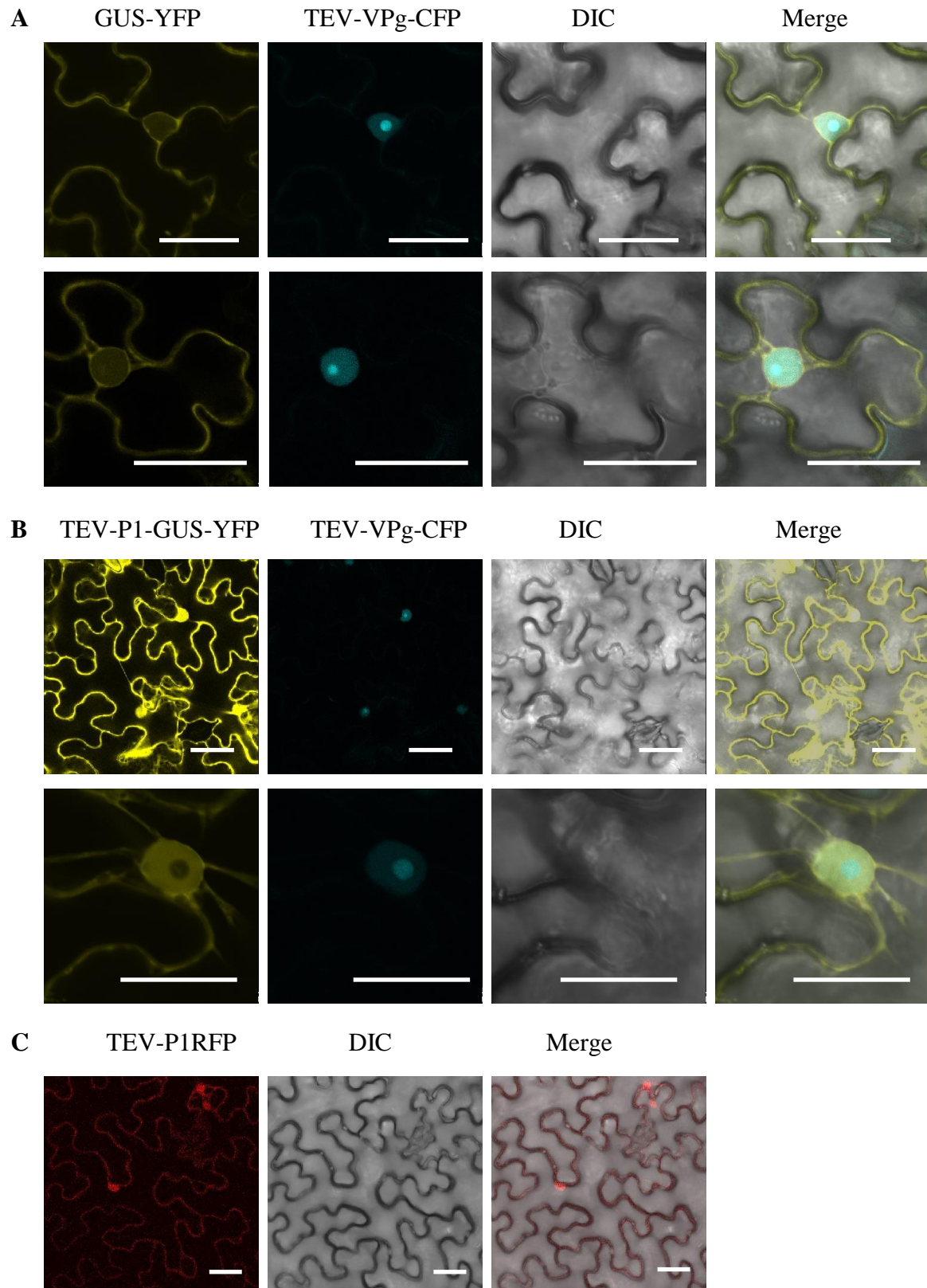


(Figure 2 continued)

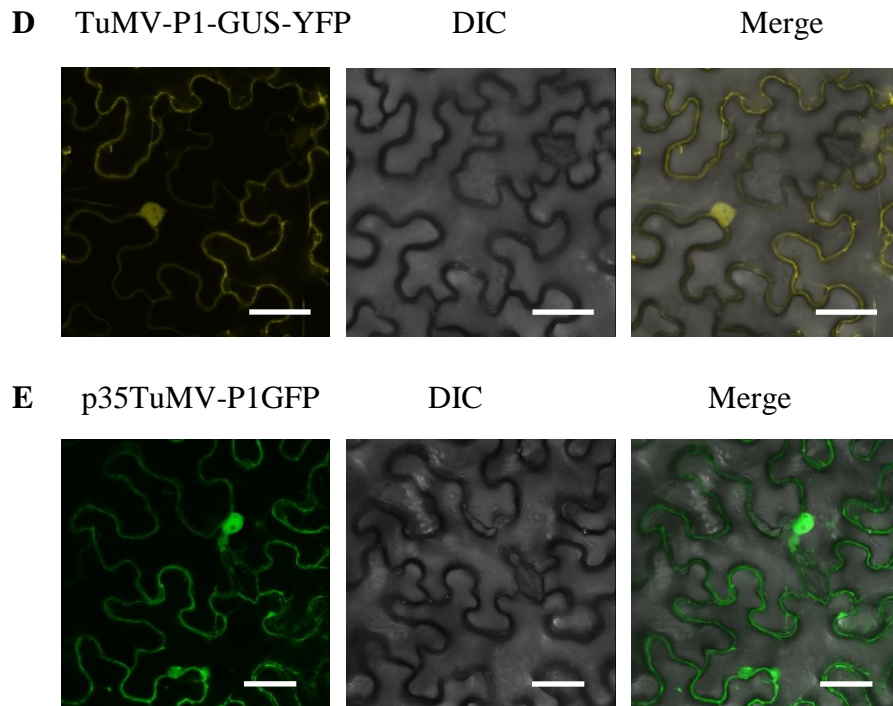


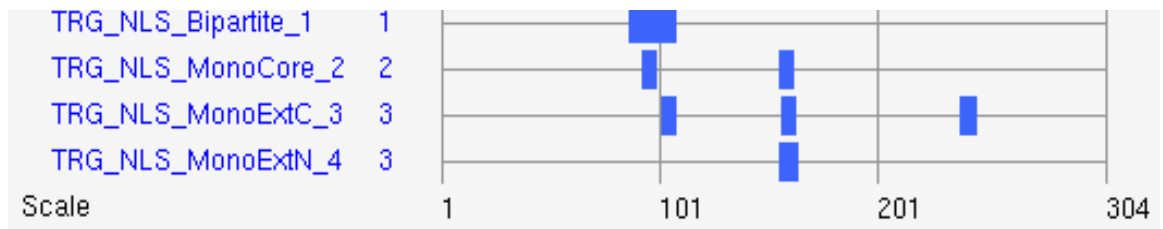
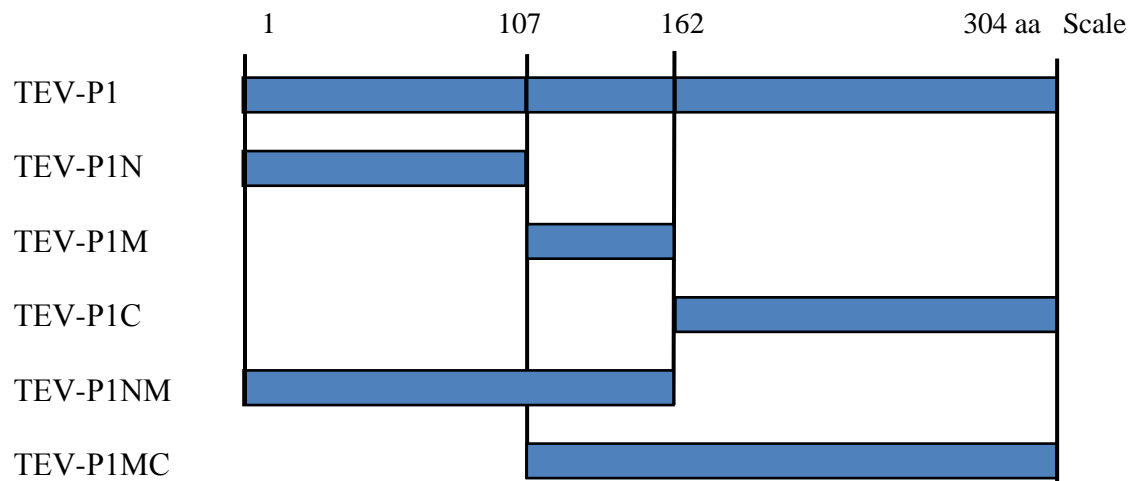
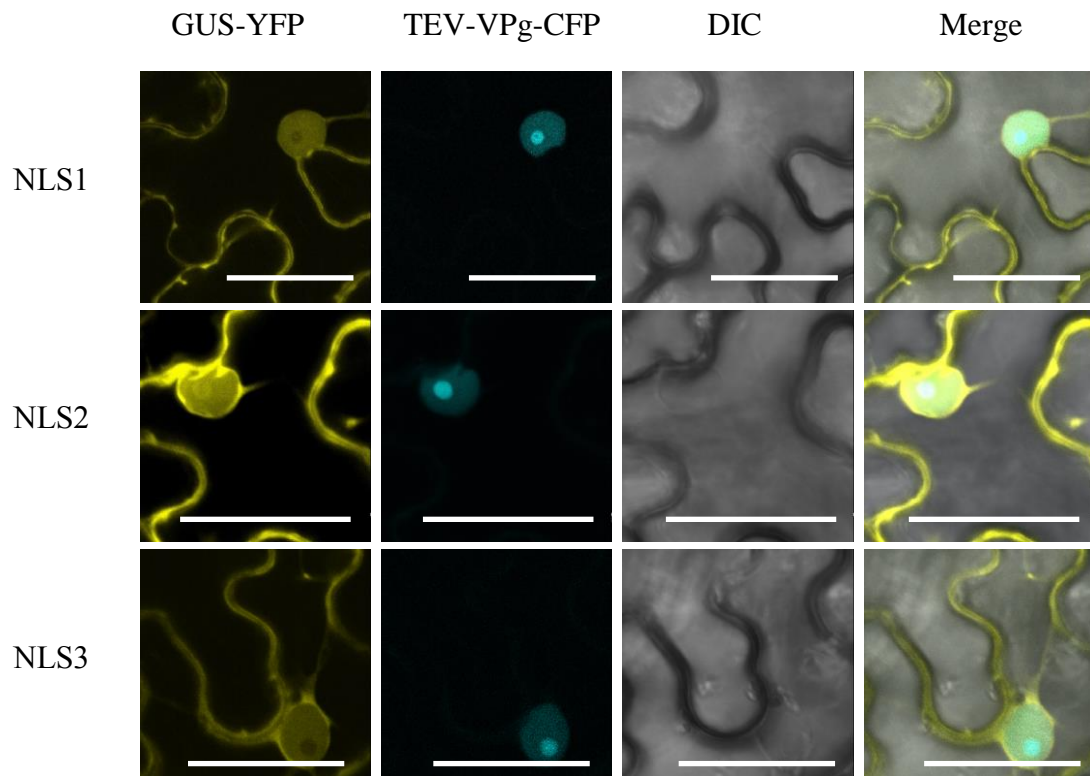
Figure 2 Subcellular localization of P1 protein in *N. benthamiana* leaf cells.

(A) GUS-YFP was used as the negative control. (B) Subcellular localization of TEV P1 in healthy *N. benthamiana* leaves. (C) Subcellular localization of TEV P1 in TEV-GFP-infected *N. benthamiana*. (D) Subcellular localization of TuMV P1 in healthy *N. benthamiana*. (E) Subcellular localization of P1 in p35TuMV-P1GFP-infected *N. benthamiana*. TEV-VPg-CFP was used as a nuclear marker. DIC, differential interference contrast. Bars, 35 μ m.

3.1.2 Determination of TEV nuclear localization signals (NLSs)

Since P1 was localized to the nucleus, the TEV P1 amino acid sequence was analyzed extensively for any possible nuclear localization signals (NLSs) using the ELM tool (<http://elm.eu.org/search/>). It was revealed that P1 contained three potential NLSs at amino acid residues 92~106 (NLS1), 155~162 (NLS2) and 238~244 (NLS3) (Figure 3A), which were located in the N-terminal (N, P1_{1~106}), middle (M, P1_{107~162}), and C-terminal regions (C, P1_{162~304}) (Figure 3B), respectively. The sequences of all three predicted NLSs were fused at the N-terminus of GUS and introduced into the plasmid pEarlyGate 101. The cDNA fragments encoding N, M and C regions of TEV P1 were cloned and recombined into the plasmid pPanGate-GUS-YFP. After transient expression in *N. benthamiana* cells and confocal analysis at 48 hpi, all the three NLSs did show the ability to direct the recombinant GUS-YFP protein into the nucleus (Figure 3C). N or M recombinant fusions were mainly localized in the nucleus, whereas the P1C-GUS-YFP fusion was distributed in both the cytoplasm and nucleus (Figure 3D). These data show that P1 contains at least three NLSs and the NLSs located in the N and M regions are very strong.

After finding out the approximate locations of NLSs, the site-directed mutagenesis was performed using overlapping PCR to mutate the potential NLS motifs. Single, double and triple site mutations were generated in both truncated and full sequences of TEV P1, and inserted into the expression vector pPanGate-GUS-YFP. Both the N region, without the NLS1, and the M part, without the NLS2, lost the ability to target the GUS-YFP protein to the nucleus (Figure 3E). But the C fragment of P1 still maintained the localization in the cytoplasm as well as nucleus without the NLS3 (Figure 3E). Regardless of single, double or triple site-directed mutagenesis into NLSs, TEV P1 remained present in the nucleus. These results confirm that all the three NLSs can work alone to target proteins into the nucleus, but there may be more NLS(s) in the C region of P1 in addition to NLS3.

A**B****C**

(Figure 3 continued)

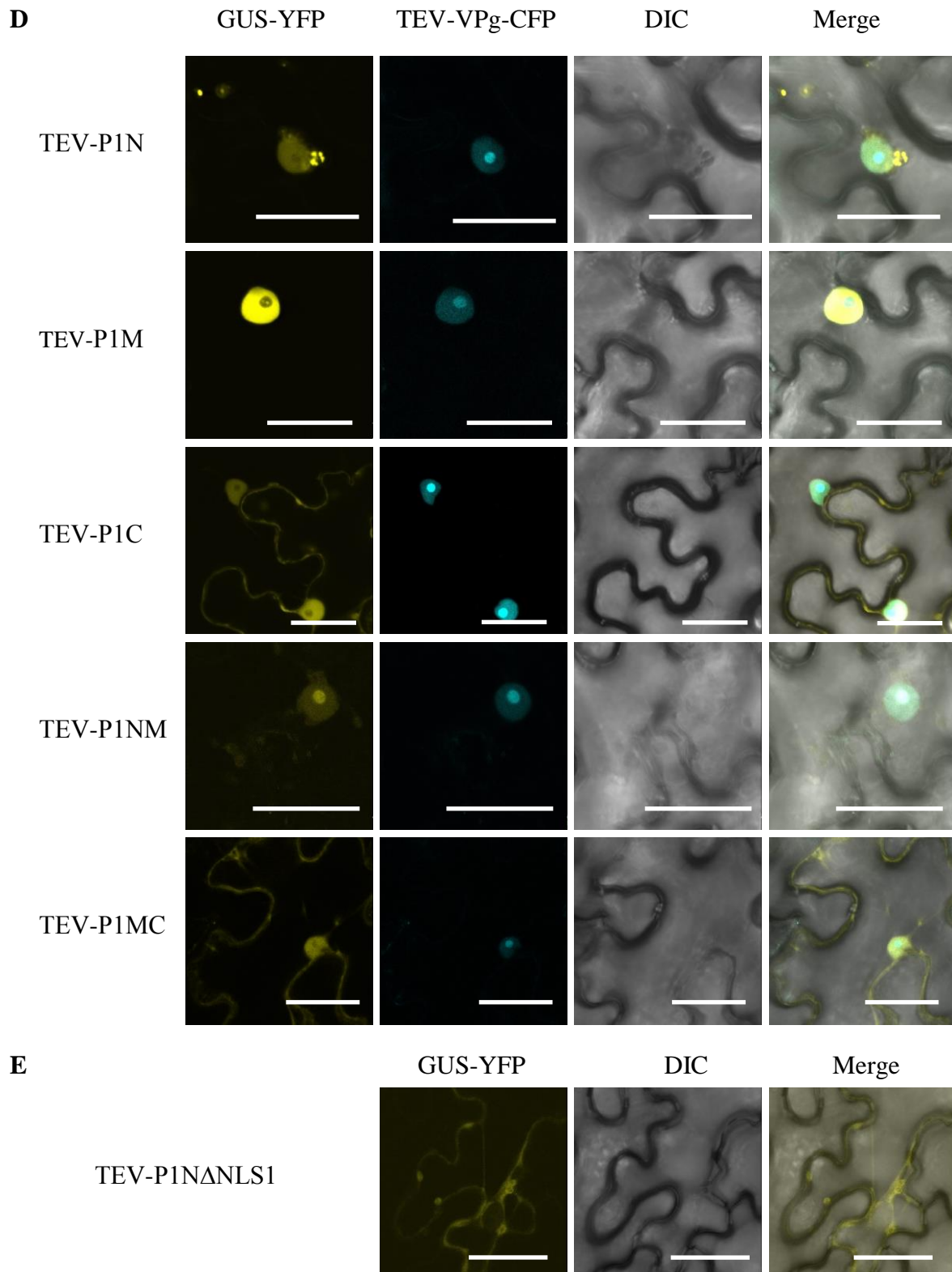
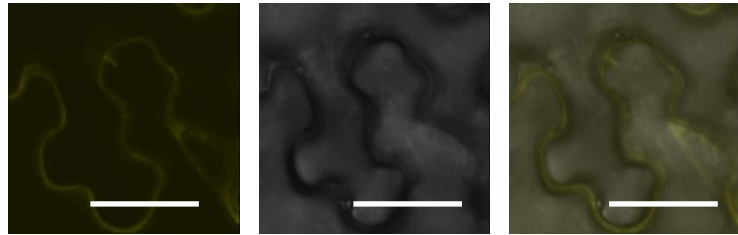
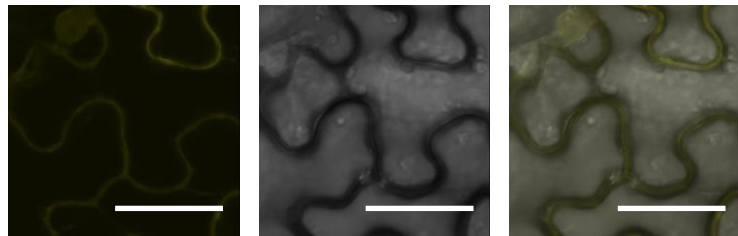


(Figure 3 continued)

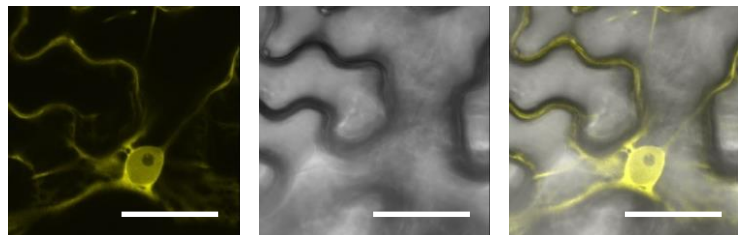
TEV-P1M Δ NLS2



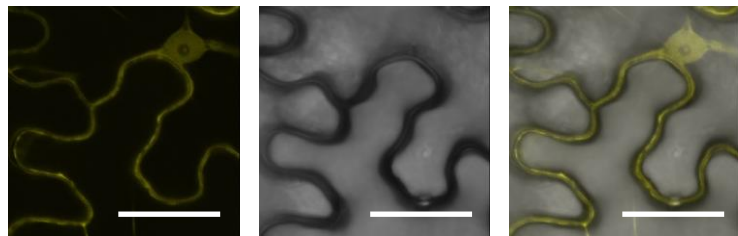
TEV-P1C Δ NLS3



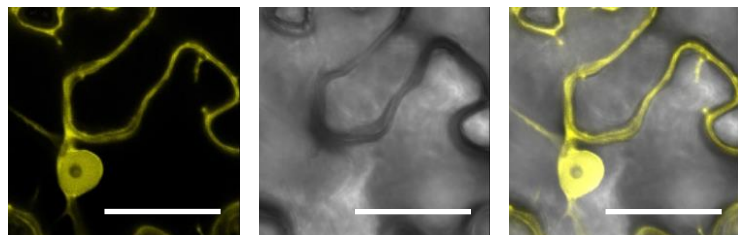
TEV-P1 Δ NLS1



TEV-P1 Δ NLS2



TEV-P1 Δ NLS3



TEV-P1 Δ NLS1&2

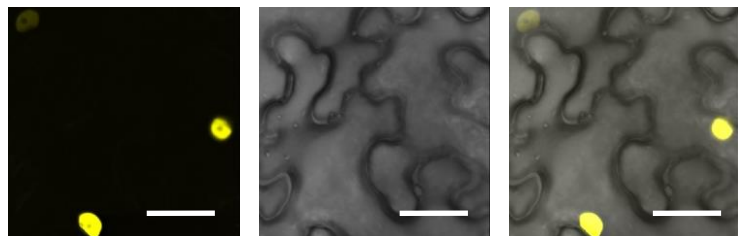


(Figure 3 continued)

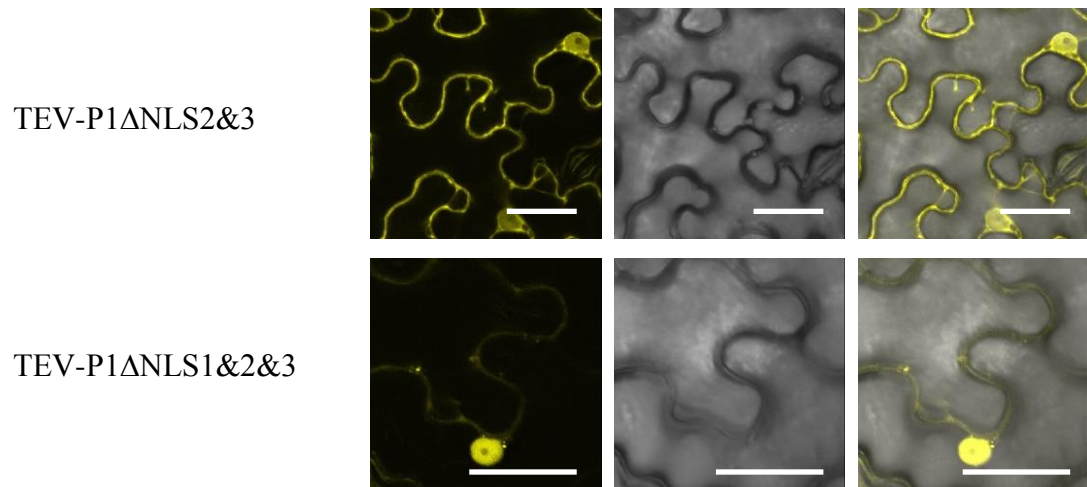


Figure 3 The determination of TEV P1 NLSs. (A) ELM analysis of TEV P1 protein sequence. (B) Partial sequences of P1. (C) (D) (E) The subcellular localization of P1 protein mutants in *N. benthamiana* cells. GUS-YFP showed in Figure 1 worked as negative control, while TEV-VPg-CFP worked as nuclear marker. DIC, differential interference contrast. Bars, 35 μ m.

3.2 Interactions between P1 and viral proteins

In this study, Y2H and BiFC assays were used to detect if P1 interacts with itself and/or other viral proteins. Interaction assays of different viruses have not always given similar results within the *Potyvirus* genus, so interactions between P1 protein and all mature potyviral proteins were tested in both TuMV and TEV using the Y2H and BiFC methods.

To determine whether the P1 protein is able to interact with viral proteins in TuMV, all 11 mature protein cistrons were cloned and transferred into vectors pGBKT7-DEST (bait) and pGADT7-DEST (prey). Co-transformants were isolated and plated on different selective media to detect activation of reporter genes. After incubation at 28°C for over a week, no positive clone was detected in yeast (data not shown). TuMV VPg and *Arabidopsis* eIF(iso)4E, which have proven to interact with each other in the Y2H assay, were used as the positive control. To confirm the protein-protein interaction results *in planta*, 11 cDNA fragments were recombined into the BiFC vectors pEarlyGate201-YN and pEarlyGate201-YC and transformed into *Agrobacterium*. Different combinations of clones were co-infiltrated *N. benthamiana* and analyzed by confocal microscopy on the daily basis, up to 5 days post inoculation (dpi). No positive fluorescence was visualized in the infiltrated leaf tissues (data not shown). TuMV CP, known to interact with itself in the BiFC assay, was used as the positive control.

In TEV, the same methods described above were applied to generate the interaction assays between the P1 protein and potyviral proteins. In all combinations except P3, the same results were obtained in both Y2H and BiFC assays (data not shown). Cloning TEV P3 was not successful probably because of its lethality in *E.coli* strain DH5 α .

3.3 Y2H screen of P1 interacting host proteins

Even though there was no interaction detected between the P1 protein and 11 potyviral proteins in TuMV and TEV, it seems impossible that a protein works alone without interaction at all with other proteins. Thus, the determination of P1 protein-host protein interactions is more urgent. Since *Arabidopsis* was used as the model host to study TuMV infection in this study, Mate & Plate™ Library - Universal *Arabidopsis*

(Normalized) in the yeast strain Y187 was purchased from Clontech for Y2H cDNA library screen to identify P1-interacting host proteins. A total of 9.43×10^7 mated clones (diploids) were screened after yeast mating using the pBGKT7-TuP1 transformed into Y2HGold as bait. Positive clones were isolated and transformed into the *E. coli* DH5 α strain for plasmid preparation and DNA sequencing. Sequencing data were analyzed online against the NCBI database. Based on BLAST results of obtained sequences, a total of 25 putative interacting protein partners of TuMV P1 were identified (Table 11). Because of the high-risk of “false positives”, the full-length of all host candidates were amplified from *Arabidopsis* cDNA and went for further confirmation using both the Y2H and BiFC systems. Only 19 were confirmed in yeast, and seven amongst them were verified in plant cells (Table 11).

Table 11 TuMV P1 interacting host candidates resulting from Y2H screen. Nineteen candidates were confirmed using the Y2H system and seven proteins were verified by both Y2H and BiFC approaches.

| Accession no | Gene description | Frequency | Y2H | BiFC |
|--------------|---|-----------|-----|------|
| GI 30687960 | Plant invertase/pectin methylesterase inhibitor domain-containing protein (<i>IPME</i>) | 10 | + | - |
| GI 334187955 | D111/G-patch domain-containing protein (<i>DDP</i>) | 3 | + | - |
| GI 30683793 | Protein N-MYC downregulated-like 2 (<i>NDL2</i>) | 9 | + | + |
| GI 145362068 | Actin depolymerizing factor 3 (<i>ADF3</i>) | 1 | + | + |
| GI 145359419 | Selenoprotein, Rdx type (<i>Rdx</i>) | 1 | - | - |
| GI 30684072 | Ubiquitin C-terminal hydrolase 3 (<i>UCH3</i>) | 1 | - | - |
| GI 186493981 | Serine/threonine-protein kinase (<i>SNT7</i>) | 1 | - | - |
| GI 145361261 | Tetratricopeptide repeat-containing protein (<i>TPR</i>) | 1 | + | + |
| GI 30686667 | Uncharacterized protein (<i>UCP1</i>) | 2 | + | - |
| GI 240256373 | Uncharacterized protein (<i>UCP2</i>) | 5 | + | - |
| GI 186507215 | Glycerol-3-phosphate dehydrogenase [NAD(+)] (<i>GPDHCl</i>) | 1 | - | - |
| GI 145360426 | Protein kinase family protein (<i>PKP</i>) | 2 | + | + |
| GI 186478280 | Sugar transporter ERD6-like 3 (<i>ESL1</i>) | 2 | + | - |
| GI 145361572 | Dessication responsive protein (<i>RD2</i>) | 1 | - | - |
| GI 145359534 | 6-phosphofructokinase 4 (<i>PFK4</i>) | 1 | + | + |
| GI 18409954 | ABC transporter G family member 25 (<i>ABCG25</i>) | 1 | + | - |
| GI 186478061 | Cytochrome oxidase assembly protein CtaG/Cox11 | 6 | + | - |
| GI 30678381 | Beta-1,4-N-acetylglucosaminyltransferase family protein (<i>AGTP</i>) | 3 | + | + |
| GI 42562333 | Uncharacterized protein (<i>UCP3</i>) | 2 | + | + |
| GI 145336439 | 60S ribosomal protein L3-1 (<i>RPI</i>) | 5 | + | - |
| GI 145335675 | Uncharacterized protein (<i>UCP4</i>) | 1 | + | - |
| GI 30688828 | Heptahelical transmembrane protein2 (<i>HHP2</i>) | 1 | + | - |
| GI 42562855 | Lysine ketoglutarate reductase trans-splicing related 1 (<i>LKR1</i>) | 1 | + | - |
| GI 145338028 | Nucleotide/sugar transporter family protein (<i>NST</i>) | 1 | + | - |
| GI 339773249 | <i>Arabidopsis thaliana</i> ecotype Col-0 mitochondrion | 1 | | |

3.4 Screening of homozygous *Arabidopsis* T-DNA knockout/knockdown lines

To identify the roles of *Arabidopsis* candidate genes in TuMV infection, *Arabidopsis* T-DNA insertion mutants carrying genetic lesions in the 22 candidate genes independently were analyzed. Forty-one *Arabidopsis* T-DNA insertion lines corresponding to the 22 candidates were selected from the TAIR database, and seed stocks were obtained from the ABRC (Table 12).

Homozygous T-DNA insertion lines were identified by PCR-based genotyping using the T-DNA left border specific primer (LbB1.3) and the gene-specific primer sets (Table 9). The progeny of self-pollinated heterozygous T-DNA insertion lines were grown and genotyped as described above. According to the preliminary genotyping results, a total of 29 homozygous *Arabidopsis* T-DNA insertion mutants corresponding to 19 candidate genes were verified (Table 13).

The gene expression of homozygous *Arabidopsis* T-DNA insertion lines was verified using RT-PCR with the gene specific primers (Table 10). Total RNA was isolated from leaf tissues of these homozygous lines and wild type *Arabidopsis* RNA was used as positive control. Based on the RT-PCR analysis, only 17 lines corresponding to 12 candidate genes were determined to be true knockout/knockdown mutants (Table 14 and Figure 4).

Eight knockout/knockdown mutant lines were challenged by TuMV and tested carefully for any (partial) resistance. qRT-PCR was performed to quantify the accumulation of TuMV RNA using primers flanking the CP region. Total RNA was isolated from the upper newly emerged leaves at 15 dpi. The *Arabidopsis Actin2* housekeeping gene was used to normalize the data. Three independent experiments, each consisting of three biological replicates, were carried out to confirm the quantitative assessment. In the *atrdx* (SALK_061798C), *atsnt7* (CS65732), *atlkr1* (SALK_129295C) and *atnst* (CS412653) mutant plants, TuMV RNA accumulation showed no significant difference with regard to that of wild type plants (Figure 5), while the *atndl2* (SALK_074252C), *attpr* (CS65556 and SALK_022668C) and *atucp3* (SALK_030248C) mutant plants showed marked

reduction comparing to that of wild type plants (Figure 9, 14, 19). Therefore, three *Arabidopsis* candidates, *AtNDL2*, *AtTPR* and *AtUCP3*, were selected for further characterization.

Table 12 List of *Arabidopsis* candidate genes and corresponding T-DNA insertion lines.

| Gene Names | TARI Locus | <i>Arabidopsis</i> T-DNA insertion lines |
|---|-------------------|---|
| <i>IPME</i> | AT5G20740 | CS436734; SAIL_1171_H11 |
| <i>DDP</i> | AT5G26610 | SALK_105440C; SALK_018458C |
| <i>NDL2</i> | AT5G11790 | SALK_059302C; SALK_074252C |
| <i>ADF3</i> | AT5G59880 | SALK_065622C; SALK_139265C |
| <i>Rdx</i> | AT5G58640 | SALK_061798C; SALK_038796C |
| <i>UCH3</i> | AT4G17510 | SALK_140822 |
| <i>SNT7</i> | AT1G68830 | CS65732; SALK_073254C; SALK_072531C |
| <i>TPR</i> | AT1G78915 | CS859833; CS65556; SALK_022668C |
| <i>GPDHC1</i> | AT2G41540 | SALK_020444 |
| <i>PKP</i> | AT2G28590 | SALK_056437; CS27216 |
| <i>ESL1</i> | AT1G08920 | CS859783; SALK_025646C |
| <i>RD2</i> | AT2G21620 | SALK_104907C |
| <i>PFK4</i> | AT5G61580 | SALK_012602C |
| <i>ABCG25</i> | AT1G71960 | SALK_016500C; SALK_128873C |
| Cytochrome coxidase assembly protein CtaG/Cox11 | AT1G02410 | SALK_003445C |
| <i>AGTP</i> | AT3G01620 | CS859576 |
| <i>UCP3</i> | AT1G26650 | SALK_080927C; SALK_030248C; SALK_123978C |
| <i>RP1</i> | AT1G43170 | SALK_019130C; SALK_045063C |
| <i>UCP4</i> | AT1G13990 | SALK_130660C; SALK_133531C |
| <i>HHP2</i> | AT4G30850 | SALK_026233C; SALK_149660C |
| <i>LKR1</i> | AT1G61240 | SALK_066115C; SALK_129295C; SALK_014631C |
| <i>NST</i> | AT3G02690 | CS412653 |

Table 13 List of homozygous *Arabidopsis* T-DNA insertion lines.

| Gene Names | TARI Locus | <i>Arabidopsis</i> T-DNA insertion lines |
|-------------------|-------------------|---|
| <i>IPME</i> | AT5G20740 | SAIL_1171_H11 |
| <i>DDP</i> | AT5G26610 | SALK_018458C |
| <i>NDL2</i> | AT5G11790 | SALK_059302C; SALK_074252C |
| <i>ADF3</i> | AT5G59880 | SALK_065622C; SALK_139265C |
| <i>Rdx</i> | AT5G58640 | SALK_061798C; SALK_038796C |
| <i>SNT7</i> | AT1G68830 | CS65732 |
| <i>TPR</i> | AT1G78915 | CS65556; SALK_022668C |
| <i>GPDHC1</i> | AT2G41540 | SALK_020444 |
| <i>PKP</i> | AT2G28590 | SALK_056437; CS27216 |
| <i>ESL1</i> | AT1G08920 | CS859783; SALK_025646C |
| <i>RD2</i> | AT2G21620 | SALK_104907C |
| <i>PFK4</i> | AT5G61580 | SALK_012602C |
| <i>AGTP</i> | AT3G01620 | CS859576 |
| <i>UCP3</i> | AT1G26650 | SALK_080927C; SALK_030248C; SALK_123978C |
| <i>RP1</i> | AT1G43170 | SALK_045063C |
| <i>UCP4</i> | AT1G13990 | SALK_130660C |
| <i>HHP2</i> | AT4G30850 | SALK_026233C; SALK_149660C |
| <i>LKR1</i> | AT1G61240 | SALK_066115C; SALK_129295C |
| <i>NST</i> | AT3G02690 | CS412653 |

Table 14 List of homozygous *Arabidopsis* T-DNA knockout/knockdown lines for TuMV infection assay.

| Gene Names | TARI Locus | <i>Arabidopsis</i> T-DNA insertion lines |
|-------------------|-------------------|---|
| <i>NDL2</i> | AT5G11790 | SALK_059302C |
| <i>Rdx</i> | AT5G58640 | SALK_061798C; SALK_038796C |
| <i>SNT7</i> | AT1G68830 | CS65732 |
| <i>TPR</i> | AT1G78915 | CS65556; SALK_022668C |
| <i>GPDHC1</i> | AT2G41540 | SALK_020444 |
| <i>PKP</i> | AT2G28590 | CS27216 |
| <i>ESL1</i> | AT1G08920 | CS859783; SALK_025646C |
| <i>PFK4</i> | AT5G61580 | SALK_012602C |
| <i>UCP3</i> | AT1G26650 | SALK_080927C; SALK_123978C |
| <i>HHP2</i> | AT4G30850 | SALK_149660C |
| <i>LKR1</i> | AT1G61240 | SALK_066115C; SALK_129295C |
| <i>NST</i> | AT3G02690 | CS412653 |

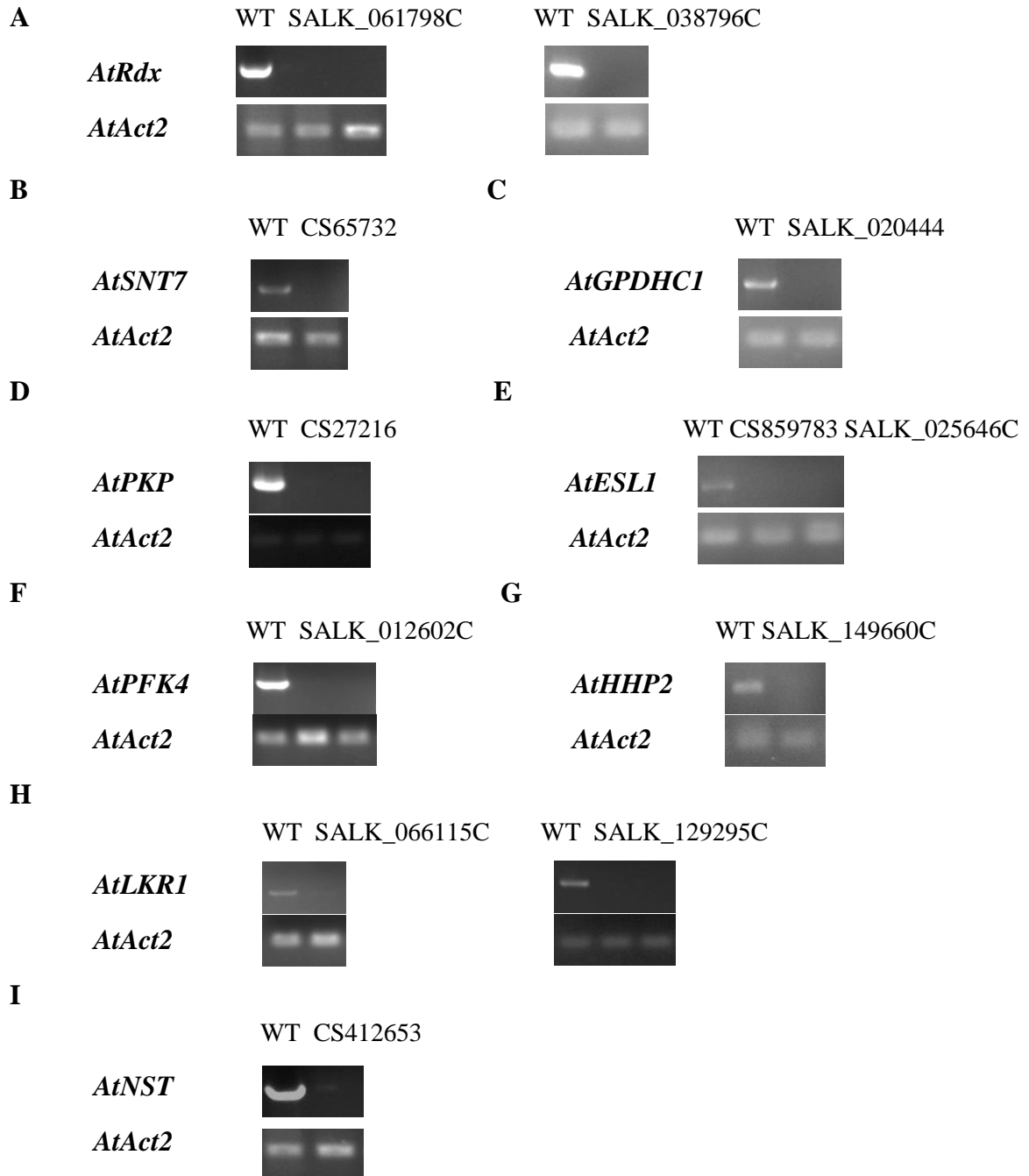


Figure 4 Gene expression analysis of homozygous *Arabidopsis* T-DNA insertion mutants. RT-PCR was conducted using *Arabidopsis* WT and mutant cDNA with gene specific primers. *AtAct2*, *Arabidopsis Actin2* was used as the internal gene control.

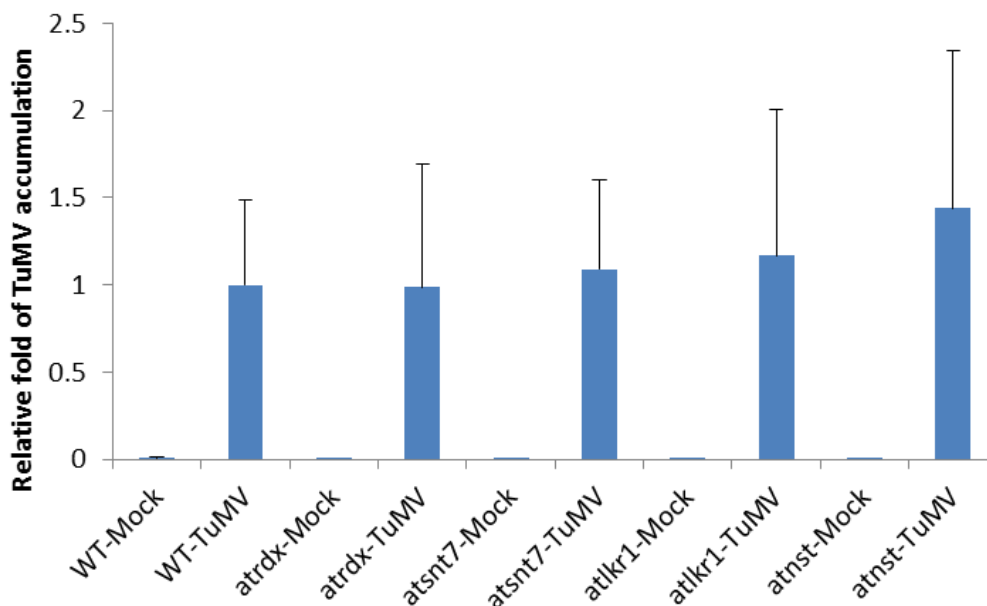


Figure 5 TuMV infection assay on *Arabidopsis* mutant and wild type plants. Total RNA used for qRT-PCR was extracted from the newly emerged leaves at 15 dpi. The internal gene control, *Arabidopsis Actin2* gene (*AtAct2*), was used to normalize the data. Error bars indicated standard deviation (n=9). No significant difference was detected from wild type plants (student's t test, $p < 0.05$).

3.5 Characterization of the *Arabidopsis* gene, *AtNDL2*

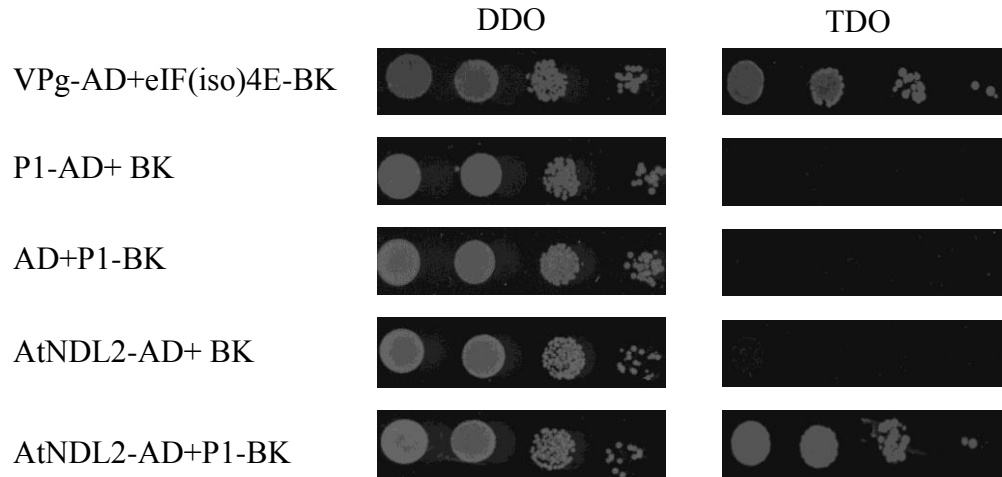
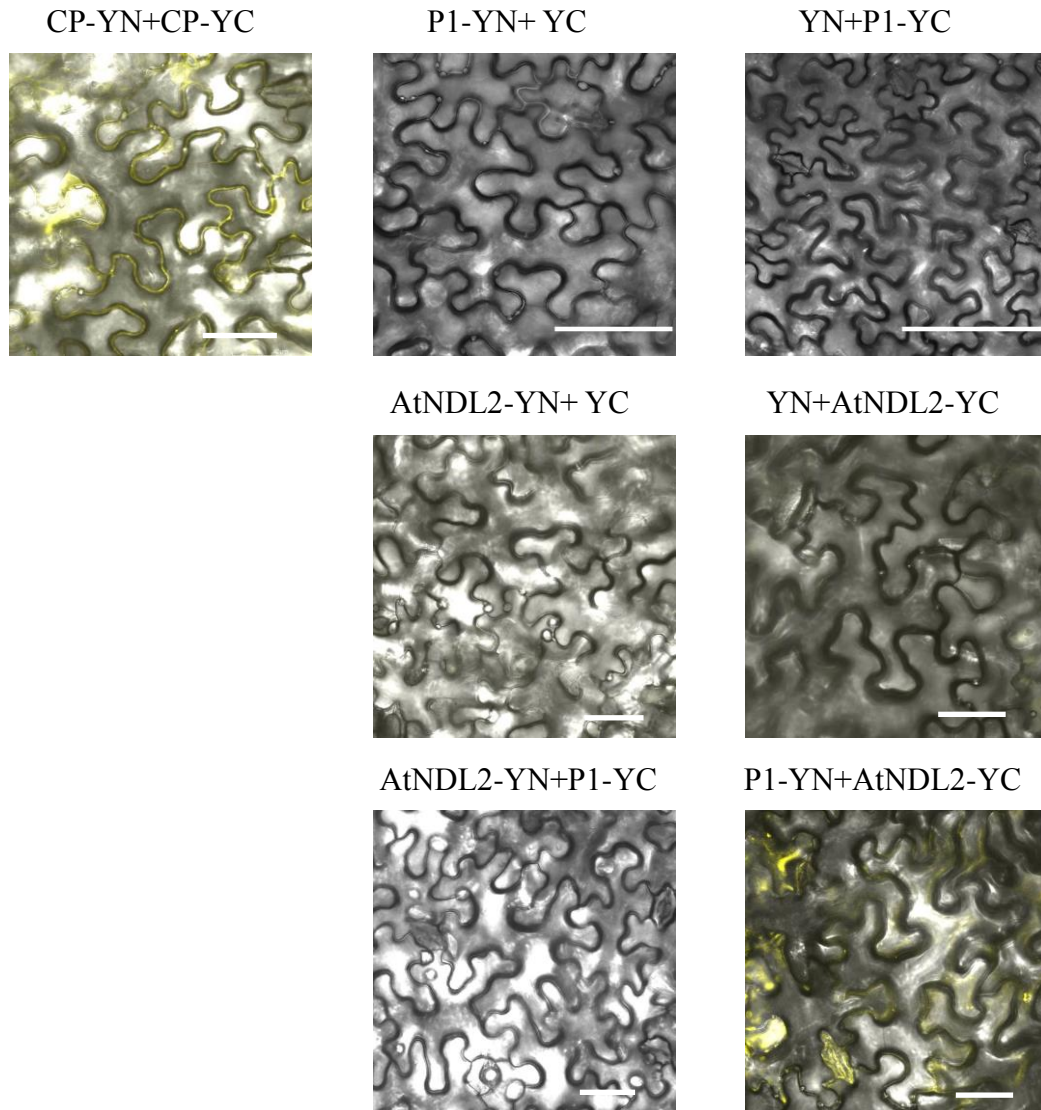
3.5.1 Interactions between *AtNDL2* and 11 potyviral proteins

The full cDNA sequence of *AtNDL2* was cloned from *Arabidopsis* cDNA and recombined into the Gateway compatible destination vector pGADT7-DEST for the Y2H assay. Protein-protein interaction between the full-length *AtNDL2* protein and TEV P1 was verified in yeast cells (Figure 6A). TuMV VPg and *Arabidopsis* eIF(iso)4E were used as the positive control. Several Y2H negative control combinations were set up to ensure the validity of the results. These combinations included P1-AD and empty BK vector, empty AD vector and P1-BK, as well as *AtNDL2*-AD and empty BK vector (Figure 6A).

To further investigate the interaction between P1 and AtNDL2 *in planta*, the BiFC assay was carried out (Figure 6B). TuMV CP-CP interaction was used as the positive control (Figure 6B). To make sure the validity of the results, several BiFC negative control combinations were applied, which included empty YN and YC of YFP vectors, AtNDL2-YN and empty YC vector, empty YN vector and AtNDL2-YC, P1-YN and empty YC vector, as well as empty YN vector and P1-YC. As observed under confocal microscopy at 3 dpi, the majority of the BiFC protein granules of AtNDL2-P1 were accumulated in the cytoplasm (Figure 6B).

To further investigate the possible interactions between AtNDL2 and other 10 TuMV proteins, *AtNDL2* was recombined into the Gateway bait vector in the Y2H assay. Co-transformants were selected and plated on the selective media SD/-Ade/-His/-Leu/-Trp. The positive and negative controls were generated as described previously. After 4 days of culture, AtNDL2 showed weak interaction with TuMV VPg (Figure 6C), and no interaction was observed with other 9 viral proteins (Figure 6C, and data not shown).

To investigate the subcellular localization of AtNDL2 *in planta*, *AtNDL2* were recombined into the vector pPanGate-GUS-YFP. AtNDL2 was present in the cytoplasm and nucleus while the negative control, GUS-YFP, was only observed in the cytoplasm (Figure 7).

A**B**

(Figure 6 continued)

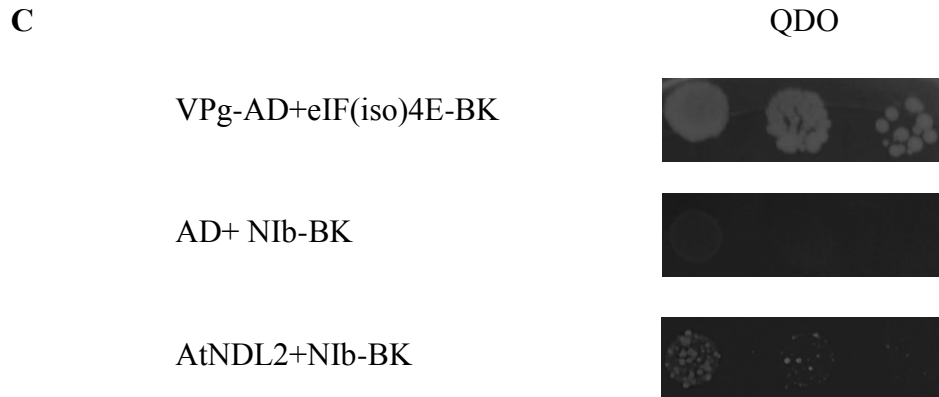


Figure 6 Protein-protein interactions between full-length *Arabidopsis* AtNDL2 and potyviral proteins. (A) Y2H assay of AtNDL2 and TuMV P1, overserved after 4 days of culture at 28°C. (B) BiFC assay of AtNDL2 and TuMV P1, observed at 3 dpi. Bars, 40 µm. (C) Y2H assay of AtNDL2 and TuMV NlB, observed after 4 days of culture at 28°C.

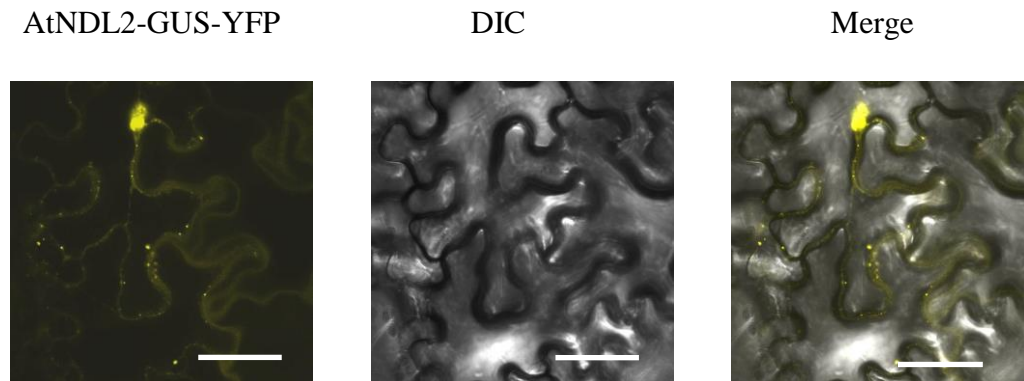


Figure 7 Subcellular localization of AtNDL2 in *N. benthamiana*. Bars, 40 µm.

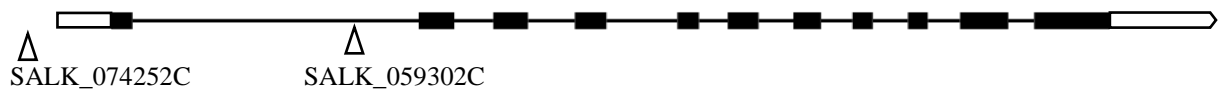
3.5.2 Verification of *Arabidopsis AtNDL2* T-DNA insertion lines

The full-length cDNA of *AtNDL2*, which contains 10 introns and 11 exons, is 1463 bp with a 5'-UTR of 132 bp, an ORF of 1035 bp, and a 3'-UTR of 296 bp (Figure 8A). It encodes a 344 aa polypeptide with a predicted molecular mass of 38.2 kDa and a PI of 5.66. The domain analysis using the Pfam program (<http://pfam.sanger.ac.uk/>) identified the Ndr domain (21 to 305 aa). Although Ndr gene family is known to be involved in cellular differentiation events, their precise cellular function is still unknown (Khatri and Mudgil, 2015).

Two *AtNDL2* T-DNA insertion lines, SALK_059302C and SALK_074252C were obtained from ABRC and analyzed using the PCR-based genotyping method. SALK_059302C contains a T-DNA insertion within intron 1 of *AtNDL2* while SALK_074252C contains an insertion within the promoter of *AtNDL2* (Figure 8A).

Homozygous T-DNA insertion lines were identified using the PCR genotyping method described earlier (Figure 8CD). RT-PCR analysis was carried out using the total RNA extracted from leaf tissues of *Arabidopsis* mutants, and wild type was operated as the positive control. Results showed that marked less expression of *AtNDL2* was detected in the T-DNA line, SALK_059302C. Thus, this line was determined to be a knockdown mutant of *AtNDL2* and named *atndl2* (Figure 8E). Another insertion line SALK_074252C showed no difference of *AtNDL2* gene expression comparing to the wild type and was abandoned for further use (Figure 8E).

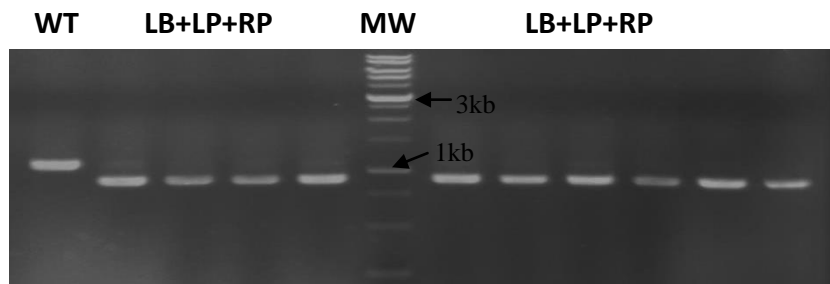
A

AT5G11790 (*AtNDL2*)

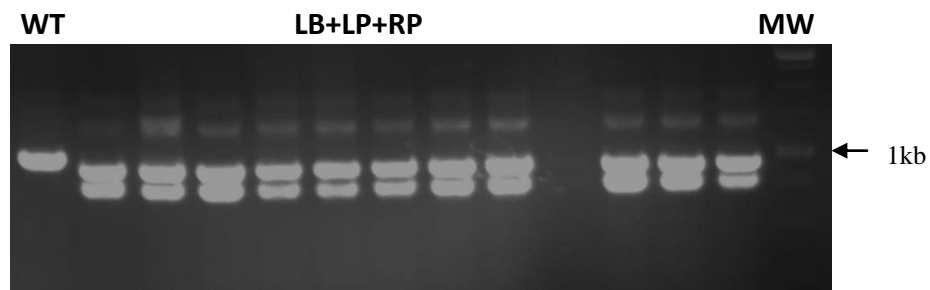
B

| Gene Name | Locus | Salk Line | T-DNA insertion sites |
|---------------|-----------|---------------------|-----------------------|
| <i>AtNDL2</i> | AT5G11790 | SALK_059302.48.65.x | Intron |
| | | SALK_074252.54.65.x | Promoter |

C

SALK_059302C

D

SALK_074252C

E

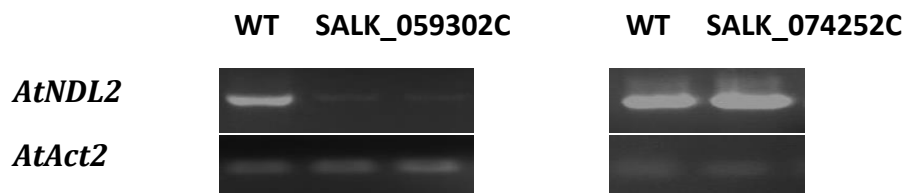


Figure 8 Genotyping and RT-PCR analysis of *Arabidopsis AtNDL2* T-DNA insertion lines.

(A) Gene structure of *AtNDL2* and T-DNA insertion sites (triangles) in *Arabidopsis* T-DNA insertion lines. Insertions of SALK_059302C and SALK_074252C are within intron 1 and promoter region of *AtNDL2* individually. Exons and introns are shown by rectangles and lines respectively. 5'-UTR and 3'-UTR are indicated as open boxes.

(B) A summary of the two *Arabidopsis AtNDL2* T-DNA insertion lines.

(C) (D) Genotyping for homozygous *Arabidopsis AtNDL2* T-DNA insertion lines, SALK_059302C and SALK_074252C. PCR screen was performed using the T-DNA left border specific primer, LBb1.3, and gene specific primer sets, LP and RP (LB+LP+RP). Genomic DNA was isolated from *Arabidopsis* leaf tissues. WT DNA was used as control. WT, wild-type *Arabidopsis*.

(E) Gene expression analysis of *AtNDL2* in homozygous T-DNA insertion mutants, SALK_059302C and SALK_074252C. RT-PCR was conducted using *Arabidopsis* WT and mutant cDNA with gene specific primers. *AtAct2*, *Arabidopsis Actin2* was used as the internal gene control.

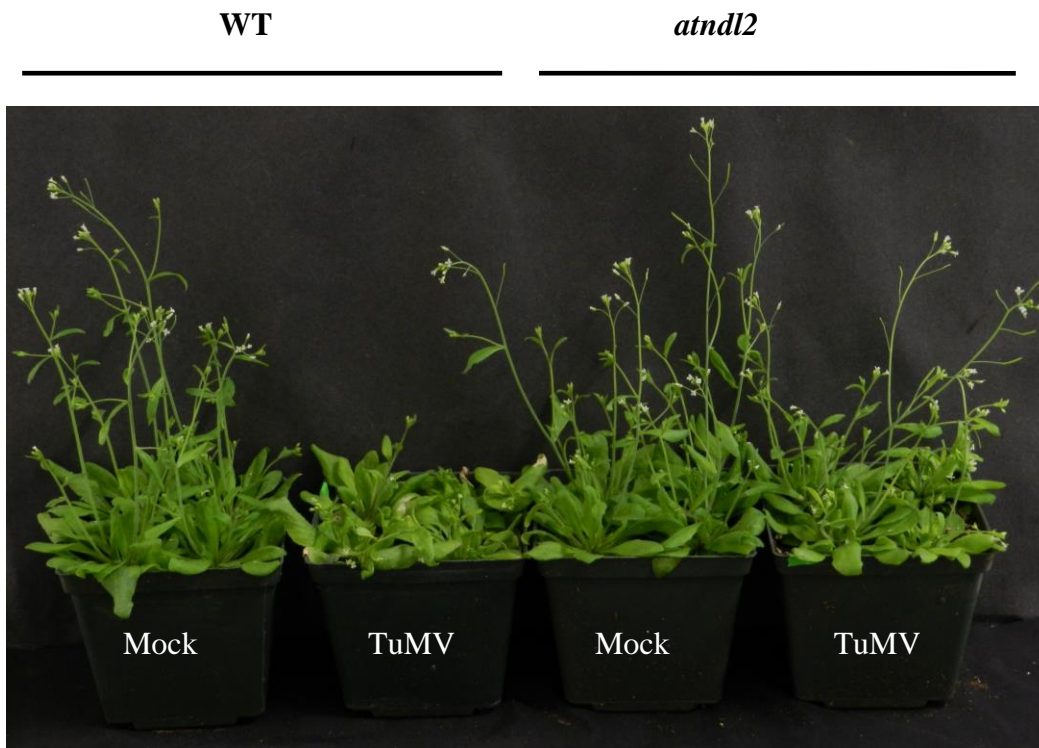
3.5.3 TuMV infection is partially inhibited in the *Arabidopsis* *AtNDL2* T-DNA knockout line

To examine if *AtNDL2* is required during TuMV infection, three-week-old *atndl2* mutant and wild-type plants were mechanically inoculated with TuMV-GFP. To monitor TuMV infection in these plants, photos were taken at 9 dpi. No distinguishable developmental difference was observed between the wild type and *atndl2* plants under the normal growth conditions (see mock-inoculated wild type and *atndl2*; Figure 9A). However, in contrast to typical TuMV symptoms including necrosis and mosaic on leaves, severe growth stunting, reduced apical dominance, curled bolts and dwarfing developed in wild type plants, *atndl2* mutants showed very minor symptoms, such as less stunted and only slight growth retardation of bolts, which suggested that *atndl2* mutants were less susceptible to TuMV infection (Figure 9A).

Along with inspections of the wild type and *atndl2* mutant plant phenotypes after infected with TuMV-GFP, qRT-PCR was performed to quantify the accumulation of TuMV RNA using primers flanking the CP region. In the *atndl2* mutant plants, TuMV accumulation showed a substantial reduction by 50% with regard to that of wild type plants at 15 dpi (Figure 9B), which paralleled the previous observation of phenotypes.

Taken together, these results indicated that *atndl2* mutants are partially resistant to TuMV, suggesting *AtNDL2* plays an important role in TuMV infection.

A



B

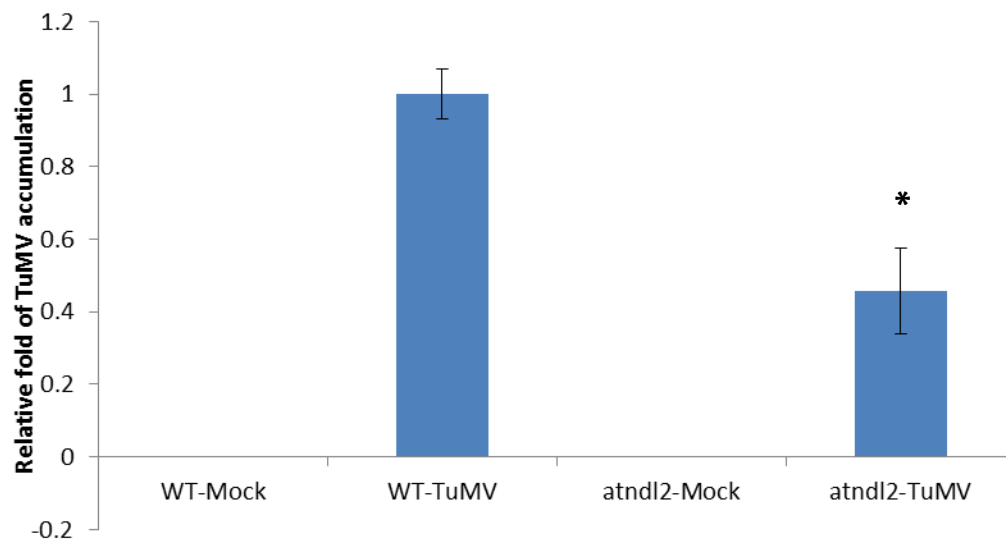


Figure 9 TuMV infection assay on *Arabidopsis atndl2* mutant and wild type plants.

(A) Representative photograph of TuMV and mock infiltrated *Arabidopsis* wild type and *atndl2* plants. Photo was taken at 9 dpi. Mock, inoculated with buffer; TuMV, inoculated with TuMV-GFP.

(B) Relative quantification of TuMV accumulation in *Arabidopsis* wild type and *atndl2* plants by qRT-PCR at 15 dpi. Total RNA was extracted from the newly emerged leaves at 15 dpi. The internal gene control, *Arabidopsis Actin2* gene (*AtAct2*), was used to normalize the data. Error bars indicated standard deviation (n=9). Asterisk represents significant difference from wild type plants (student's t test, $p < 0.05$).

3.5.4 Co-localization of AtNDL2 with VRC

To explore its possible functional role during viral infection, the subcellular localization of AtNDL2 was examined in the presence of TuMV infection *in planta*. The *AtNDL2* coding sequence was cloned into the plasmid pGWB 454/554 and transiently expressed in *N. benthamiana* leaves, which was pre-inoculated with the infectious clone pCambiaTunos/6KGFP. The potyviral 6K2 has proven to be an integral membrane protein which induces the formation of ER-derived vesicles (Schaad et al., 1997). Consistent with the report, green fluorescence emitted from pCambiaTunos/6KGFP was visualized at the VRC in infected *N. benthamiana* leaf epidermal cells. In contrast to the distribution of AtNDL2 in the cytoplasm and nucleus when expressed alone (Figure 7), AtNDL2 was strongly co-localized with the chloroplast-associated 6K2 vesicles during TuMV infection (Figure 10).

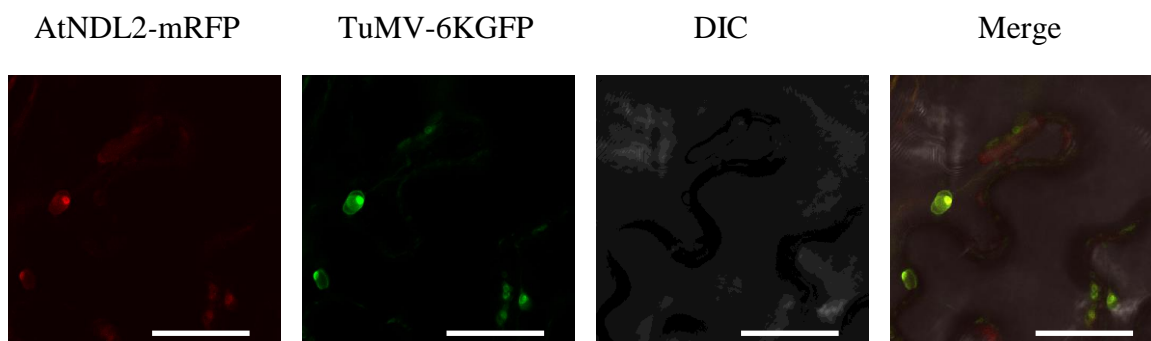


Figure 10 Co-localization of AtNDL2 with VRC in TuMV-infected *N. benthamiana* epidermal cells. Bars, 25 μm .

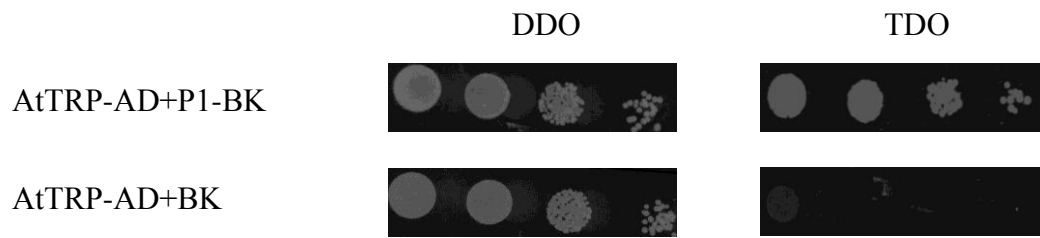
3.6 Characterization of the *Arabidopsis* gene, *AtTPR*

3.6.1 Interactions between AtTPR and 11 potyviral proteins

The Y2H method was carried out and confirmed the positive interaction between TuMV P1 and the full-length AtTPR proteins (Figure 11A). Positive and negative controls were performed as described before. The BiFC assay was used to further verify this protein-protein interaction *in planta* (Figure 11B), while positive and negative controls ensured the validity of the positive results. To further examine the interactions between AtTPR and other 10 TuMV proteins, the Y2H assay was used. However, AtTPR showed no detectable interaction with any of other 10 viral proteins (data not shown).

To localize AtTPR *in planta*, the plant expression vector containing the recombinant DNA sequence encoding the AtTPR-GUS-YFP fusion protein was agroinfiltrated into *N. benthamiana* leaves. The observation by confocal microscopy at 48 hpi displayed the distribution of AtTPR in the cytoplasm as puncta (Figure 12).

A



B

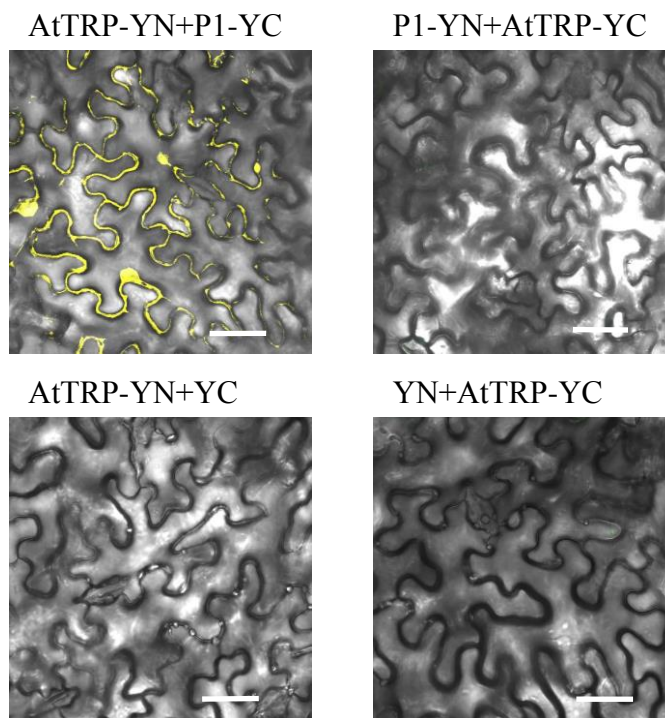


Figure 11 Protein-protein interactions between *Arabidopsis* AtTRP and TuMV proteins. (A) Y2H assay of AtTRP and TuMV P1, observed after 4 days of culture at 28°C. (B) BiFC assay of AtTRP and TuMV P1 at 3 dpi. Bars, 40 μm.

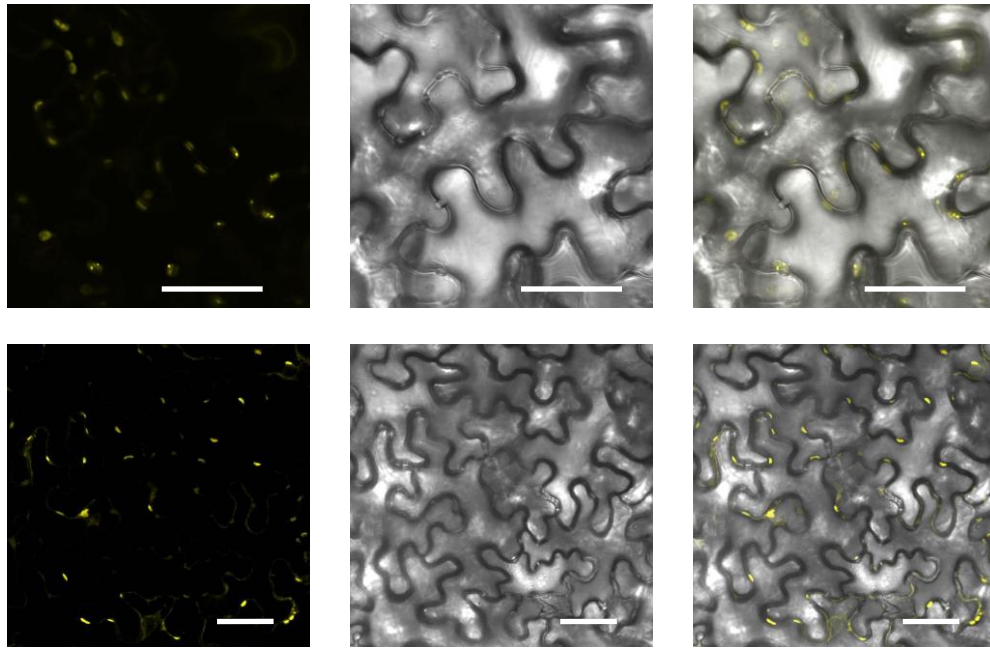


Figure 12 Subcellular localization of AtTRP in *N. benthamiana*. Bars, 40 μm .

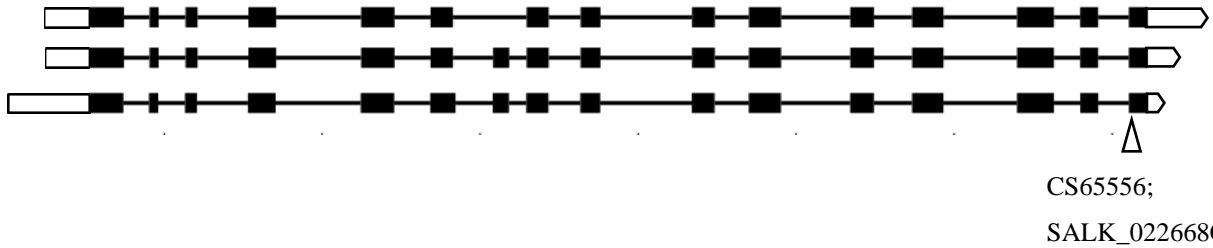
3.6.2 Verification of *Arabidopsis AtTPR* T-DNA insertion lines

The full-length cDNA of *AtTPR* is 1460 bp with a 5'-UTR of 138 bp, an ORF of 1158 bp, and a 3'-UTR of 164 bp (Figure 13A). It encodes a 385 aa polypeptide with a predicted molecular mass of 42.6 kDa and a PI of 7.95. The domain analysis using the Pfam program (<http://pfam.sanger.ac.uk/>) identified a tetratricopeptide repeat (TPR) domain (174 to 361 aa). The TPR domain, a structural motif present in a wide range of proteins, binds specific peptide ligands in a variety of biological systems (Davies et al., 2005; Hammerschmidt, 2009; Loebenstein, 2009).

The homozygous insertions of two *AtTPR* T-DNA insertion lines, CS65556 and SALK_022668C, were positively identified by PCR-based genotyping as described earlier (Figure 13C). And both lines contain the T-DNA insertion within the last intron of *AtTPR* (Figure 13A).

The RT-PCR analysis of total RNA extracted from leaf tissues of mutant lines with wild type as a positive control failed to detect any expression of *AtTPR*. Thus, both of these lines, CS65556 and SALK_022668C, were confirmed to be knockout mutants of *AtTPR* and named *attp-1* and *attp-2* respectively (Figure 13D).

A

AT1G78915 (*AtTPR*)

B

| Gene Name | Locus | Stock | Associated Polymorphisms | T-DNA insertion sites |
|--------------|-----------|--------------|--------------------------|-----------------------|
| <i>AtTPR</i> | AT1G78915 | CS65556 | SALK_022668.34.70.x | Exon |
| | | SALK_022668C | SALK_022668.34.70.x | Exon |

C



D

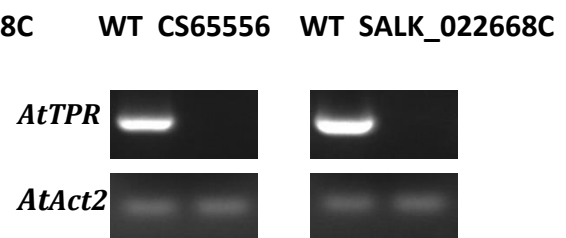


Figure 13 Genotyping and RT-PCR analysis of *Arabidopsis AtTPR* T-DNA insertion lines.

(A) Gene structure of *AtTPR* and T-DNA insertion sites (triangles) in *Arabidopsis* T-DNA insertion lines. Insertions of CS65556 and SALK_022668C are within the last intron of *AtTPR*. Exons and introns are shown by rectangles and lines respectively. 5'-UTR and 3'-UTR are indicated as open boxes.

(B) A summary of the two *Arabidopsis AtTPR* T-DNA insertion lines.

(C) Genotyping for homozygous *Arabidopsis AtTPR* T-DNA insertion lines, CS65556 and SALK_022668C. PCR screen was performed using the T-DNA left border specific primer, Lbb1.3, and gene specific primer sets, LP and RP (LB+LP+RP). Genomic DNA was isolated from *Arabidopsis* leaf tissues.

(D) Gene expression analysis of *AtTPR* in homozygous T-DNA insertion mutants, CS65556 and SALK_022668C. RT-PCR was conducted using *Arabidopsis* wild type and mutant cDNA with gene specific primers. *AtAct2* was used as the internal gene control.

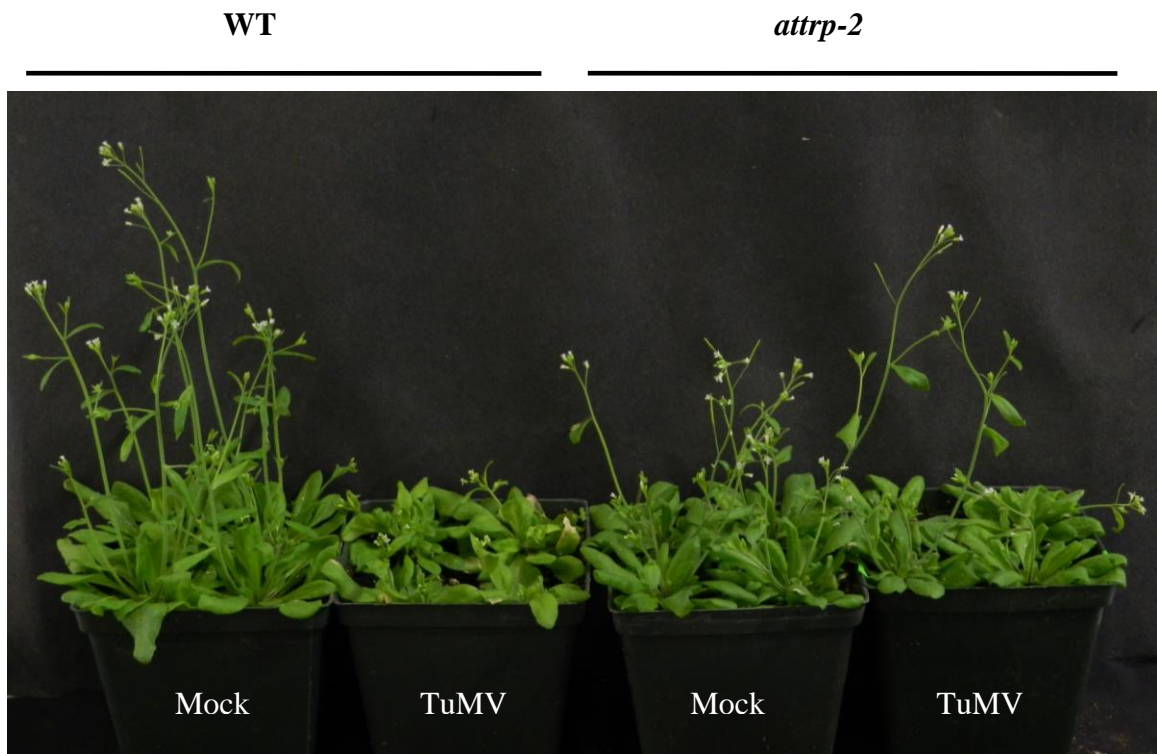
3.6.3 TuMV infection is partially inhibited in *Arabidopsis AtTPR* T-DNA knockout lines

Under normal growth conditions, *attp* mutants showed vegetative growth defects, like stunted stem (see mock-inoculated wild type and *attp-2*; Figure 14A), but displayed almost normal flowering development and seed production, which suggested that knockout of *AtTPR* negatively affects plant growth.

In order to investigate if *AtTPR* is required for TuMV infection, *attp* mutant and wild-type plants were mechanically inoculated with TuMV-GFP. Mild disease symptoms, such as slight growth retardation and less mosaic and necrosis on leaves, were found in the mutant plants in comparison with TuMV-infected wild-type plants, which displayed severe viral symptoms (Figure 14A). Consistent with the phenotype observation of *attp* mutant and wild-type plants, qRT-PCR analysis revealed that in the two *attp* mutant plants, TuMV accumulation was reduced by about 70% with respect to that of wild type plants at 15 dpi (Figure 14B).

Taken together, these data suggested that *AtTPR* is needed for both plant development and TuMV infection.

A



B

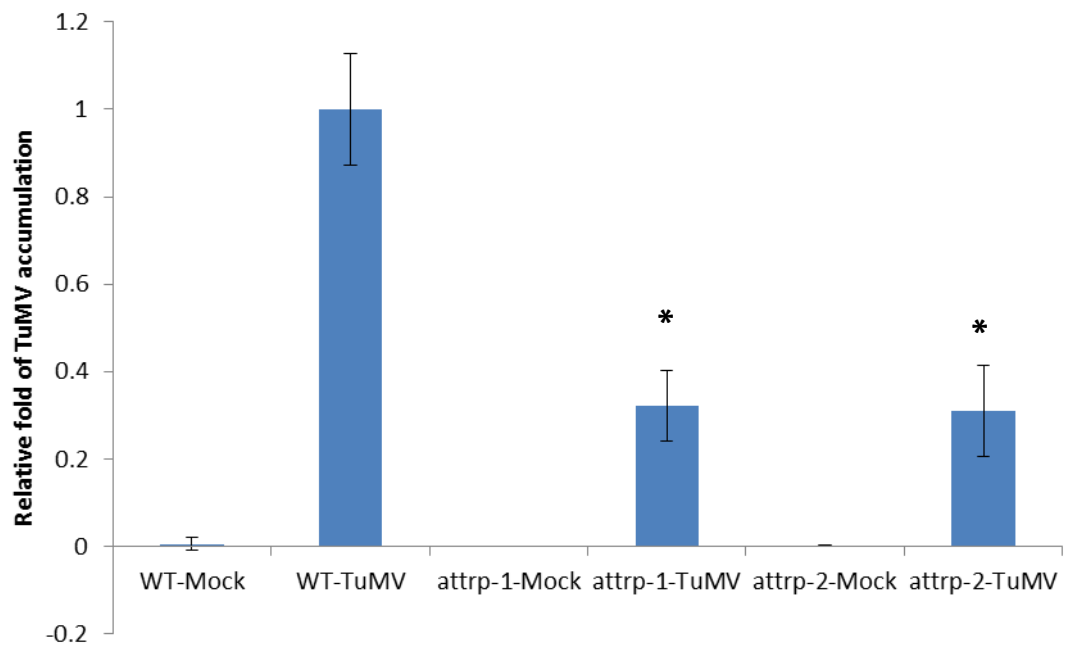


Figure 14 TuMV infection assay on *Arabidopsis atrrp* mutant and wild type plants.

(A) Phenotyping of TuMV and mock infiltrated *Arabidopsis atrrp* and wild type plants at 9 dpi. Mock, inoculated with buffer; TuMV, inoculated with TuMV-GFP.

(B) Relative quantification of TuMV accumulation in *Arabidopsis atrrp* and wild type plants by qRT-PCR at 15 dpi. Total RNA was extracted from the newly emerged leaves at 15 dpi. *AtAct2* was used as the internal gene control to normalize all values. Error bars indicated standard deviation (n=9). Asterisk represented significant difference comparing to wild type plants (student's t test, $p < 0.05$).

3.6.4 Co-localization of AtTRP with VRC

To investigate the potential role of *AtTRP* in viral infection, the subcellular localization of AtTRP was observed in the presence of pCambiaTunos/6KGFP infection *in planta*. In contrast to the localization of AtTRP in the cytoplasm when expressed alone (Figure 12), AtTRP was largely visualized in the chloroplast-bound 6K2 vesicles during TuMV infection (Figure 15).

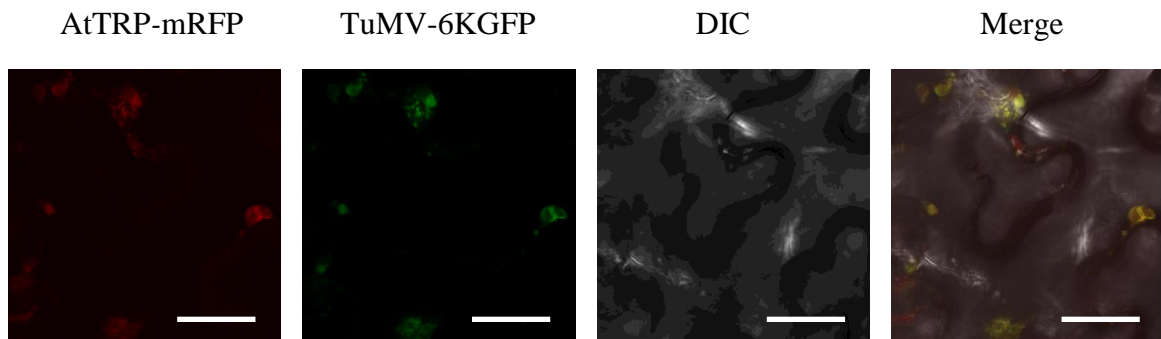


Figure 15 Co-localization of AtTRP with VRC in TuMV-infected *N. benthamiana* leaves. Bars, 25 μm .

3.7 Characterization of the *Arabidopsis* gene, *AtUCP3*

3.7.1 Interactions between *AtUCP3* and 11 potyviral proteins

Both Y2H and BiFC assays were performed and confirmed the protein-protein interaction between *AtUCP3* and TuMV P1 (Figure 16A, B). To investigate interactions between *AtUCP3* and other 10 viral proteins, another Y2H assay was carried out, but no interaction was detected between *AtUCP3* and any of the 10 viral proteins (data not shown). To localize *AtUCP3* *in planta*, an expression vector containing the full length cDNA of *AtUCP3* inserted in frame upstream of the GUS-YFP coding sequence was generated and agroinfiltrated into *N. benthamiana* leaf cells. The *AtUCP3* signal was observed in the nucleus using confocal microscopy at 48 hpi (Figure 17).

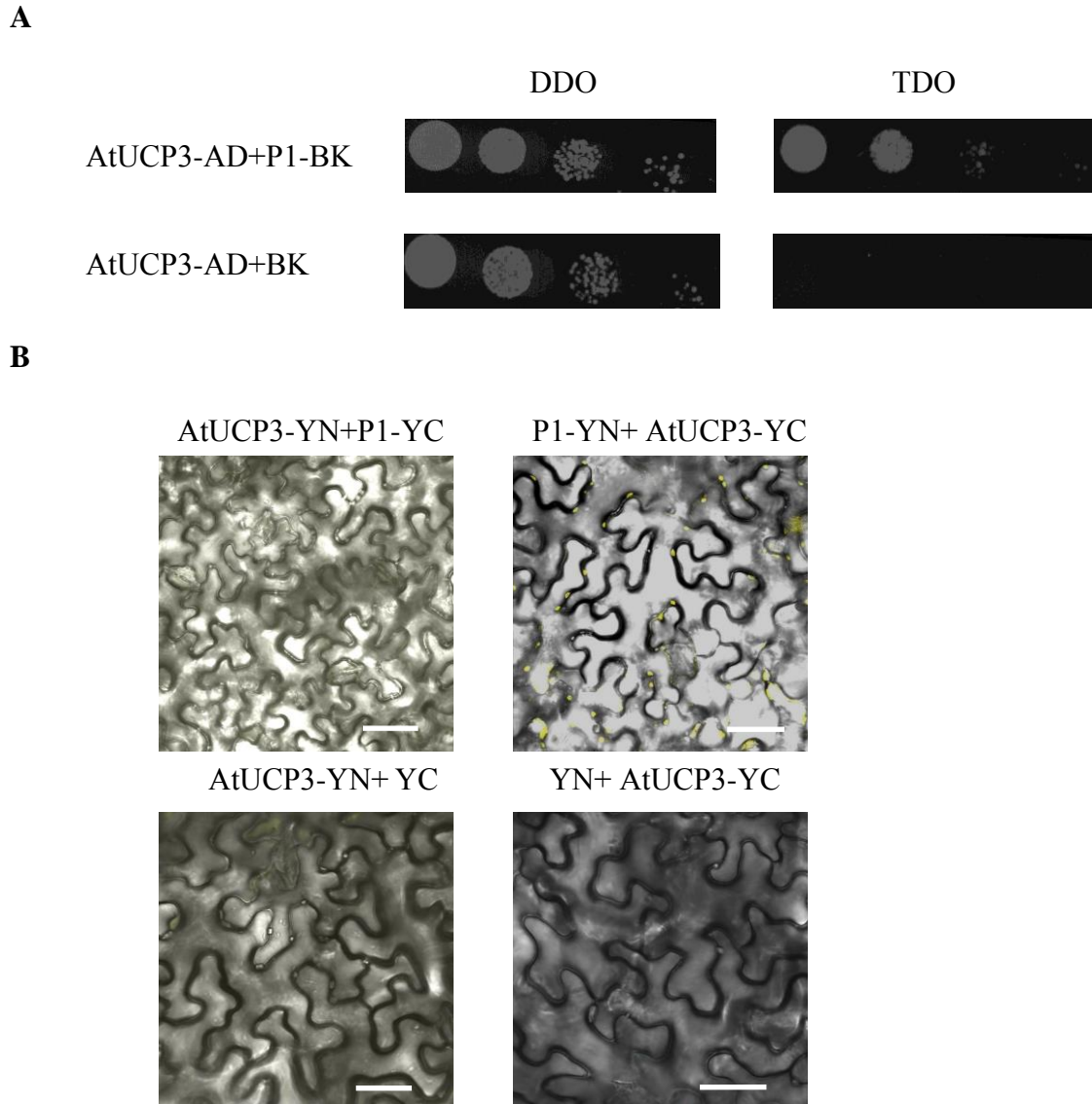


Figure 16 Interactions between full-length *Arabidopsis* AtUCP3 and potyviral proteins. (A) Y2H assay of AtUCP3 and TuMV P1 after 4 days of culture at 28°C. (B) BiFC assay of AtUCP3 and TuMV P1 at 3 dpi. Bars, 40 µm.

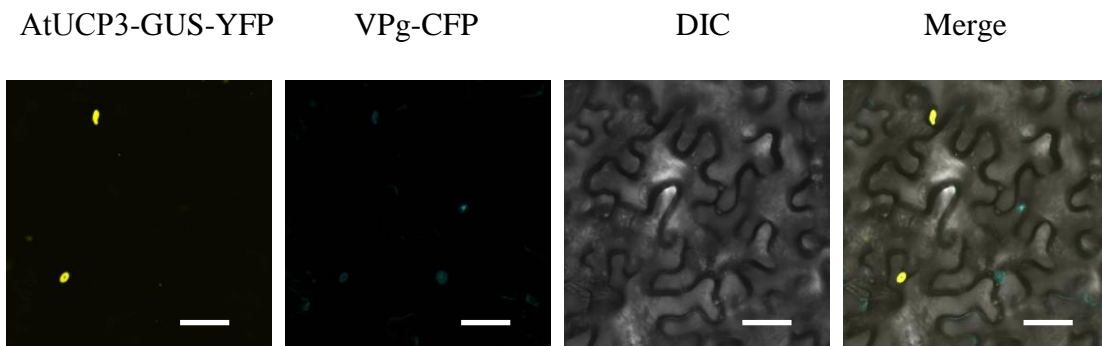


Figure 17 Subcellular localization of AtUCP3 in *N. benthamiana* at 48 hpi. Bars, 40 μm .

3.7.2 Verification of *Arabidopsis AtUCP3* T-DNA insertion lines

The full-length cDNA of *AtUCP3* is 1472 bp in length with a 5'-UTR of 246 bp, an ORF of 1008 bp, and a 3'-UTR of 218 bp (Figure 18A), and encodes a 335 aa polypeptide with a predicted molecular mass of 37 kDa and a PI of 7.786. The domain analysis using the Pfam program (<http://pfam.sanger.ac.uk/>) identified no integrated domain.

The homozygosity of three *AtUCP3* T-DNA insertion lines, SALK_080927C, SALK_030248C and SALK_123978C, was confirmed by PCR genotyping as described previously (Figure 18CDE). The RT-PCR analysis of mutant lines failed to amplify *AtUCP3* in the T-DNA insertion lines, SALK_080927C and SALK_123978C. Thus, these two lines were confirmed to be knockout mutant lines of *AtUCP3* and named *atucp3-1* and *atucp3-2* correspondingly (Figure 18F). Another line SALK_030248C showed no difference of *AtUCP3* gene expression comparing to wild type (Figure 18F).

A

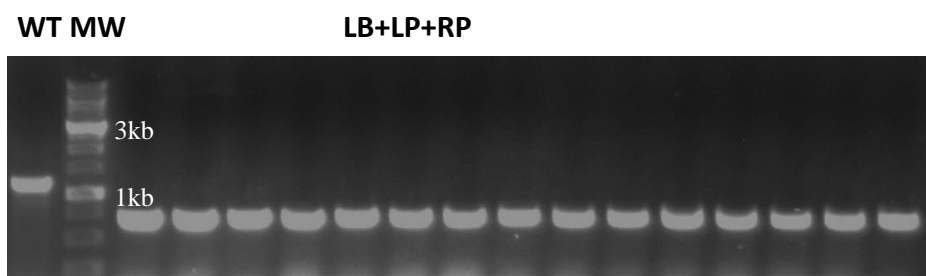
AT1G26650 (*AtUCP3*)

B

| Gene Name | Locus | Salk Line | T-DNA insertion sites |
|---------------|-----------|---------------------|-----------------------|
| <i>AtUCP3</i> | AT5G11790 | SALK_080927.55.75.x | Exon |
| | | SALK_030248.55.00.x | Exon |
| | | SALK_123978.24.60.x | Exon |

C

SALK_080927C



D

SALK_030248C

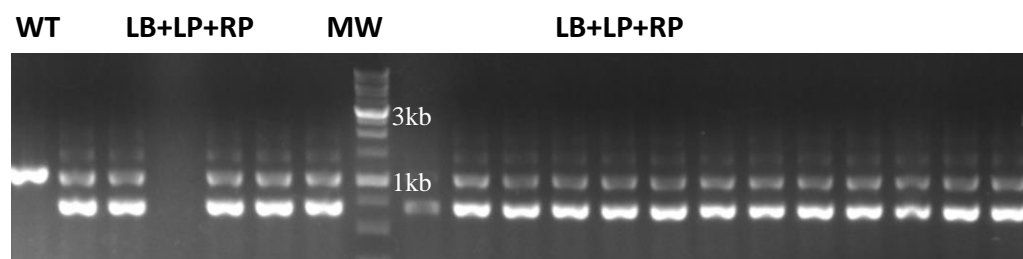
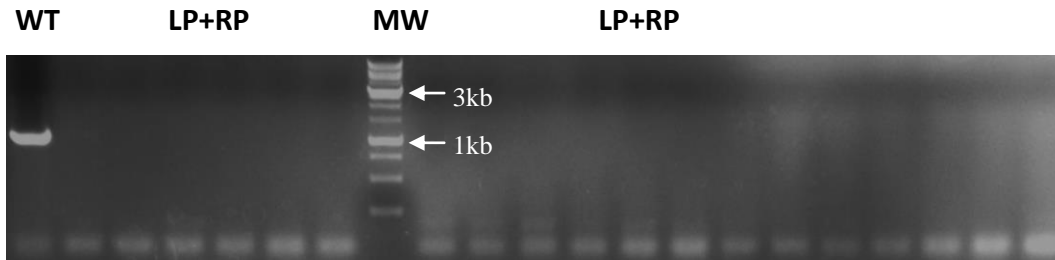
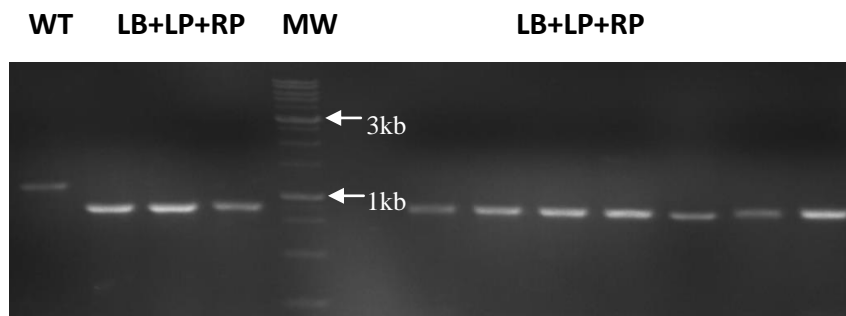


(Figure 14 continued)



E

SALK_123978C



F

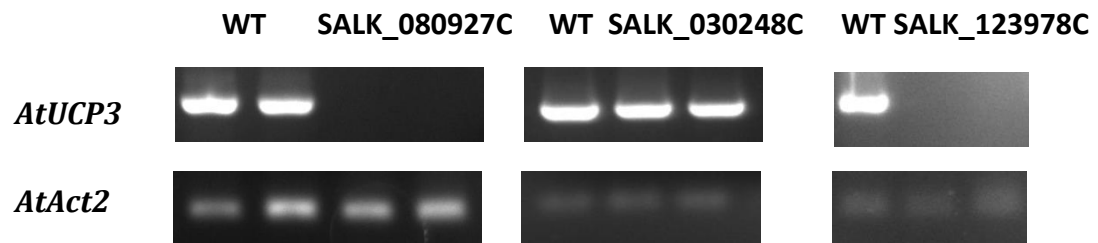


Figure 18 Genotyping and RT-PCR analysis of *Arabidopsis AtUCP3* T-DNA insertion lines.

(A) Gene structure of *AtUCP3* and T-DNA insertion sites (triangles) in *Arabidopsis* T-DNA insertion lines. 5'-UTR and 3'-UTR are indicated as open boxes.

(B) A summary of the two *Arabidopsis AtUCP3* T-DNA insertion lines.

(C) (D) (E) Genotyping for homozygous *Arabidopsis AtUCP3* T-DNA insertion lines, SALK_080927C, SALK_030248C and SALK_123978C. PCR screen was performed using the T-DNA left border specific primer, LBb1.3, and gene specific primer sets, LP and RP. Genomic DNA was isolated from *Arabidopsis* leaf tissues. Wild type DNA was used as control.

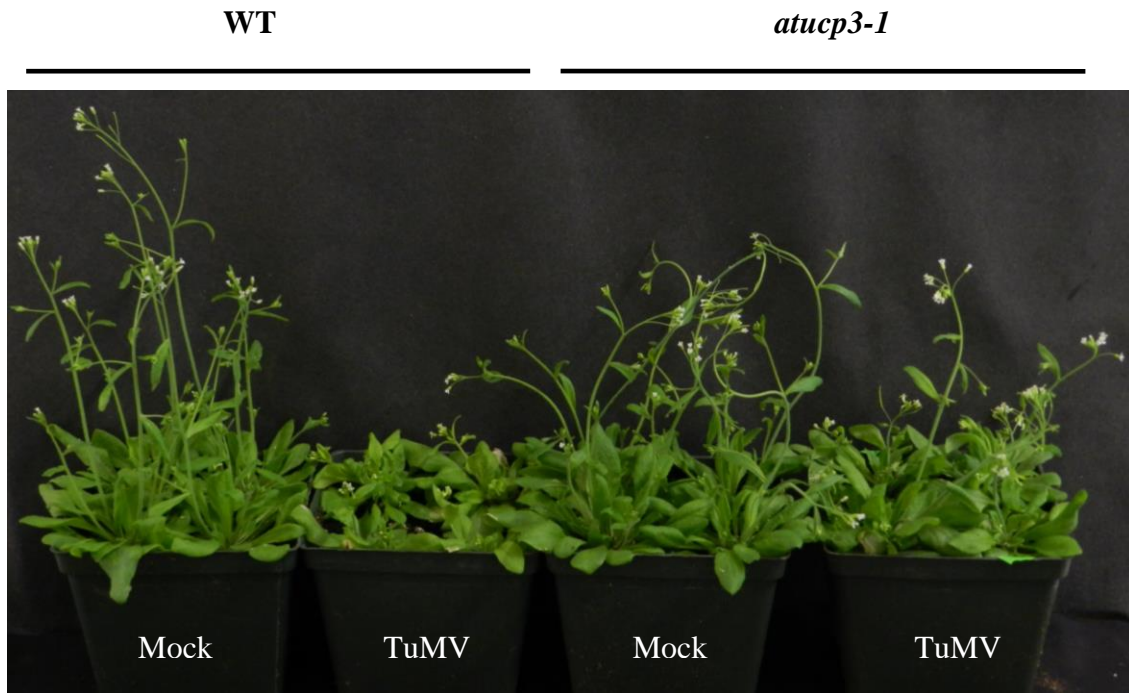
(F) Gene expression analysis of *AtUCP3* in homozygous T-DNA insertion mutants. RT-PCR was conducted using *Arabidopsis* wild type and mutant cDNA with gene specific primers. *Actin2* was used as the internal gene control.

3.7.3 Partial resistance of the *Arabidopsis AtUCP3* T-DNA knockout line to TuMV

Under normal culture conditions, *atucp3-1* mutants developed slight retardation and curling of bolts, but displayed almost normal flowering development and seed production with respect to wild type plants (see mock-inoculated wild type and *atucp3-1*; Figure 19A).

To investigate whether *AtUCP3* is needed for TuMV infection, *atucp3-1* mutant and wild-type plants were mechanically inoculated with TuMV-GFP. Less severe disease symptoms were observed on the mutant plants (Figure 19A). Plus, qRT-PCR of *atucp3-1* mutant and wild-type plants showed a marked reduction of viral RNA accumulation, by about 60%, in *atucp3-1* mutants compared to that of wild type plants at 15 dpi (Figure 19B). Taken together, these results revealed that *AtUCP3* is required for TuMV infection.

A



B

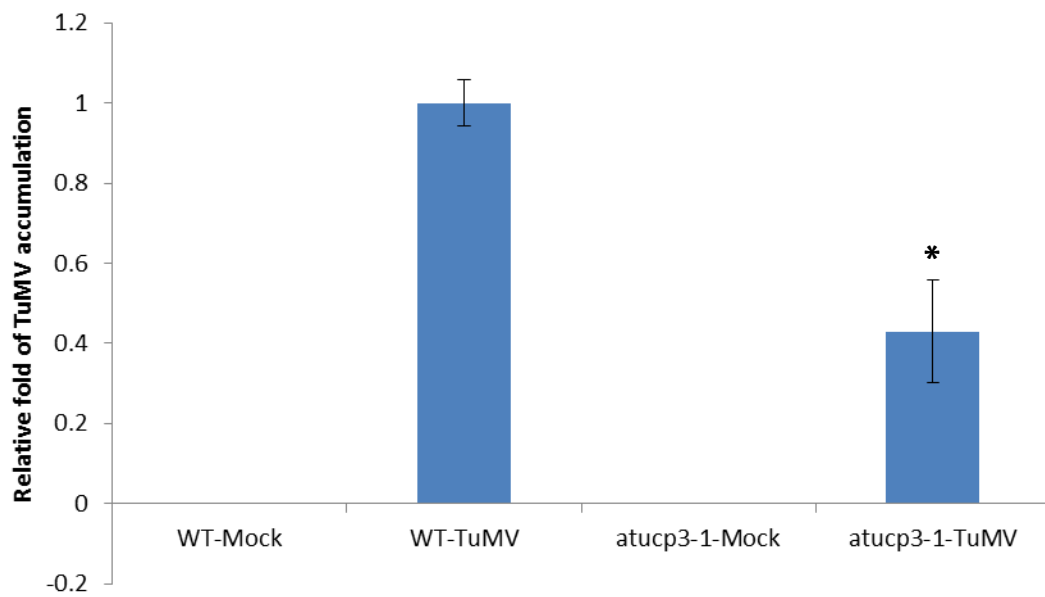


Figure 19 TuMV infection assay on *Arabidopsis atucp3-1* and wild type plants.

(A) Phenotyping of TuMV and mock infiltrated *Arabidopsis* WT and *atucp3-1* plants at 9 dpi.

(B) Relative quantification of TuMV accumulation in *Arabidopsis atucp3-1* and wild type plants by qRT-PCR. Total RNA was extracted from the newly emerged leaves at 15 dpi. *AtAct2* was used as the internal gene control to normalize all values. Error bars indicated standard deviation (n=9). Asterisk represented significant difference comparing to wild type plants (student's t test, $p < 0.05$).

3.7.4 Co-localization of AtUCP3 with VRC

The subcellular localization of AtUCP3 was also detected in the presence of pCambiaTunos/6KGFP infection in *N. benthamiana*. In contrast to the localization of AtUCP3 in the nucleus when expressed alone (Figure 17), AtUCP3 was mainly observed in the chloroplast-associated 6K2 vesicles during TuMV infection (Figure 20).

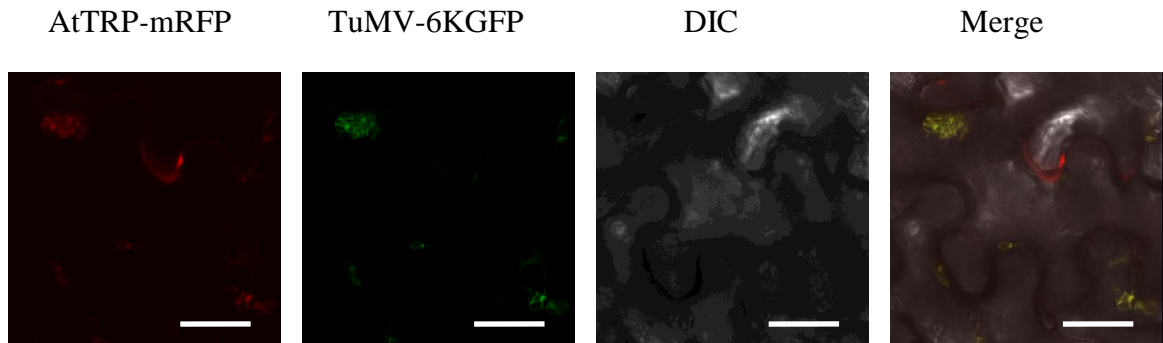


Figure 20 Co-localization of AtUCP3 with VRC in TuMV-infected *N. benthamiana* leaf tissues. Bars, 25 μm .

3.8 P1 functions other than being a protease

To explore new functional roles of P1 in virus infection, mutations were introduced into the P1 coding region of TEV and TuMV (Figure 21). In the mutant P1S, the serine residue in the P1 protease active site was mutated to an alanine residue, which abolished the P1 protease function. In the mutant P1(null)/HC, the P1/HC-Pro cleavage site was mutated and could not be recognized and cut by the P1 protease. In the mutant P1(nia)/HC, the P1/HC-Pro cleavage site was replaced by NIb/CP cleavage site, which could be cut by the NIa protease. In the mutant Δ P1, the whole P1 was deleted from the infectious clone.

N. benthamiana plants were inoculated by parental plasmid p35TEV/GFP and its descended mutation plasmids using biolistic bombardment. Plants inoculated with p35TEV/GFP-P1S, p35TEV/GFP-P1(null)/HC, p35TEV/GFP-P1S&P1(null)/HC and p35TEV/GFP- Δ P1 did not show any green fluorescence under UV light, while plants infected with p35TEV/GFP, p35TEV/GFP-P1(nia)/HC and p35TEV/GFP-P1S&P1(nia)/HC showed green fluorescence along with obvious disease symptoms at 9 dpi (Figure 22A). To quantify the accumulation of TEV, qRT-PCR was carried out. The total RNA was isolated from the newly emerged leaves at 10 dpi. Consistent with the previous phenotype observation of TEV-infected plants, qRT-PCR analysis revealed that virus RNA accumulation of p35TEV/GFP-P1S, p35TEV/GFP-P1(null)/HC, p35TEV/GFP-P1S&P1(null)/HC and p35TEV/GFP- Δ P1 was markedly reduced, while p35TEV/GFP-P1(nia)/HC and p35TEV/GFP-P1S&P1(nia)/HC showed similar expression level of CP comparing to that of p35TEV/GFP (Figure 22B). The expression level of the *N. benthamiana* housekeeping gene *Actin* was used to normalize these data.

Taken together, these data indicated that the P1 proteinase activity is not required but its separation from HC-Pro is essential for viral infection. It also suggested that P1 may be involved in other non-proteolytic function(s), such as viral amplification and/or cell-to-cell transportation, which needs further exploration.

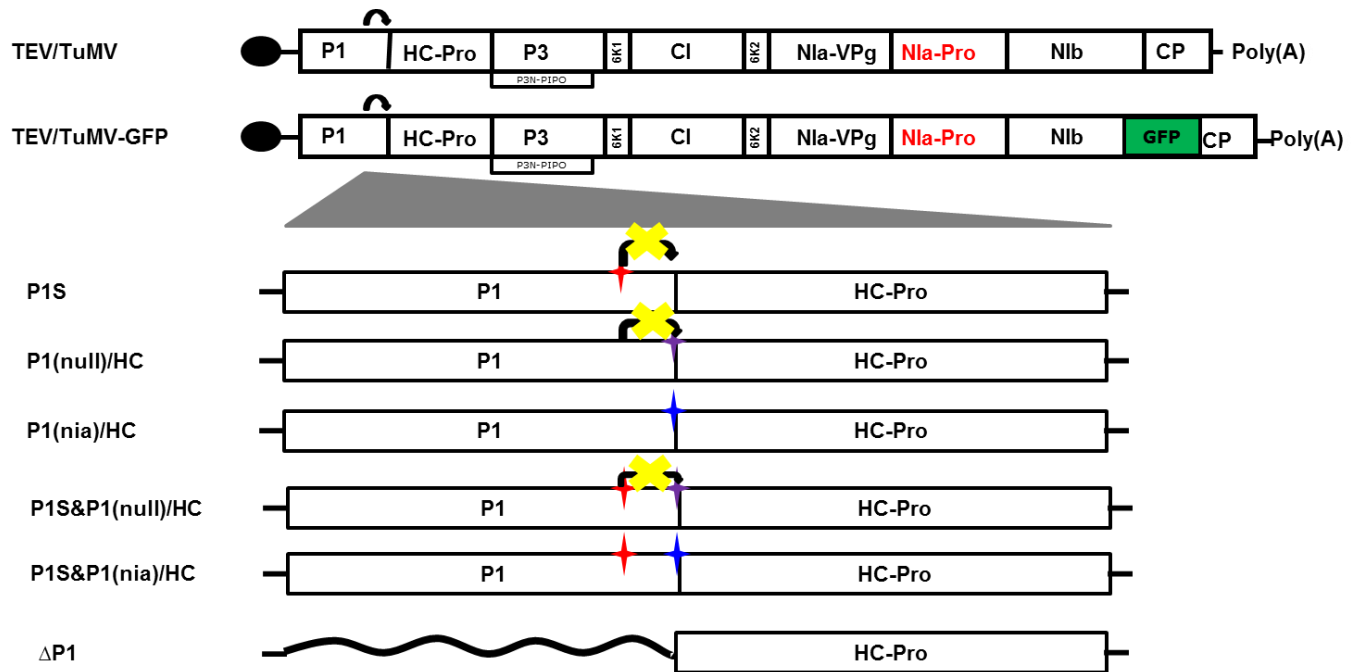


Figure 21 Diagrammatic representation of relevant portions of the p35TEV and p35TuMV plasmids. The boxes indicate the viral proteins and GFP coding sequences.

The bent arrows indicate the function of P1 self-cleavage. The red stars indicate the active site of P1. The purple stars indicate the mutated P1/HC-Pro cleavage site. The blue stars indicate the introduced NIa cleavage site. The wavy line indicates the full deletion of P1 coding region.

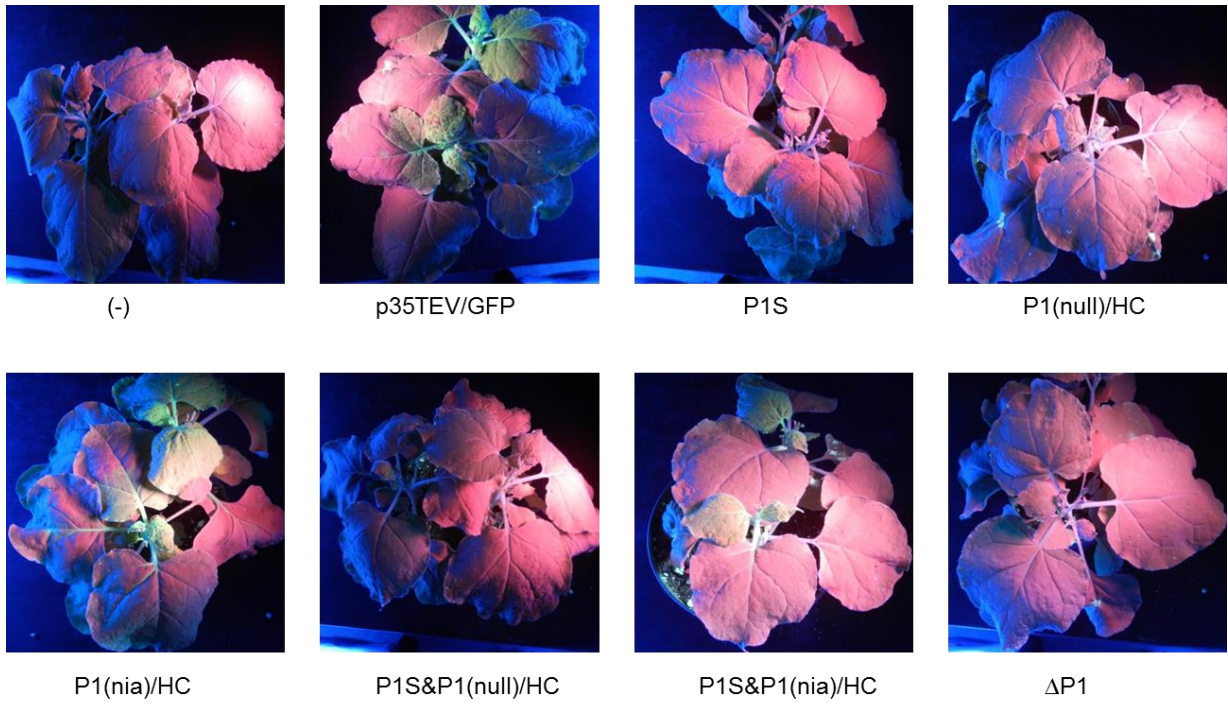
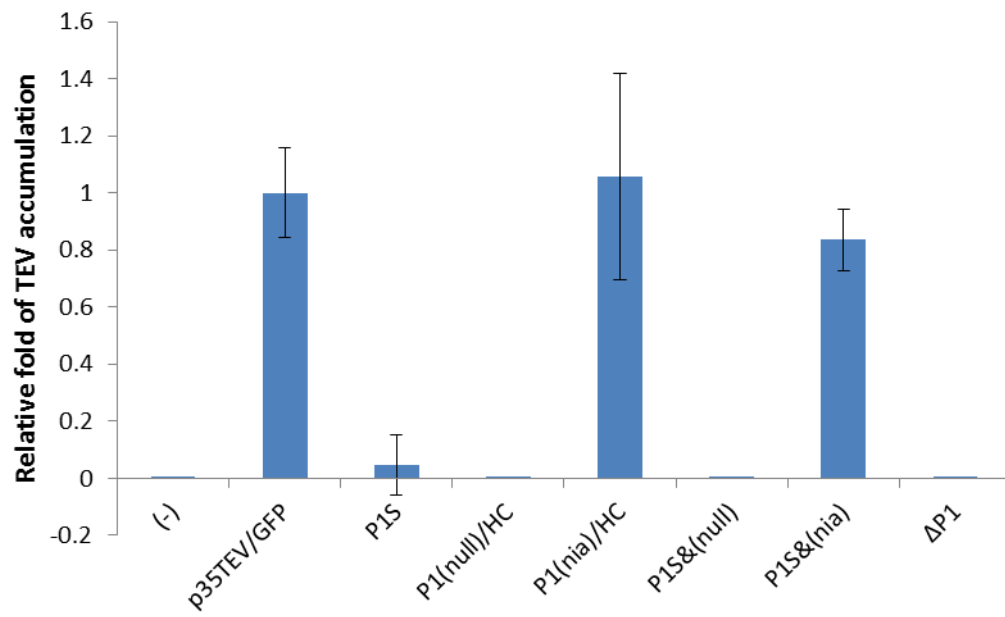
A**B**

Figure 22 TEV infection assay on *N. benthamiana* plants.

(A) Phenotyping of TEV/GFP infected *N. benthamiana* under UV light at 9 dpi.

(B) Relative quantification of TEV accumulation in *N. benthamiana* plants by qRT-PCR. Total RNA was extracted from the newly emerged leaves at 10 dpi. *NbAct*, *N. benthamiana Actin*, was used as the internal gene control to normalize all values. Error bars indicated standard deviation (n=5).

Chapter 4 Discussion

4.1 Subcellular localization of the P1 protein

In order to perform its proper function during biological processes, a protein needs to be directed to the right cellular compartment. In turn, subcellular localization of a viral protein can give us some idea of its functional roles in the virus life cycle. Thus, I started my project with the investigation of the subcellular localization of TuMV and TEV P1 proteins in the presence and absence of virus infection. Both TuMV and TEV P1 proteins remained within the cytoplasm and nucleus, with or without viral infection (Figure 2). Unpublished data from our lab has indicated that SMV-L P1 also localizes in the cytoplasm and nucleus (Chen et al., unpublished).

To determine if the nuclear targeting of P1 is a common feature among potyviruses, P1 amino acid sequences of four potyvirus species and two strains of the same virus were analyzed for NLSs using the ELM tool (Table 15). Besides the three NLSs confirmed in TEV P1, P1s of TuMV, SMV-L and SMV-G5 were predicted one monopartite NLS each, but no NLS was detected in LMV. These results suggest that P1's nuclear targeting is consistent among some potyviruses but may not be detected among all of them. Predicted NLS sequences showed divergence among different potyviruses, but conservative in the same species. This may be because P1 is the most divergent potyviral protein with regard to both length and amino acid sequence (Valli et al., 2007).

Proteins larger than 60~70 kDa in size generally require specific targeting signals, called NLSs in order to achieve transport into the nucleus. Even much smaller proteins enter the nucleus via an active mechanism, rather than diffusion through the nuclear pore, as it is more efficient and easier to regulate (Rajamäki and Valkonen, 2009). I identified three NLSs in TEV P1 that are able to function independently, but there could exist more NLSs at work. In 2014, Martínez and Daròs indicated that TEV P1 exhibited a dynamic subcellular localization, trafficking into the nucleus particularly targeting the nucleolus at the early stage of virus infection, and then back to the cytoplasm. Additionally, they identified a functional nucleolar localization signal (NoLS) and a nuclear export signal

(NES) (Martínez and Daròs, 2014). It's worth pointing out that I didn't observe nucleolus localization in my research, even at the very beginning of the viral infection. Given that nuclear import and export processes are crucial for eukaryotic cells, it is still mysterious as to why proteins encrypted by plus-strand RNA viruses which replicate in the cytoplasm must be transported to the nucleus (Miller and Krijnse-Locker, 2008). There are suggestions that nuclear-localized proteins might be involved in recruitment and redistribution of certain nuclear components in order to gain access to host's replication and repair machinery, transport of viral genomes, integration of the viral genome into the host genome, or suppression of host defences (Krichevsky et al., 2006; Haupt et al., 2008; Solovyev and Savenkov, 2014). Actually, the well-recognized potyviral suppressor, HC-Pro, functions outside of the nucleus (Kasschau et al., 2003). It was suggested that P1 could not work as a suppressor, itself, but could assist HC-Pro in RNA silencing suppression (Kasschau and Carrington, 1998; Valli et al., 2006). It is possible that P1 may function through targeting the nucleus. Another hypothesis is that P1 is involved in hijacking cellular signaling and transcriptional machinery in order to play an important role in virus replication. Interestingly, in another potyvirus, SPFMV, a truncated protein, P1N-PISPO, which is generated from frame slippage at the P1 cistron, was proven to be an RSS (Mingot et al., 2016). The nucleolus has been documented to be involved in stress sensing, gene silencing and cell cycle regulation (Pontes et al., 2006; Boisvert et al., 2007). Viral proteins in the nucleolus could modulate nucleolar particles to facilitate viral replication (Hiscox, 2007). Undoubtedly, future efforts are required to elucidate the mechanism behind the nuclear localization of P1 protein, which could be important in the development of novel virus control strategies. P1 was proposed to be part of the potyviral VRC (Merits et al., 1999), which could be a good explanation of its cytoplasmic localization. If molecular interaction partners of P1 during the virus infection cycle could be identified, this conclusion would be perfectly supplemented.

Table 15 List of predicted NLSs of potyviral P1s using ELM. np, not predicted.

| Potyvirus | GenBank Accession Number | NLS Amino Acid Sequence | NLS Position | NLS Type |
|-----------|--------------------------|-------------------------|--------------|-------------|
| TEV | M11458.1 | GKRRKVSNNKRNRR | 92-106 | Bipartite |
| | | AKRFRKNE | 155-162 | Monopartite |
| | | PKRKKQKN | 238-244 | Monopartite |
| TuMV | AF169561.2 | PSMKKRTV | 207-214 | Monopartite |
| LMV | X97705.1 | np | np | np |
| SMV-L | EU871724.1 | KGKRVKV | 198-204 | Monopartite |
| SMV-G5 | AY294044.1 | KGKRVKV | 199-205 | Monopartite |

4.2 Protein-protein interaction

Protein-protein interactions play pivotal roles during most, if not every, biological stages. Any molecular function of a protein must be exerted as a component in a protein complex (Phizicky and Fields, 1995; Guo et al., 2001). Naturally, the analysis of interactions amongst proteins can provide a wide array of biological insights, so the analysis of protein-protein interaction has become a popular and important part of studying protein function and understanding the molecular mechanisms underlying these biological processes (Phizicky and Fields, 1995; Guo et al., 2001; Lee et al., 2002; Yambao et al., 2003; Kang et al., 2004; Parrish et al., 2006; Guo et al., 2008; Lin et al., 2009).

Of the commonly used methods, the Y2H system (Fields and Song, 1989) represents a rapid and sensitive approach for identifying protein-protein interactions *in vivo* and has been used extensively to screen and identify protein-interacting partners and confirm protein-protein interactions. As cost- and time-efficient as it is, Y2H should be treated with caution since results sometimes prove to be “false negatives” or “false positives”. The best way to eliminate false positives and negatives is to verify the interaction data obtained from Y2H experiments using other interaction methods carried out under native conditions (Brückner et al., 2009).

Consequently, another commonly used approach, the BiFC assay (Hu et al., 2002), was used here to verify protein-protein interactions. This assay allows direct visualization of protein interactions in living plant cells, which allows the proteins to be expressed, post-translationally modified and folded in their native cellular environment. Plus, BiFC can remedy one shortcoming of the Y2H system, in which additional complex factors required for two proteins to interact (i.e., through third or even fourth partners) are absent (Kerppola, 2013). However, one limitation of the BiFC approach is that it is not able to detect real-time interaction, since there is delay from the time when the fusion partners interact to the time when the complex generates detectable fluorescence (Hu et al., 2002). So if the interaction is transient or unstable, there is a good chance that it cannot be

captured using BiFC. Also, the fluorophore can only be properly folded together if the two fusion proteins are in close enough proximity (Miller et al., 2015).

Overall, while both Y2H, to identify, and BiFC, to confirm, protein-protein interactions were used in my study, it is still virtually impossible to reveal all protein interactions taking place in biological processes.

4.2.1 P1's potyviral interaction partners

In the virus life cycle, many pivotal cellular processes, such as the formation of VRC, assembly of viral particles, virus intercellular and long-distance movements, are dependent on various protein complexes that are formed via protein-protein interactions (Guo et al., 2001; Guo et al., 2008). Consequently, the detection of any interactions between P1 and other multifunctional potyviral proteins could identify potential roles of P1 during the virus life cycle.

Unfortunately, the presented work was not able to distinguish any potyviral proteins interacting with P1 from either TEV or TuMV, using Y2H or BiFC methods. Previously, efforts have been made to study the molecular interaction partners of P1 protein. Merits et al. (1999) was able to detect interactions between P1 with itself, HC-Pro, P3, CI, VPg, NIa and NIb from *Potato virus A* (PVA) using two *in vitro* methods. But, only the interaction of P1 and CI was verified using the Y2H assay. Two years later, a weak but reproducible interaction between P1 and CI in PVA was confirmed by Guo et al. (2001) *in vivo*. And, the interaction between P1 and VPg was detected in *Papaya ringspot virus* type P (PRSV-P) using Y2H (Shen et al., 2010). In the case of *Wheat streak mosaic virus* (WSMV), Choi et al. (2000) found the self-interaction of P1, as well as interactions between P1 and subdomains of CI in the Y2H system. Interactions of P1 with P1, HC-Pro, P3 and CI were discovered *in vitro*, as well (Choi et al., 2000). Lin et al. (2009) applied the Y2H method and identified the interaction of P1 with itself, 6K1, CI, VPg, NIa and CP in *Shallot stripe yellow virus* (SYSV) but found no interaction using Pinellia isolate of SMV (SMV-P). Zilian et al. (2011) optimized the BiFC system and were able to show that P1 interacted with CI, VPg, NIa and CP in PPV. It is worth noting that TEV P1 was reported to interact with itself, HC-Pro and CP using a protein pull-down method

(Martínez and Daròs, 2014). Interestingly, despite several interactions being detected by one method and not shown by another, some of these interactions showed consistency with each other amongst different potyviruses, but this was not shown in my research. Not only have no studies shown any interactions between P1 and potyviral proteins in TuMV, but some researchers have also suggested that there are no interactions involving P1 from other potyviruses (Urcuqui-Inchima et al., 1999; López et al., 2001; Kang et al., 2004; Shi et al., 2007; Lin et al., 2009). It is believed that interactions between viral proteins are not universal amongst different potyviruses, especially, since P1 is the least conservative protein among potyviruses in regards to both length and amino acid sequence.

Importantly, all interaction data must be interpreted with caution no matter which method is used. Even though no interactions were determined in this research, it might be too arbitrary to conclude that P1 does not interact with other viral proteins in TuMV or TEV. If there are weak or transient interactions, both Y2H and BiFC assays may not be able to capture them. More approaches may be applied to verify the results of this work and previous studies.

4.2.2 P1's host interaction partners

Viral infection requires complicated interactions between the virus and its host (Hyodo and Okuno, 2016). On one hand, due to the limited number of proteins, the virus must hijack host factors for its own molecular processes, such as mRNA transcription, protein translation, transportation, and so on. On the other hand, host factors could also regulate viral proteins, either to assist or destroy their proper functions (Hull, 2013). Therefore, experiments were performed to identify P1's host interaction partners.

Following the Y2H screening against the Universal *Arabidopsis* cDNA library (Normalized) using TuMV P1 as bait, 25 putative host factors were isolated (Table 11). These host proteins can be specified into three categories: false positives, positives but without biological significance, and positives with biological significance, based on interaction analysis and infection assays. The full-length cDNA sequence of all *Arabidopsis* candidates was amplified and used to confirm the protein-protein interaction.

Only 19 out of 25 were detected to interact with P1 in the Y2H system, and seven among the 19 were double-confirmed using BiFC (Table 11). The proteins verified by neither method were grouped into false positives. Proteins from this group may never have the chance to come into contact with P1 under native conditions and hence, their interactions with P1 may represent non-biological purposes. The other P1 interaction partners, as well as some interesting candidates in the first group, were selected for TuMV infection assays to study their roles in the virus infection cycle. *Arabidopsis* knockout/knockdown mutants were tested against TuMV for any possible virus resistance, and three candidates were chosen for more thorough characteristic study.

P1 was previously reported to interact with host factors such as the Rieske Fe/S proteins (SMV, Shi et al., 2007), the 60S ribosome subunits and some other host proteins such as the heat shock protein 70 (HSP70) (TEV, Martínez and Daròs, 2014). HSP70 is a chaperone protein that is believed to be involved in the response to various biotic and abiotic stresses (Aparicio et al., 2005). However, none of the proteins previously reported were detected in my study. The reasons may be due to the inherent limitations of the Y2H system, poor representation of mRNA transcript levels in the cDNA expression library, or the divergence of P1 among potyviruses.

4.3 Host proteins identified to be involved in potyviral infection

In this research, three novel P1-interacting *Arabidopsis* proteins, AtNDL2, AtTPR and AtUCP3, were identified and the corresponding *Arabidopsis* homozygous T-DNA insertion lines were used to functionally characterize the requirement of those plant factors during TuMV infectious processes. I found that *AtNDL2*, *AtTPR* and *AtUCP3* knockout/knockdown plants showed less ability to support TuMV infection, suggesting that these proteins have important functions in the virus infection cycle (Figure 9, 14, 19). To our knowledge, this report is the first indication that those three *Arabidopsis* proteins, AtNDL2, AtTPR and AtUCP3, may be involved in virus infection in plants. In this study, those three plant proteins were also found to co-localize with the TuMV 6K2 vesicles in virus-infected cells (Figure 10, 15, 20). The potyvirus VRC contains viral replication-associated proteins (such as NIa, 6K2-NIa, and NIb), viral genomic RNA (carrying VPg),

dsRNA, and host factors (such as eIF(iso)4E, PABP2, and eEF1A) (Cotton et al., 2009). It is possible that those three proteins are recruited by potyviruses for viral replication/translation. These results were supported by the research of Merits et al. (1999) suggesting that P1 may be involved in VRC formation. In addition to interaction with P1, the AtNDL2 protein also interacted with TuMV NIB (Figure 6C). So, it is possible that AtNDL2 was involved in virus accumulation through NIB and, or instead of, P1.

For AtNDL2, the *Arabidopsis* genome encodes two other homologs, AtNDL1 and AtNDL3. Although the exact molecular function of AtNDL proteins is still elusive, it is proposed that they are involved in auxin regulation, cell differentiation and abiotic stress response (Khatri and Mudgil, 2015). The subcellular localization of AtNDL2 was in both the cytoplasm and nucleus (Figure 7), which was the same as TuMV P1. Nevertheless, the co-localization of AtNDL2 and P1 was only present in the cytoplasm when using the BiFC method (Figure 6B), possibly because their localizations were altered in the presence of each other. For the second host candidate, AtTPR, its precise biological function is unclear, but many proteins containing the TPR domains are present across all kingdoms. The TPR is a structural motif consisting of 3~16 tandem-repeats of 34 amino acids residues (D'Andrea and Regan, 2003). This motif is known to be responsible for protein-protein interactions, either assembling active multiprotein complexes or mediating the folding of a number of substrates (Akad et al., 2005; Davies et al., 2005). TPR proteins have shown involvement in diverse biological processes, such as plant hormonal regulation, salt/osmotic stress responses, abscisic acid (ABA) sensitivity, protein kinase inhibition, transcriptional modulation, cell-cycle regulation, mitochondrial and peroxisomal protein transportation, neurogenesis and protein folding (Rosado et al., 2006; Hammerschmidt, 2009; Loebenstein, 2009). Moreover, a direct engagement of the TPR motif in plant pathogenic resistance was reported with RAR1 interactor protein. Two TPR proteins, RAR1 and its interacting partner SGT1, are proposed to function with cytosolic HSP90 in co-chaperoning roles that are essential for disease resistance triggered by a number of R proteins (Hubert et al., 2003; Takahashi et al., 2003). In particular, RAR1 is an early convergence point in the R genes mediated signaling pathway (Azevedo et al., 2002). Given the name of the third candidate, AtUCP3, it's

straightforward that not much is known about it. It is currently unknown what the precise roles of these three host proteins play during viral infection and their underlying biological mechanisms. Studies could be continued to discover these mechanisms and which part of P1 is most important in regard to these protein-protein interactions.

4.4 P1 functions

In my study, it was shown that deletion of the whole P1 cistron from the TEV infectious clone totally abolished the ability for genome amplification (Figure 22). Also, the P1S and P1(null)/HC mutants were nonviable in plants. The P1S mutant encodes a non-functional P1 protease, while the P1(null)/HC mutant encodes a non-recognized cleavage site between P1/HC-Pro. Substitution of a cleavage site distinguished by a heterologous protease, NIa, between P1/HC-Pro fully recovered the infectivity of the P1S mutant. These results revealed that P1 plays important roles other than its proteolytic activity, and separation of P1 from HC-Pro is essential for both of them to function properly. Together with the data of cellular localization and interaction partners, it is rational to conclude that P1 may possess critical functions during viral genome amplification.

4.5 Major findings and future directions

Collectively, the knowledge obtained from this study has provided new insights into the functions of potyviral P1 protein in viral infection and host-virus interaction, which can be applied to develop novel strategies against potyviruses and related viruses and hopefully put into practice eventually.

It has been addressed before that P1 may be engaged in virus replication (Verchot and Carrington, 1995b; Verchot and Carrington, 1995a; Merits et al., 1999; Rohožková and Navrátil, 2011; Martínez and Daròs, 2014). My study corroborated these findings. A list of potential host factors has been identified using the Y2H screen. But, due to the limited time, only three *Arabidopsis* proteins were selected for detailed molecular characterization. *atndl2*, *attpr* and *atucp3* knockout/knockdown plants demonstrated reduced symptoms to TuMV infection. To the best of my knowledge, this is the first report indicating that plant NDL2, TPR and UCP3 proteins are required for potyviral

infection. However, the list of the untested host proteins still represents a useful reservoir of potential potyviral interacting host proteins. The experimental design and analysis approach used in this study can also serve as the template for further investigation of the other untested host factors.

Even though considerable effort has been dedicated and noteworthy knowledge has been accumulated, the majority of host factors involved in virus infection are still unidentified, and many questions raised by this project are still unresolved. Deeper functional characterization of every positive candidate will, no doubt, expand our knowledge in the different types of viral-host interaction involved during infection. With more effort, better understanding of the mechanisms underlying viral replication and plant viral defence, as well as identification of more host factors will be obtained, which can provide new sources of recessive resistance and be utilized to design engineered resistance in crops.

References

- Abdul-Razzak, A., Guiraud, T., Peypelut, M., Walter, J., Houvenaghel, M.C., Candresse, T., Le Gall, O., and German-Retana, S.** (2009). Involvement of the cylindrical inclusion (CI) protein in the overcoming of an eIF4E-mediated resistance against *Lettuce mosaic potyvirus*. *Molecular Plant Pathology* **10**, 109-113.
- Adams, M., Antoniw, J., and Fauquet, C.** (2005a). Molecular criteria for genus and species discrimination within the family *Potyviridae*. *Archives of Virology* **150**, 459-479.
- Adams, M.J., Antoniw, J.F., and Beaudoin, F.** (2005b). Overview and analysis of the polyprotein cleavage sites in the family *Potyviridae*. *Molecular Plant Pathology* **6**, 471-487.
- Akad, A., Teverovsky, E., Gidoni Elad, D., Kirshner, B., Rav-David, D., Czosnek, H., and Loebenstein, G.** (2005). Resistance to *Tobacco mosaic virus* and *Botrytis cinerea* in tobacco transformed with complementary DNA encoding an inhibitor of viral replication-like protein. *Annals of Applied Biology* **147**, 89-100.
- Alvarado, V., and Scholthof, H.B.** (2009). Plant responses against invasive nucleic acids: RNA silencing and its suppression by plant viral pathogens. *Seminars in Cell and Developmental Biology* **20**, 1032-1040.
- Anandalakshmi, R., Pruss, G.J., Ge, X., Marathe, R., Mallory, A.C., Smith, T.H., and Vance, V.B.** (1998). A viral suppressor of gene silencing in plants. *Proceedings of the National Academy of Sciences* **95**, 13079-13084.
- Anurag, S.** (2013). Virus-induced symptoms in plants: A review of interactions between viral trafficking and RNA silencing. *Philippine Agricultural Scientist* **96**, 210-218.
- Aparicio, F., Thomas, C.L., Lederer, C., Niu, Y., Wang, D., and Maule, A.J.** (2005). Virus induction of heat shock protein 70 reflects a general response to protein accumulation in the plant cytosol. *Plant Physiology* **138**, 529-536.
- Arbatova, J., Lehto, K., Pehu, E., and Pehu, T.** (1998). Localization of the P1 protein of *Potato Y potyvirus* in association with cytoplasmic inclusion bodies and in the cytoplasm of infected cells. *Journal of General Virology* **79**, 2319-2323.
- Atreya, C.D.** (1992). Application of genome sequence information in potyvirus taxonomy: an overview. *Archives of Virology. Supplementum* **5**, 17-23.
- Azevedo, C., Sadanandom, A., Kitagawa, K., Freialdenhoven, A., Shirasu, K., and Schulze-Lefert, P.** (2002). The RAR1 interactor SGT1, an essential component of *R* gene-triggered disease resistance. *Science* **295**, 2073-2076.

- Barrett, A.J.** (1994). *Proteolytic enzymes: Serine and cysteine peptidases.* (Academic Press).
- Bartels, M., French, R., Graybosch, R.A., and Tatineni, S.** (2016). *Triticum mosaic virus* exhibits limited population variation yet shows evidence of parallel evolution after replicated serial passage in wheat. *Virology* **492**, 92-100.
- Baulcombe, D.** (2004). RNA silencing in plants. *Nature* **431**, 356-363.
- Beauchemin, C., Boutet, N., and Laliberté, J.-F.** (2007). Visualization of the interaction between the precursors of VPg, the viral protein linked to the genome of *Turnip mosaic virus*, and the translation eukaryotic initiation factor iso 4E in *planta*. *Journal of Virology* **81**, 775-782.
- Bedoya, L.C., and Daròs, J.-A.** (2010). Stability of *Tobacco etch virus* infectious clones in plasmid vectors. *Virus Research* **149**, 234-240.
- Belkhadir, Y., Subramaniam, R., and Dangl, J.L.** (2004). Plant disease resistance protein signaling: NBS-LRR proteins and their partners. *Current Opinion in Plant Biology* **7**, 391-399.
- Bendahmane, A., Köhm, B.A., Dedi, C., and Baulcombe, D.C.** (1995). The coat protein of *Potato virus X* is a strain-specific elicitor of *Rx1*-mediated virus resistance in potato. *The Plant Journal* **8**, 933-941.
- Berggard, T., Linse, S., and James, P.** (2007). Methods for the detection and analysis of protein-protein interactions. *Proteomics* **7**, 2833-2842.
- Bisgrove, S.R., Simonich, M.T., Smith, N.M., Sattler, A., and Innes, R.W.** (1994). A disease resistance gene in *Arabidopsis* with specificity for two different pathogen avirulence genes. *The Plant Cell* **6**, 927-933.
- Bivalkar-Mehla, S., Vakharia, J., Mehla, R., Abreha, M., Kanwar, J.R., Tikoo, A., and Chauhan, A.** (2011). Viral RNA silencing suppressors (RSS): Novel strategy of viruses to ablate the host RNA interference (RNAi) defense system. *Virus Research* **155**, 1-9.
- Blanc, S., López-Moya, J.-J., Wang, R., García-Lampasona, S., Thornbury, D.W., and Pirone, T.P.** (1997). A specific interaction between coat protein and helper component correlates with aphid transmission of a potyvirus. *Virology* **231**, 141-147.
- Blanc, S., Ammar, E., Garcia-Lampasona, S., Dolja, V., Llave, C., Baker, J., and Pirone, T.** (1998). Mutations in the potyvirus helper component protein: effects on interactions with virions and aphid stylets. *Journal of General Virology* **79**, 3119-3122.

- Boisvert, F.M., Van Koningsbruggen, S., Navascués, J., and Lamond, A.I.** (2007). The multifunctional nucleolus. *Nature Reviews Molecular Cell Biology* **8**, 574-585.
- Brantley, J.D., and Hunt, A.G.** (1993). The N-terminal protein of the polyprotein encoded by the potyvirus *Tobacco vein mottling virus* is an RNA-binding protein. *Journal of General Virology* **74**, 1157-1157.
- Brigneti, G., Voinnet, O., Li, W.X., Ji, L.H., Ding, S.W., and Baulcombe, D.C.** (1998). Viral pathogenicity determinants are suppressors of transgene silencing in *Nicotiana benthamiana*. *The EMBO Journal* **17**, 6739-6746.
- Brückner, A., Polge, C., Lentze, N., Auerbach, D., and Schlattner, U.** (2009). Yeast two-hybrid, a powerful tool for systems biology. *International Journal of Molecular Sciences* **10**, 2763-2788.
- Bruening, G.** (2006). Resistance to infection. Natural resistance mechanisms of plants to viruses (Springer Netherlands), pp. 211-240.
- Buck, K.W.** (1996). Comparison of the replication of positive-stranded RNA viruses of plants and animals. *Advances in Virus Research* **47**, 159.
- Burguán, J.** (2006). Virus induced RNA silencing and suppression: Defence and counter defence. *Journal of Plant Pathology* **88**, 233-244.
- Caplan, J., and Dinesh-Kumar, S.** (2006). Recognition and signal transduction associated with *R* gene-mediated resistance. Natural resistance mechanisms of plants to viruses (Springer), pp. 73-98.
- Carbonell, A., Dujovny, G., García, J.A., and Valli, A.** (2012). The *Cucumber vein yellowing virus* silencing suppressor P1b can functionally replace HC-Pro in *Plum pox virus* infection in a host-specific manner. *Molecular Plant-Microbe Interactions* **25**, 151-164.
- Carr, J.P., Lewsey, M.G., and Palukaitis, P.** (2010). Signaling in induced resistance. *Advances in Virus Research* **76**, 57-121.
- Carrington, J.C., Jensen, P.E., and Schaad, M.C.** (1998). Genetic evidence for an essential role for potyvirus CI protein in cell-to-cell movement. *The Plant Journal* **14**, 393-400.
- Charron, C., Nicolai, M., Gallois, J.L., Robaglia, C., Moury, B., Palloix, A., and Caranta, C.** (2008). Natural variation and functional analyses provide evidence for co-evolution between plant eIF4E and potyviral VPg. *The Plant Journal* **54**, 56-68.

- Chisholm, S.T., Coaker, G., Day, B., and Staskawicz, B.J.** (2006). Host-microbe interactions: shaping the evolution of the plant immune response. *Cell* **124**, 803-814.
- Choi, I.R., Stenger, D.C., and French, R.** (2000). Multiple interactions among proteins encoded by the mite-transmitted *Wheat streak mosaic tritimovirus*. *Virology* **267**, 185-198.
- Chung, B.Y.-W., Miller, W.A., Atkins, J.F., and Firth, A.E.** (2008). An overlapping essential gene in the *Potyviridae*. *Proceedings of the National Academy of Sciences* **105**, 5897-5902.
- Clark, C.A., Davis, J.A., Abad, J.A., Cuellar, W.J., Fuentes, S., Kreuze, J.F., Gibson, R.W., Mukasa, S.B., Tugume, A.K., Tairo, F.D., and Valkonen, J.P.T.** (2012). Sweetpotato viruses: 15 years of progress on understanding and managing complex diseases. *Plant Disease* **96**, 168-185.
- Clemente-Moreno, M.J., Hernández, J.A., and Diaz-Vivancos, P.** (2015). Sharka: How do plants respond to *Plum pox virus* infection? *Journal of Experimental Botany* **66**, 25-35.
- Collier, S.M., and Moffett, P.** (2009). NB-LRRs work a “bait and switch” on pathogens. *Trends in Plant Science* **14**, 521-529.
- Cooley, M.B., Pathirana, S., Wu, H.J., Kachroo, P., and Klessig, D.F.** (2000). Members of the *Arabidopsis* *HRT/RPP8* family of resistance genes confer resistance to both viral and oomycete pathogens. *The Plant Cell* **12**, 663-676.
- Cotton, S., Grangeon, R., Thivierge, K., Mathieu, I., Ide, C., Wei, T., Wang, A., and Laliberté, J.-F.** (2009). *Turnip mosaic virus* RNA replication complex vesicles are mobile, align with microfilaments, and are each derived from a single viral genome. *Journal of Virology* **83**, 10460-10471.
- Covey, S.N.** (1997). Plants combat infection by gene silencing. *Nature* **385**, 781-782.
- Csorba, T., Kontra, L., and Burgyán, J.** (2015). Viral silencing suppressors: Tools forged to fine-tune host-pathogen coexistence. *Virology* **479-480**, 85-103.
- Cui, H., and Wang, A.** (2016). *Plum Pox Virus* 6K1 protein is required for viral replication and targets the viral replication complex at the early stage of infection. *Journal of Virology* **90**, 5119-5131.
- Cui, X., Wei, T., Chowda-Reddy, R., Sun, G., and Wang, A.** (2010). The *Tobacco etch virus* P3 protein forms mobile inclusions via the early secretory pathway and traffics along actin microfilaments. *Virology* **397**, 56-63.
- D'Andrea, L.D., and Regan, L.** (2003). TPR proteins: the versatile helix. *Trends in Biochemical Sciences* **28**, 655-662.

- Dangl, J.L., and Jones, J.D.** (2001). Plant pathogens and integrated defence responses to infection. *Nature* **411**, 826-833.
- Davies, T.H., Ning, Y.-M., and Sánchez, E.R.** (2005). Differential control of glucocorticoid receptor hormone-binding function by tetratricopeptide repeat (TPR) proteins and the immunosuppressive ligand FK506. *Biochemistry* **44**, 2030-2038.
- de Ronde, D., Butterbach, P., and Kormelink, R.** (2014). Dominant resistance against plant viruses. *Frontiers in Plant Science* **5**.
- Diaz-Pendon, J.A., Truniger, V., Nieto, C., Garcia - Mas, J., Bendahmane, A., and Aranda, M.A.** (2004). Advances in understanding recessive resistance to plant viruses. *Molecular Plant Pathology* **5**, 223-233.
- Durrant, W., and Dong, X.** (2004). Systemic acquired resistance. *Annual Review of Phytopathology* **42**, 185-209.
- Earley, K.W., Haag, J.R., Pontes, O., Opper, K., Juehne, T., Song, K., and Pikaard, C.S.** (2006). Gateway-compatible vectors for plant functional genomics and proteomics. *The Plant Journal* **45**, 616-629.
- Faoro, F., and Gozzo, F.** (2015). Is modulating virus virulence by induced systemic resistance realistic? *Plant Science* **234**, 1-13.
- Fernández, A., Guo, H.S., Sáenz, P., Simón-Buela, L., de Cedrón, M.G., and García, J.A.** (1997). The motif V of *Plum pox potyvirus* CI RNA helicase is involved in NTP hydrolysis and is essential for virus RNA replication. *Nucleic Acids Research* **25**, 4474-4480.
- Fetchko, M., and Stagljar, I.** (2004). Application of the split-ubiquitin membrane yeast two-hybrid system to investigate membrane protein interactions. *Methods* **32**, 349-362.
- Fields, S., and Song, O.-k.** (1989). A novel genetic system to detect protein protein interactions. *Nature* **340**, 245 - 246
- Fraser, R., and Van Loon, L.C.** (1986). Genes for resistance to plant viruses. *Critical Reviews in Plant Sciences* **3**, 257-294.
- Galvez, L.C., Banerjee, J., Pinar, H., and Mitra, A.** (2014). Engineered plant virus resistance. *Plant Science* **228**, 11-25.
- Gao, Z., Johansen, E., Evers, S., Thomas, C.L., Noel Ellis, T., and Maule, A.J.** (2004). The potyvirus recessive resistance gene, *sbm1*, identifies a novel role for translation initiation factor eIF4E in cell-to-cell trafficking. *The Plant Journal* **40**, 376-385.

- Ghoshal, B., and Sanfaçon, H.** (2015). Symptom recovery in virus-infected plants: Revisiting the role of RNA silencing mechanisms. *Virology* **479-480**, 167-179.
- Gilliland, A., Murphy, A., and Carr, J.** (2006). Induced resistance mechanisms. *Natural resistance mechanisms of plants to viruses* (Springer), pp. 125-145.
- Giner, A., Lakatos, L., García-Chapa, M., López-Moya, J.J., and Burgyán, J.** (2010). Viral protein inhibits RISC activity by argonaute binding through conserved WG/GW motifs. *PLoS Pathogens* **6**, e1000996.
- Gottula, J., and Fuchs, M.** (2009). Toward a quarter century of pathogen-derived resistance and practical approaches to plant virus disease control. *Advances in Virus Research* **75**, 161-183.
- Guo, D., Rajamäki, M.-L., and Valkonen, J.** (2008). Protein-protein interactions: the yeast two-hybrid system. *Plant virology protocols: From viral sequence to protein function*, 421-439.
- Guo, D., Rajamäki, M.-L., Saarma, M., and Valkonen, J.P.** (2001). Towards a protein interaction map of potyviruses: protein interaction matrixes of two potyviruses based on the yeast two-hybrid system. *Journal of General Virology* **82**, 935-939.
- Hammerschmidt, R.** (2009). Systemic acquired resistance. *Advances in botanical research*, pp. 173-222.
- Hannon, G.J.** (2002). RNA interference. *Nature* **418**, 244-251.
- Haupt, S., Ziegler, A., and Torrance, L.** (2008). Localization of viral proteins in plant cells: Protein tagging. *Plant virology protocols: From viral sequence to protein function*, 463-473.
- Heinlein, M.** (2015). Plant virus replication and movement. *Virology* **479-480**, 657-671.
- Hiscox, J.A.** (2007). RNA viruses: Hijacking the dynamic nucleolus. *Nature Reviews Microbiology* **5**, 119-127.
- Hu, C.-D., Chinenov, Y., and Kerppola, T.K.** (2002). Visualization of interactions among bZIP and Rel family proteins in living cells using bimolecular fluorescence complementation. *Molecular Cell* **9**, 789-798.
- Huang, C.J., Qian, Y.J., Li, Z.H., and Zhou, X.P.** (2012). Virus-induced gene silencing and its application in plant functional genomics. *Science China Life Sciences* **55**, 99-108.
- Hubert, D.A., Tornero, P., Belkhadir, Y., Krishna, P., Takahashi, A., Shirasu, K., and Dangl, J.L.** (2003). Cytosolic HSP90 associates with and modulates the *Arabidopsis* RPM1 disease resistance protein. *The EMBO Journal* **22**, 5679-5689.

- Hull, R.** (2009). Mechanical inoculation of plant viruses. *Current protocols in microbiology*, 16B.16.11-16B.16.14.
- Hull, R.** (2013). *Plant virology*. (Academic press).
- Hyodo, K., and Okuno, T.** (2016). Pathogenesis mediated by proviral host factors involved in translation and replication of plant positive-strand RNA viruses. *Current Opinion in Virology* **17**, 11-18.
- Jiang, J., and Laliberté, J.-F.** (2011). The genome-linked protein VPg of plant viruses-a protein with many partners. *Current Opinion in Virology* **1**, 347-354.
- Jin, H., and Zhu, J.K.** (2010). A viral suppressor protein inhibits host RNA silencing by hooking up with Argonautes. *Genes and Development* **24**, 853-856.
- Jones, R.A.C.** (2006). Control of plant virus diseases. *Advances in virus research*, K. Maramorosch, A.J. Shatkin, and J.M. Thresh **67**, 205-244.
- Kang, B.C., Yeam, I., and Jahn, M.M.** (2005a). Genetics of plant virus resistance. *Annual Review of Phytopathology*, pp. 581-621.
- Kang, B.C., Yeam, I., Frantz, J.D., Murphy, J.F., and Jahn, M.M.** (2005b). The *pvr1* locus in *Capsicum* encodes a translation initiation factor eIF4E that interacts with *Tobacco etch virus* VPg. *The Plant Journal* **42**, 392-405.
- Kang, S.-H., Lim, W.-S., and Kim, K.-H.** (2004). A protein interaction map of *Soybean mosaic virus* strain G7H based on the yeast two-hybrid system. *Molecules and Cells* **18**, 122-126.
- Karran, R.A., and Sanfaçon, H.** (2014). *Tomato ringspot virus* coat protein binds to Argonaute 1 and suppresses the translation repression of a reporter gene. *Molecular Plant-Microbe Interactions* **27**, 933-943.
- Kasschau, K.D., and Carrington, J.C.** (1998). A counterdefensive strategy of plant viruses: suppression of posttranscriptional gene silencing. *Cell* **95**, 461-470.
- Kasschau, K.D., Cronin, S., and Carrington, J.C.** (1997). Genome amplification and long-distance movement functions associated with the central domain of *Tobacco etch potyvirus* helper component-proteinase. *Virology* **228**, 251-262.
- Kasschau, K.D., Xie, Z., Allen, E., Llave, C., Chapman, E.J., Krizan, K.A., and Carrington, J.C.** (2003). P1/HC-Pro, a viral suppressor of RNA silencing, interferes with *Arabidopsis* development and miRNA function. *Developmental Cell* **4**, 205-217.
- Kekarainen, T., Savilahti, H., and Valkonen, J.P.** (2002). Functional genomics on *Potato virus A*: virus genome-wide map of sites essential for virus propagation. *Genome Research* **12**, 584-594.

- Kerppola, T.K.** (2013). Bimolecular fluorescence complementation (BiFC) analysis of protein interactions in live cells. *Cold spring harbor protocols* **2013**, pdb. prot076497.
- Khatri, N., and Mudgil, Y.** (2015). Hypothesis: NDL proteins function in stress responses by regulating microtubule organization. *Frontiers in Plant Science* **6**.
- Kon, T., and Ikegami, M.** (2009). RNA silencing in plants and its suppression by plant viruses. *CAB Reviews: Perspectives in Agriculture, Veterinary Science, Nutrition and Natural Resources* **4**, 1-16.
- Kopp, A., Kondrák, M., and Bánfalvi, Z.** (2015). Review article: Molecular mechanisms of resistance to *Potato virus X* and *Y* in potato. *Acta Phytopathologica et Entomologica Hungarica* **50**, 151-160.
- Krichevsky, A., Kozlovsky, S.V., Gafni, Y., and Citovsky, V.** (2006). Nuclear import and export of plant virus proteins and genomes. *Molecular Plant Pathology* **7**, 131-146.
- La Scola, B., Audic, S., Robert, C., Jungang, L., de Lamballerie, X., Drancourt, M., Birtles, R., Claverie, J.-M., and Raoult, D.** (2003). A giant virus in amoebae. *Science* **299**, 2033-2033.
- La Scola, B., Desnues, C., Pagnier, I., Robert, C., Barrassi, L., Fournous, G., Merchat, M., Suzan-Monti, M., Forterre, P., and Koonin, E.** (2008). The virophage as a unique parasite of the giant mimivirus. *Nature* **455**, 100-104.
- Lee, K.-C., Lin, S.-S., Yeh, S.-D., and Wong, S.-M.** (2002). Interactions between Nuclear Inclusion Protein a (NIa) and Nuclear Inclusion Protein b (NIb) of *Zucchini yellow mosaic virus* and *Papaya ringspot virus*. *Plant Pathology* **11**, 80.
- Léonard, S., Viel, C., Beauchemin, C., Daigneault, N., Fortin, M.G., and Laliberte, J.F.** (2004). Interaction of VPg-Pro of *Turnip mosaic virus* with the translation initiation factor 4E and the poly(A)-binding protein *in planta*. *Journal of General Virology* **85**, 1055-1063.
- Les Erickson, F., Holzberg, S., Calderon-Urrea, A., Handley, V., Axtell, M., Corr, C., and Baker, B.** (1999). The helicase domain of the TMV replicase proteins induces the *N*-mediated defence response in tobacco. *The Plant Journal* **18**, 67-75.
- Lin, L., Shi, Y., Luo, Z., Lu, Y., Zheng, H., Yan, F., Chen, J., Chen, J., Adams, M., and Wu, Y.** (2009). Protein-protein interactions in two potyviruses using the yeast two-hybrid system. *Virus Research* **142**, 36-40.
- Liu, Y., Burch-Smith, T., Schiff, M., Feng, S., and Dinesh-Kumar, S.P.** (2004). Molecular chaperone Hsp90 associates with resistance protein N and its signaling proteins SGT1 and Rar1 to modulate an innate immune response in plants. *Journal of Biological Chemistry* **279**, 2101-2108.

- Llave, C.** (2010). Virus-derived small interfering RNAs at the core of plant-virus interactions. *Trends in Plant Science* **15**, 701-707.
- Loebenstein, G.** (2009). Local lesions and induced resistance. *Advances in Virus Research* **75**, 73-117.
- López, L., Urzainqui, A., Domínguez, E., and García, J.A.** (2001). Identification of an N-terminal domain of the *Plum pox potyvirus* CI RNA helicase involved in self-interaction in a yeast two-hybrid system. *Journal of General Virology* **82**, 677-686.
- Lu, Q., Tang, X., Tian, G., Wang, F., Liu, K., Nguyen, V., Kohalmi, S.E., Keller, W.A., Tsang, E.W., and Harada, J.J.** (2010). *Arabidopsis* homolog of the yeast TREX-2 mRNA export complex: components and anchoring nucleoporin. *The Plant Journal* **61**, 259-270.
- Lu, R., Malcuit, I., Moffett, P., Ruiz, M.T., Peart, J., Wu, A.J., Rathjen, J.P., Bendahmane, A., Day, L., and Baulcombe, D.C.** (2003). High throughput virus-induced gene silencing implicates heat shock protein 90 in plant disease resistance. *The EMBO Journal* **22**, 5690-5699.
- Ma, J., Zhu, C., Wen, F., Xu, H., and Li, X.Q.** (2015). Strategic RNA silencing for plant viral resistance. *Somatic genome manipulation: Advances, methods, and applications* (Springer New York), pp. 237-252.
- Maia, I.G., Haenni, A.L., and Bernardi, F.** (1996). Potyviral HC-Pro: A multifunctional protein. *Journal of General Virology* **77**, 1335-1341.
- Mäki-Valkama, T., Valkonen, J.P., Kreuze, J.F., and Pehu, E.** (2000a). Transgenic resistance to PVYO associated with post-transcriptional silencing of P1 transgene is overcome by PVYN strains that carry highly homologous P1 sequences and recover transgene expression at infection. *Molecular Plant-Microbe Interactions* **13**, 366-373.
- Mäki-Valkama, T., Pehu, T., Santala, A., Valkonen, J.P., Koivu, K., Lehto, K., and Pehu, E.** (2000b). High level of resistance to *potato virus Y* by expressing P1 sequence in antisense orientation in transgenic potato. *Molecular Breeding* **6**, 95-104.
- Martin, G.B., Bogdanove, A.J., and Sessa, G.** (2003). Understanding the functions of plant disease resistance proteins. *Annual Review of Plant Biology* **54**, 23-61.
- Martínez, F., and Daròs, J.A.** (2014). *Tobacco etch virus* protein P1 traffics to the nucleolus and associates with the host 60S ribosomal subunits during infection. *Journal of Virology* **88**, 10725-10737.
- Maule, A., Leh, V., and Lederer, C.** (2002). The dialogue between viruses and hosts in compatible interactions. *Current Opinion in Plant Biology* **5**, 279-284.

- Maule, A.J., Caranta, C., and Boulton, M.I.** (2007). Sources of natural resistance to plant viruses: Status and prospects: Review. *Molecular Plant Pathology* **8**, 223-231.
- Mbanzibwa, D.R., Tian, Y., Mukasa, S.B., and Valkonen, J.P.** (2009). *Cassava brown streak virus (Potyviridae)* encodes a putative Maf/HAM1 pyrophosphatase implicated in reduction of mutations and a P1 proteinase that suppresses RNA silencing but contains no HC-Pro. *Journal of Virology* **83**, 6934-6940.
- McDowell, J.M., Dhandaydham, M., Long, T.A., Aarts, M.G.M., Goff, S., Holub, E.B., and Dangl, J.L.** (1998). Intragenic recombination and diversifying selection contribute to the evolution of downy mildew resistance at the *RPP8* locus of *Arabidopsis*. *The Plant Cell* **10**, 1861-1874.
- Merits, A., Guo, D., Järvekülg, L., and Saarma, M.** (1999). Biochemical and genetic evidence for interactions between *Potato A potyvirus*-encoded proteins P1 and P3 and proteins of the putative replication complex. *Virology* **263**, 15-22.
- Miller, K.E., Kim, Y., Huh, W.-K., and Park, H.-O.** (2015). Bimolecular fluorescence complementation (BiFC) analysis: Advances and recent applications for genome-wide interaction studies. *Journal of Molecular Biology* **427**, 2039-2055.
- Miller, S., and Krijnse-Locker, J.** (2008). Modification of intracellular membrane structures for virus replication. *Nature Reviews Microbiology* **6**, 363-374.
- Mingot, A., Valli, A., Rodamilans, B., León, D.S., Baulcombe, D.C., García, J.A., and López-Moya, J.J.** (2016). The P1N-PISPO trans-frame gene of *Sweet potato feathery mottle potyvirus* is produced during virus infection and functions as an RNA silencing suppressor. *Journal of Virology* **90**, 3543-3557.
- Moffett, P.** (2009). Mechanisms of recognition in dominant *R* gene mediated resistance. *Advances in Virus Research* **75**, 1-33.
- Moissiard, G., and Voinnet, O.** (2004). Viral suppression of RNA silencing in plants. *Molecular Plant Pathology* **5**, 71-82.
- Moreno, M., Bernal, J., Jim, I., and Rodr, E.** (1998). Resistance in plants transformed with the P1 or P3 gene of *Tobacco vein mottling potyvirus*. *Journal of General Virology* **79**, 2819-2827.
- Moreno, M., Brandwagt, B.F., Shaw, J.G., and Rodríguez-Cerezo, E.** (1999). Infectious virus in transgenic plants inoculated with a nonviable, P1-proteinase defective mutant of a potyvirus. *Virology* **257**, 322-329.
- Moury, B., Charron, C., Janzac, B., Simon, V., Gallois, J.L., Palloix, A., and Caranta, C.** (2014). Evolution of plant eukaryotic initiation factor 4E (eIF4E) and potyvirus genome-linked protein (VPg): A game of mirrors impacting resistance spectrum and durability. *Infection, genetics and evolution* **27**, 472-480.

- Moury, B., Morel, C., Johansen, E., Guilbaud, L., Souche, S., Ayme, V., Caranta, C., Palloix, A., and Jacquemond, M.** (2004). Mutations in *Potato virus Y* genome-linked protein determine virulence toward recessive resistances in *Capsicum annuum* and *Lycopersicon hirsutum*. *Molecular Plant-Microbe Interactions* **17**, 322-329.
- Nakagawa, T., Suzuki, T., Murata, S., Nakamura, S., Hino, T., Maeo, K., Tabata, R., Kawai, T., Tanaka, K., and Niwa, Y.** (2007). Improved Gateway binary vectors: High-performance vectors for creation of fusion constructs in transgenic analysis of plants. *Bioscience, Biotechnology, and Biochemistry* **71**, 2095-2100.
- Nakahara, K.S., Shimada, R., Choi, S.-H., Yamamoto, H., Shao, J., and Uyeda, I.** (2010). Involvement of the P1 cistron in overcoming eIF4E-mediated recessive resistance against *Clover yellow vein virus* in pea. *Molecular Plant-Microbe Interactions* **23**, 1460-1469.
- Nelson, R.S., and Citovsky, V.** (2005). Plant viruses. Invaders of cells and pirates of cellular pathways. *Plant Physiology* **138**, 1809-1814.
- Ng, J.C., and Perry, K.L.** (2004). Transmission of plant viruses by aphid vectors. *Molecular Plant Pathology* **5**, 505-511.
- Nicaise, V., Roux, M., and Zipfel, C.** (2009). Recent advances in PAMP-triggered immunity against bacteria: Pattern recognition receptors watch over and raise the alarm. *Plant Physiology* **150**, 1638-1647.
- Nicaise, V., German-Retana, S., Sanjuán, R., Dubrana, M.P., Mazier, M., Maisonneuve, B., Candresse, T., Caranta, C., and LeGall, O.** (2003). The eukaryotic translation initiation factor 4E controls lettuce susceptibility to the potyvirus *Lettuce mosaic virus*. *Plant Physiology* **132**, 1272-1282.
- Nieto, C., Morales, M., Orjeda, G., Clepet, C., Monfort, A., Sturbois, B., Puigdomenech, P., Pitrat, M., Caboche, M., and Dogimont, C.** (2006). An *eIF4E* allele confers resistance to an uncapped and non-polyadenylated RNA virus in melon. *The Plant Journal* **48**, 452-462.
- Olsper, A., Chung, B.Y.W., Atkins, J.F., Carr, J.P., and Firth, A.E.** (2015). Transcriptional slippage in the positive-sense RNA virus family *Potyviridae*. *EMBO Reports* **16**, 995-1004.
- Omarov, R.T., and Scholthof, H.B.** (2012). Biological chemistry of virus-encoded suppressors of RNA silencing: An overview. *Methods in molecular biology*, pp. 39-56.
- Padgett, H.S., and Beachy, R.N.** (1993). Analysis of a *Tobacco mosaic virus* strain capable of overcoming *N* gene-mediated resistance. *The Plant Cell* **5**, 577-586.

- Padmanabhan, M., Cournoyer, P., and Dinesh-Kumar, S.** (2009). The leucine-rich repeat domain in plant innate immunity: A wealth of possibilities. *Cellular Microbiology* **11**, 191-198.
- Pallas, V., and García, J.A.** (2011). How do plant viruses induce disease? Interactions and interference with host components. *Journal of General Virology* **92**, 2691-2705.
- Pålsson-McDermott, E., and O'Neill, L.** (2007). Building an immune system from nine domains. *Biochemical Society Transactions* **35**, 1437-1444.
- Palukaitis, P.** (2011). The road to RNA silencing is paved with plant-virus interactions. *Plant Pathology Journal* **27**, 197-206.
- Palukaitis, P., and MacFarlane, S.** (2006). Viral counter-defense molecules. Natural resistance mechanisms of plants to viruses (Springer Netherlands), pp. 165-185.
- Palukaitis, P., Carr, J.P., and Schoelz, J.E.** (2008). Plant-virus interactions. *Methods in molecular biology* **451**, 3-19.
- Palukaitis, P., Groen, S.C., and Carr, J.P.** (2013). The Rumsfeld paradox: Some of the things we know that we don't know about plant virus infection. *Current Opinion in Plant Biology* **16**, 513-519.
- Parrish, J.R., Gulyas, K.D., and Finley, R.L.** (2006). Yeast two-hybrid contributions to interactome mapping. *Current Opinion in Biotechnology* **17**, 387-393.
- Pasin, F., Simón-Mateo, C., and García, J.A.** (2014). The hypervariable amino-terminus of P1 protease modulates potyviral replication and host defense responses. *PLoS Pathogens* **10**, e1003985.
- Pearson, H.** (2008). 'Virophage' suggests viruses are alive. *Nature News* **454**, 677-677.
- Phizicky, E.M., and Fields, S.** (1995). Protein-protein interactions: Methods for detection and analysis. *Microbiological Reviews* **59**, 94-123.
- Picard, D.** (2002). Heat-shock protein 90, a chaperone for folding and regulation. *Cellular and Molecular Life Sciences CMLS* **59**, 1640-1648.
- Pontes, O., Li, C.F., Nunes, P.C., Haag, J., Ream, T., Vitins, A., Jacobsen, S.E., and Pikaard, C.S.** (2006). The *Arabidopsis* chromatin-modifying nuclear siRNA pathway involves a nucleolar RNA processing center. *Cell* **126**, 79-92.
- Porebski, S., Bailey, L.G., and Baum, B.R.** (1997). Modification of a CTAB DNA extraction protocol for plants containing high polysaccharide and polyphenol components. *Plant Molecular Biology Reporter* **15**, 8-15.

- Pruss, G., Ge, X., Shi, X.M., Carrington, J.C., and Vance, V.B.** (1997). Plant viral synergism: The potyviral genome encodes a broad-range pathogenicity enhancer that transactivates replication of heterologous viruses. *The Plant Cell* **9**, 859-868.
- Pumplin, N., and Voinnet, O.** (2013). RNA silencing suppression by plant pathogens: Defence, counter-defence and counter-counter-defence. *Nature Reviews Microbiology* **11**, 745-760.
- Puustinen, P., and Mäkinen, K.** (2004). Uridylylation of the potyvirus VPg by viral replicase NIb correlates with the nucleotide binding capacity of VPg. *Journal of Biological Chemistry* **279**, 38103-38110.
- Rafiqi, M., Bernoux, M., Ellis, J.G., and Dodds, P.N.** (2009). In the trenches of plant pathogen recognition: Role of NB-LRR proteins. *Seminars in Cell & Developmental Biology* (Elsevier), pp. 1017-1024.
- Rajamäki, M.-L., and Valkonen, J.P.** (2009). Control of nuclear and nucleolar localization of nuclear inclusion protein a of picorna-like *Potato virus A* in *Nicotiana* species. *The Plant Cell* **21**, 2485-2502.
- Rajamäki, M.-L., Mäki-Valkama, T., Mäkinen, K., and Valkonen, J.P.T.** (2009). Infection with potyviruses. *Annual Plant Reviews, Plant-Pathogen Interactions* **11**, 68.
- Rajamäki, M.L., Kelloniemi, J., Alminait, A., Kekarainen, T., Rabenstein, F., and Valkonen, J.P.T.** (2005). A novel insertion site inside the potyvirus P1 cistron allows expression of heterologous proteins and suggests some P1 functions. *Virology* **342**, 88-101.
- Rawlings, N.D., and Barrett, A.J.** (1993). Evolutionary families of peptidases. *Biochemistry Journal* **290**, 205-218.
- Reddy, D.V., Sudarshana, M.R., Fuchs, M., Rao, N.C., and Thottappilly, G.** (2009). Genetically engineered virus-resistant plants in developing countries: Current status and future prospects. *Advances in Virus Research* **75**, 185-220.
- Riechmann, J.L., Laín, S., and García, J.A.** (1992). Highlights and prospects of potyvirus molecular biology. *Journal of General Virology* **73**, 1-16.
- Ritzenthaler, C.** (2005). Resistance to plant viruses: Old issue, news answers? *Current Opinion in Biotechnology* **16**, 118-122.
- Robaglia, C., and Caranta, C.** (2006). Translation initiation factors: A weak link in plant RNA virus infection. *Trends in Plant Science* **11**, 40-45.
- Rohožková, J., and Navrátil, M.** (2011). P1 peptidase- A mysterious protein of family *Potyviridae*. *Journal of Biosciences* **36**, 189-200.

- Rojas, M.R., Zerbini, F.M., Allison, R.F., Gilbertson, R.L., and Lucas, W.J.** (1997). Capsid protein and helper component-proteinase function as potyvirus cell-to-cell movement proteins. *Virology* **237**, 283-295.
- Roossinck, M.J.** (2010). Lifestyles of plant viruses. *Philosophical Transactions of the Royal Society B: Biological Sciences* **365**, 1899-1905.
- Rosa, C., and Falk, B.W.** (2014). Virus-resistant crops and trees. *Plant biotechnology: Experience and future prospects* (Springer international publishing), pp. 155-168.
- Rosado, A., Schapire, A.L., Bressan, R.A., Harfouche, A.L., Hasegawa, P.M., Valpuesta, V., and Botella, M.A.** (2006). The *Arabidopsis* tetratricopeptide repeat-containing protein TTL1 is required for osmotic stress responses and abscisic acid sensitivity. *Plant Physiology* **142**, 1113-1126.
- Roth, B.M., Pruss, G.J., and Vance, V.B.** (2004). Plant viral suppressors of RNA silencing. *Virus Research* **102**, 97-108.
- Roudet-Tavert, G., Michon, T., Walter, J., Delaunay, T., Redondo, E., and Le Gall, O.** (2007). Central domain of a potyvirus VPg is involved in the interaction with the host translation initiation factor eIF4E and the viral protein HcPro. *Journal of General Virology* **88**, 1029-1033.
- Ruffel, S., Gallois, J., Lesage, M., and Caranta, C.** (2005). The recessive potyvirus resistance gene *pot-1* is the tomato orthologue of the pepper *pvr2-eIF4E* gene. *Molecular Genetics and Genomics* **274**, 346-353.
- Ruffel, S., Gallois, J.-L., Moury, B., Robaglia, C., Palloix, A., and Caranta, C.** (2006). Simultaneous mutations in translation initiation factors eIF4E and eIF (iso) 4E are required to prevent *pepper vein mottle virus* infection of pepper. *Journal of General Virology* **87**, 2089-2098.
- Ruffel, S., Dussault, M.H., Palloix, A., Moury, B., Bendahmane, A., Robaglia, C., and Caranta, C.** (2002). A natural recessive resistance gene against *potato virus Y* in pepper corresponds to the eukaryotic initiation factor 4E (eIF4E). *The Plant Journal* **32**, 1067-1075.
- Rybicki, E.P.** (2015). A top ten list for economically important plant viruses. *Archives of Virology* **160**, 17-20.
- Sacco, M.A., and Moffett, P.** (2009). Disease resistance genes: Form and function. *Molecular Plant-Microbe Interactions*. Wallingford, UK: CABI, 94-141.
- Sadowy, E., Milner, M., and Haenni, A.-L.** (2001). Proteins attached to viral genomes are multifunctional. *Advances in Virus Research* **57**, 185-262.
- Saito, T., Yamanaka, K., Watanabe, Y., Takamatsu, N., Meshi, T., and Okada, Y.** (1989). Mutational analysis of the coat protein gene of *tobacco mosaic virus* in

relation to hypersensitive response in tobacco plants with the *N'* gene. *Virology* **173**, 11-20.

- Salvador, B., Saénz, P., Yangüez, E., Quiot, J.B., Quiot, L., Delgadillo, M.O., García, J.A., and Simón-Mateo, C.** (2008). Host-specific effect of P1 exchange between two potyviruses. *Molecular Plant Pathology* **9**, 147-155.
- Sanchez, F., Wang, X., Jenner, C., Walsh, J., and Ponz, F.** (2003). Strains of *Turnip mosaic potyvirus* as defined by the molecular analysis of the coat protein gene of the virus. *Virus Research* **94**, 33-43.
- Sanfaçon, H.** (2015). Plant translation factors and virus resistance. *Viruses* **7**, 3392-3419.
- Schaad, M.C., Jensen, P.E., and Carrington, J.C.** (1997). Formation of plant RNA virus replication complexes on membranes: Role of an endoplasmic reticulum-targeted viral protein. *The EMBO Journal* **16**, 4049-4059.
- Scholthof, K.B.G., Adkins, S., Czosnek, H., Palukaitis, P., Jacquot, E., Hohn, T., Hohn, B., Saunders, K., Candresse, T., Ahlquist, P., Hemenway, C., and Foster, G.D.** (2011). Top 10 plant viruses in molecular plant pathology. *Molecular Plant Pathology* **12**, 938-954.
- Sharma, N., Sahu, P.P., Puranik, S., and Prasad, M.** (2013). Recent advances in plant-virus interaction with emphasis on small interfering RNAs (siRNAs). *Molecular Biotechnology* **55**, 63-77.
- Shen, W.T., Wang, M.Q., Yan, P., Gao, L., and Zhou, P.** (2010). Protein interaction matrix of *Papaya ringspot virus* type P based on a yeast two-hybrid system. *Acta Virologica* **54**, 49-54.
- Shi, Y., Chen, J., Hong, X., Chen, J., and Adams, M.J.** (2007). A potyvirus P1 protein interacts with the Rieske Fe/S protein of its host. *Molecular Plant Pathology* **8**, 785-790.
- Sibley, C.R., Seow, Y., and Wood, M.J.** (2010). Novel RNA-based strategies for therapeutic gene silencing. *Molecular Therapy* **18**, 466-476.
- Siddiqui, S.A., Sarmiento, C., Kiisma, M., Koivumäki, S., Lemmetty, A., Truve, E., and Lehto, K.** (2008). Effects of viral silencing suppressors on *Tobacco ringspot virus* infection in two *Nicotiana* species. *Journal of General Virology* **89**, 1502-1508.
- Solovyev, A.G., and Savenkov, E.I.** (2014). Factors involved in the systemic transport of plant RNA viruses: The emerging role of the nucleus. *Journal of Experimental Botany* **65**, 1689-1697.

- Sorel, M., Garcia, J.A., and German-Retana, S.** (2014). The potyviridae cylindrical inclusion helicase: A key multipartner and multifunctional protein. *Molecular Plant-Microbe Interactions* **27**, 215-226.
- Soumounou, Y., and Laliberté, J.-F.** (1994). Nucleic acid-binding properties of the P1 protein of *Turnip mosaic potyvirus* produced in *Escherichia coli*. *The Journal of General Virology* **75**, 2567-2573.
- Spetz, C., and Valkonen, J.P.** (2004). Potyviral 6K2 protein long-distance movement and symptom-induction functions are independent and host-specific. *Molecular Plant-Microbe Interactions* **17**, 502-510.
- Srivastava, S., and Prasad, V.** (2014). Induction of defence responses for biological control of plant diseases. *Biological controls for preventing food deterioration: Strategies for pre- and postharvest management* (Wiley Blackwell), pp. 321-339.
- Stein, N., Perovic, D., Kumlehn, J., Pellió, B., Stracke, S., Streng, S., Ordon, F., and Graner, A.** (2005). The eukaryotic translation initiation factor 4E confers multiallelic recessive *Bymovirus* resistance in *Hordeum vulgare* (L.). *The Plant Journal* **42**, 912-922.
- Strange, R.N., and Scott, P.R.** (2005). Plant disease: A threat to global food security. *Phytopathology* **43**.
- Takács, A., Gáborjányi, R., Horváth, J., and Kazinczi, G.** (2014). Virus-virus interactions. *Plant virus-host interaction: Molecular approaches and viral evolution*, pp. 385-394.
- Takahashi, A., Casais, C., Ichimura, K., and Shirasu, K.** (2003). HSP90 interacts with RAR1 and SGT1 and is essential for RPS2-mediated disease resistance in *Arabidopsis*. *Proceedings of the National Academy of Sciences* **100**, 11777-11782.
- Takahashi, H., Suzuki, M., Natsuaki, K., Shigyo, T., Hino, K., Teraoka, T., Hosokawa, D., and Ehara, Y.** (2001). Mapping the virus and host genes involved in the resistance response in *Cucumber mosaic virus*-infected *Arabidopsis thaliana*. *Plant and Cell Physiology* **42**, 340-347.
- Takahashi, H., Miller, J., Nozaki, Y., Sukamto, Takeda, M., Shah, J., Hase, S., Ikegami, M., Ehara, Y., and Dinesh-Kumar, S.P.** (2002). *RCY1*, an *Arabidopsis thaliana* *RPP8/HRT* family resistance gene, conferring resistance to *Cucumber mosaic virus* requires salicylic acid, ethylene and a novel signal transduction mechanism. *The Plant Journal* **32**, 655-667.
- Tameling, W.I., and Joosten, M.H.** (2007). The diverse roles of NB-LRR proteins in plants. *Physiological and Molecular Plant Pathology* **71**, 126-134.

- Tameling, W.I., Elzinga, S.D., Darmin, P.S., Vossen, J.H., Takken, F.L., Haring, M.A., and Cornelissen, B.J.** (2002). The tomato *R* gene products I-2 and MI-1 are functional ATP binding proteins with ATPase activity. *The Plant Cell* **14**, 2929-2939.
- Tatineni, S., Qu, F., Li, R., Jack Morris, T., and French, R.** (2012). *Triticum mosaic poacevirus* enlists P1 rather than HC-Pro to suppress RNA silencing-mediated host defense. *Virology* **433**, 104-115.
- Tavert-Roudet, G., Ravelonandro, M., Bachelier, J.-C., and Dunez, J.** (1998). Transgenic *Nicotiana benthamiana* plants containing the P1 gene of *Plum pox virus* are resistant to virus challenge. *European Journal of Plant Pathology* **104**, 103-107.
- Tenoever, B.R.** (2013). RNA viruses and the host microRNA machinery. *Nature Reviews Microbiology* **11**, 169-180.
- Thivierge, K., Nicaise, V., Dufresne, P.J., Cotton, S., Laliberté, J.F., Le Gall, O., and Fortin, M.G.** (2005). Plant virus RNAs. Coordinated recruitment of conserved host functions by (+) ssRNA viruses during early infection events. *Plant Physiology* **138**, 1822-1827.
- Thivierge, K., Cotton, S., Dufresne, P.J., Mathieu, I., Beauchemin, C., Ide, C., Fortin, M.G., and Laliberté, J.-F.** (2008). Eukaryotic elongation factor 1A interacts with *Turnip mosaic virus* RNA-dependent RNA polymerase and VPg-Pro in virus-induced vesicles. *Virology* **377**, 216-225.
- Thompson, J.R., and Tepfer, M.** (2010). Assessment of the benefits and risks for engineered virus resistance. *Advances in Virus Research* **76**, 33-56.
- Thresh, J.** (2006). Crop viruses and virus diseases: A global perspective. *Virus diseases and crop biosecurity* (Springer), pp. 9-32.
- Tomlinson, J.** (1987). Epidemiology and control of virus diseases of vegetables. *Annals of Applied Biology* **110**, 661-681.
- Ueda, H., Yamaguchi, Y., and Sano, H.** (2006). Direct interaction between the *Tobacco mosaic virus* helicase domain and the ATP-bound resistance protein, N factor during the hypersensitive response in tobacco plants. *Plant Molecular Biology* **61**, 31-45.
- Untiveros, M., Olsper, A., Artola, K., Firth, A.E., Kreuze, J.F., and Valkonen, J.P.T.** (2016). A novel sweet potato potyvirus open reading frame (ORF) is expressed via polymerase slippage and suppresses RNA silencing. *Molecular Plant Pathology*.
- Urcuqui-Inchima, S., Haenni, A.L., and Bernardi, F.** (2001). Potyvirus proteins: A wealth of functions. *Virus Research* **74**, 157-175.

- Urcuqui-Inchima, S., Walter, J., Drugeon, G., German-Retana, S., Haenni, A.-L., Candresse, T., Bernardi, F., and Le Gall, O.** (1999). Potyvirus helper component-proteinase self-interaction in the yeast two-hybrid system and delineation of the interaction domain involved. *Virology* **258**, 95-99.
- Valli, A., López-Moya, J.J., and García, J.A.** (2007). Recombination and gene duplication in the evolutionary diversification of P1 proteins in the family *Potyviridae*. *Journal of General Virology* **88**, 1016-1028.
- Valli, A., Martín-Hernández, A.M., López-Moya, J.J., and García, J.A.** (2006). RNA silencing suppression by a second copy of the P1 serine protease of *Cucumber vein yellowing Ipomovirus*, a member of the family *Potyviridae* that lacks the cysteine protease HCPro. *Journal of Virology* **80**, 10055-10063.
- Van Der Biezen, E.A., and Jones, J.D.** (1998). Plant disease-resistance proteins and the gene-for-gene concept. *Trends in Biochemical Sciences* **23**, 454-456.
- Vargason, J.M., Szittyá, G., Burgyán, J., and Tanaka Hall, T.M.** (2003). Size selective recognition of siRNA by an RNA silencing suppressor. *Cell* **115**, 799-811.
- Vaucheret, H.** (2006). Post-transcriptional small RNA pathways in plants: Mechanisms and regulations. *Genes and Development* **20**, 759-771.
- Verchot, J.** (2014). The ER quality control and ER associated degradation machineries are vital for viral pathogenesis. *Frontiers in Plant Science* **5**.
- Verchot, J., and Carrington, J.C.** (1995a). Debilitation of plant potyvirus infectivity by P1 proteinase-inactivating mutations and restoration by second-site modifications. *Journal of Virology* **69**, 1582-1590.
- Verchot, J., and Carrington, J.C.** (1995b). Evidence that the potyvirus P1 proteinase functions *in trans* as an accessory factor for genome amplification. *Journal of Virology* **69**, 3668-3674.
- Verchot, J., Koonin, E.V., and Carrington, J.C.** (1991). The 35-kDa protein from the N-terminus of the potyviral polyprotein functions as a third virus-encoded proteinase. *Virology* **185**, 527-535.
- Verchot, J., Herndon, K.L., and Carrington, J.C.** (1992). Mutational analysis of the tobacco etch potyviral 35-kDa proteinase: identification of essential residues and requirements for autoproteolysis. *Virology* **190**, 298-306.
- Verma, R.K., Mishra, R., Sharma, P., Choudhary, D.K., and Gaur, R.K.** (2014). Systemic infection of potyvirus: A compatible interaction between host and viral proteins. *Approaches to plant stress and their management* (Springer India), pp. 353-363.

- Voinnet, O.** (2005). Induction and suppression of RNA silencing: Insights from viral infections. *Nature Reviews Genetics* **6**, 206-220.
- Walsh, J.A., and Jenner, C.E.** (2002). *Turnip mosaic virus* and the quest for durable resistance. *Molecular Plant Pathology* **3**, 289-300.
- Wang, A.** (2013). Molecular isolation and functional characterization of host factors required in the virus infection cycle for disease control in plants. *CAB Reviews: Perspectives in Agriculture, Veterinary Science, Nutrition and Natural Resources* **8**.
- Wang, A.** (2015). Dissecting the molecular network of virus-plant interactions: The complex roles of host factors. *Annual Review of Phytopathology*, pp. 45-66.
- Wang, A., and Krishnaswamy, S.** (2012). Eukaryotic translation initiation factor 4E-mediated recessive resistance to plant viruses and its utility in crop improvement. *Molecular Plant Pathology* **13**, 795-803.
- Wassenegger, M.** (2002a). Gene silencing. *International Review of Cytology*, pp. 61-113.
- Wassenegger, M.** (2002b). Gene silencing-based disease resistance. *Transgenic Research* **11**, 639-653.
- Waterhouse, P.M., Wang, M.B., and Finnegan, E.J.** (2001). Role of short RNAs in gene silencing. *Trends in Plant Science* **6**, 297-301.
- Wei, T., Zhang, C., Hou, X., Sanfaçon, H., and Wang, A.** (2013). The SNARE protein Syp71 is essential for *Turnip mosaic virus* infection by mediating fusion of virus-induced vesicles with chloroplasts. *PLoS Pathogens* **9**, e1003378.
- Wei, T., Zhang, C., Hong, J., Xiong, R., Kasschau, K.D., Zhou, X., Carrington, J.C., and Wang, A.** (2010). Formation of complexes at plasmodesmata for potyvirus intercellular movement is mediated by the viral protein P3N-PIPO. *PLoS Pathogens* **6**, e1000962.
- Westwood, J.H., Lewsey, M.G., Murphy, A.M., Tungadi, T., Bates, A., Gilligan, C.A., and Carr, J.P.** (2014). Interference with jasmonic acid-regulated gene expression is a general property of viral suppressors of RNA silencing but only partly explains virus-induced changes in plant-aphid interactions. *Journal of General Virology* **95**, 733-739.
- Whitham, S., Dinesh-Kumar, S., Choi, D., Hehl, R., Corr, C., and Baker, B.** (1994). The product of the *Tobacco mosaic virus* resistance gene *N*: Similarity to toll and the interleukin-1 receptor. *Cell* **78**, 1101-1115.

- Wieczorek, P., and Obrepalska-Stepłowska, A.** (2015). Suppress to survive- Implication of plant viruses in PTGS. *Plant Molecular Biology Reporter* **33**, 335-346.
- Wingard, S.A.** (1928). Hosts and symptoms of ring spot, a virus disease of plants. *Journal of Agricultural Research* **37**, 127-153.
- Yadav, N., and Khurana, S.M.P.** (2015). Plant virus detection and diagnosis: Progress and challenges. *Frontier discoveries and innovations in interdisciplinary microbiology* (Springer India), pp. 97-132.
- Yambao, M.L.M., Masuta, C., Nakahara, K., and Uyeda, I.** (2003). The central and C-terminal domains of VPg of *Clover yellow vein virus* are important for VPg-HCPro and VPg-VPg interactions. *Journal of General Virology* **84**, 2861-2869.
- Young, B.A., Stenger, D.C., Qu, F., Morris, T.J., Tatineni, S., and French, R.** (2012). Tritimovirus P1 functions as a suppressor of RNA silencing and an enhancer of disease symptoms. *Virus Research* **163**, 672-677.
- Zaitlin, M., and Palukaitis, P.** (2000). Advances in understanding plant viruses and virus diseases. *Annual Review of Phytopathology*, pp. 117-143.
- Zhang, C., Wu, Z., Li, Y., and Wu, J.** (2015). Biogenesis, function, and applications of virus-derived small RNAs in plants. *Frontiers in Microbiology* **6**.
- Zhang, L., Chen, H., Brandizzi, F., Verchot, J., and Wang, A.** (2015b). The UPR branch IRE1-*bZIP60* in plants plays an essential role in viral infection and is complementary to the only UPR pathway in yeast. *PLoS Genetics* **11**, e1005164.
- Zhang, Y.Y., Li, H.X., Ouyang, B., and Ye, Z.B.** (2006). Regulation of eukaryotic initiation factor 4E and its isoform: Implications for antiviral strategy in plants. *Journal of Integrative Plant Biology* **48**, 1129-1139.
- Zhao, J.H., Hua, C.L., Fang, Y.Y., and Guo, H.S.** (2016). The dual edge of RNA silencing suppressors in the virus-host interactions. *Current Opinion in Virology* **17**, 39-44.
- Zhao, Y., DelGrosso, L., Yigit, E., Dempsey, D.M.A., Klessig, D.F., and Wobbe, K.K.** (2000). The amino terminus of the coat protein of *Turnip crinkle virus* is the AVR factor recognized by resistant *Arabidopsis*. *Molecular Plant-Microbe Interactions* **13**, 1015-1018.
- Ziebell, H.** (2016). Plant defence and viral interference. *Plant-virus interactions: Molecular biology, intra- and intercellular transport* (Springer International Publishing), pp. 123-159.

- Zilian, E., and Maiss, E.** (2011). Detection of plum pox potyviral protein-protein interactions *in planta* using an optimized mRFP-based bimolecular fluorescence complementation system. *Journal of General Virology* **92**, 2711-2723.
- Zipfel, C.** (2008). Pattern-recognition receptors in plant innate immunity. *Current Opinion in Immunology* **20**, 10-16.
- Zvereva, A.S., and Pooggin, M.M.** (2012). Silencing and innate immunity in plant defense against viral and non-viral pathogens. *Viruses* **4**, 2578-2597.

Curriculum Vitae

Qiuyue Pan

EDUCATION

Department of Biology, Western University

London, Ontario, Canada

2010 ~ present, Ph.D. of Biology

College of Horticulture, Northwest A&F University

Yangling, Shaanxi, China

2009 ~ 2010, Master of Agriculture (Incomplete)

College of Agronomy, Northwest A&F University

Yangling, Shaanxi, China

2005 ~ 2009, Bachelor of Agronomy (Honors)

HONORS AND AWARDS

| | |
|-------------|---------------------------------------|
| 2006 ~ 2007 | China National Scholarship |
| 2009 | Outstanding Graduate of University |
| 2010 ~ 2014 | China Scholarship Council Scholarship |
| 2010~2015 | Western Graduate Research Scholarship |

RELATED WORK EXPERIENCE

| | |
|-------------|---|
| 2010 ~ 2011 | Teaching Assistant, Western University, London, Ontario |
| 2011 ~ 2015 | Research Assistant, AAFC, London, Ontario |
| 2015 ~ 2016 | Teaching Assistant, Western University, London, Ontario |